Dendritic Cell Targeted Therapy Utilising Porous Silicon Nanoparticles for the Induction of Immunological Tolerance

Sebastian O. Stead

School of Medicine
Discipline of Medicine

December 2018

CONTENTS

ABSTRACT

The work depicted in this thesis, explores the use of drug loaded porous silicon nanoparticles (pSiNP) targeted to dendritic cells both *in vitro* and *in vivo*. Paper one explores the *in vitro* application of rapamycin loaded, DC-SIGN pSiNP to induces a maturation resistant, tolerogenic state within human monocyte derived DC. Furthermore, it explores the poor stimulatory ability of these tolerogenic DC within an allogeneic immune system. The study concluded that nanoparticles functionalised with DC-SIGN antibody, were capable of tracking to human monocyte derived DC expeditiously compared to their isotype counterparts. DC-SIGN pSiNP were also able to release their payload and induce a tolerogenic state in DC *in vitro*. Paper two develops the work from paper one exploring the *in vivo* tracking capability of the nanoparticle within both murine and non-human primate animal models. Within mice, the functionalisation of the pSiNP with antibodies permitting targeting to DC (CD11c receptor) significantly enhanced their tracking abilities to splenic DC populations, compared to isotype pSiNP. Within both murine and non-human primate animal models, a serendipitous discovery was the enhanced kidney tracking abilities of the DC targeting pSiNP. This opens the door for the development of potentially new drug delivery methods more localised to the kidneys. Following *in vivo* tracking experiments, paper two explored the ability of drug and peptide loaded nanoparticle to enhance regulatory T-cell populations *in vivo* by targeting DC. It was concluded that the CD11c pSiNP were capable of significantly increasing the number of splenic regulatory T-cells when compared to the control animals, which did not receive pSiNP. These two papers identify a novel strategy for promoting drug delivery to a scarce cell population and the ability to promote regulatory T-cell generation *in vivo* without *ex vivo* modification of DC, which is more commonly seen today. The results show promise for future development of an enhanced drug delivery method to modify the immune system.

DECLARATION

I certify that this work contains no material which has been accepted for the award of any other degree or diploma in any university or other tertiary institution and, to the best of my knowledge and belief, contains no material previously published or written by another person, except where due reference has been made in the text. In addition, I certify that no part of this work will, in the future, be used in a submission for any other degree or diploma in any university or other tertiary institution without the prior approval of the University of Adelaide and where applicable, any partner institution responsible for the joint-award of this degree. I give consent to this copy of my thesis when deposited in the University Library, being made available for loan and photocopying, subject to the provisions of the Copyright Act 1968. The author acknowledges that copyright of published works contained within this thesis resides with the copyright holder(s) of those works. I also give permission for the digital version of my thesis to be made available on the web, via the University's digital research repository, the Library catalogue and also through web search engines, unless permission has been granted by the University to restrict access for a period of time.

Sebastian O. Stead

December 2018

To my parents, Kym and Greg,
I dedicate this thesis.
If it wasn't for your care, support and love,
I would not be the person I am today.

ACKNOWLEDGEMENTS

I would like to thank my principal supervisor, Professor Toby Coates, who has been an amazing mentor to me for over the past 3 year. I am truly grateful for the time, enthusiasm, encouragement and intellectual expertise he has provided throughout my studies. During my time under his tutelage, Prof. Coates has provided me with many opportunities, developing my abilities as both a student and as a professional, which have helped me acquire priceless skills for my future. I'd also like to thank Prof. Coates for his wholehearted support with my goal to pursue graduate medicine after my PhD. I have learnt a lot from him with regards to doctor-patient interactions and the level of duty and expertise a doctor can provide, not just to his patients but also significant contributions in the field of medicine in Australia. I have no doubt that this insight will be endlessly useful during my time as a medical student and practicing doctor. I'd also like to thank my co-supervisor Dr. Robert Carroll for his continued assistance throughout my PhD. He has offered me a lot of useful feedback on data presentation which was endlessly useful, especially with the number of presentation I have performed throughout my studies. His method of presenting has become permanently integrated into my future presentation, offering me a lifelong skill that I am incredibly grateful for.

I want to thank my co-supervisor Professor Nico Voelcker, for supplying me with open use of his laboratory space and intellectual expertise, which contributed to a significant proportion of my research. Without his knowledge and skills, this project would not have been possible. I also want to thank Prof. Voelcker for providing me with his time and assistance consistently throughout my PhD and also his willingness to help with publication revision, especially on short notice. His help contributed significantly to my ability to write high level manuscripts and publish my data in high impact journals.

I would like to thank my co-supervisor, Dr. Steven McInnes, for his assistance, expertise and fundamental training with regards to manufacturing nanoparticles. This knowledge provided the crux of my research and a majority of my skills in chemistry have stemmed from discussion and meetings with him over the past 3 years. This knowledge has enriched my learning experience, providing me with an in-depth view and appreciation for the field of nanomedicine. I also want to thank Dr. Darling Rojas-Canales for her time and intellectual contributions to experimental design, during the crucial early stages. She set me on the right footing for the remaining years and offered helpful insight into being a PhD student.

Someone who I cannot go without thanking is Mrs. Svjetlana Kireta. She has been monumentally helpful during my PhD, teaching me the fundamentals of a majority of my research protocols. Not only that, Svjetlana has offered her assistance consistently throughout my research, especially with regards to the animals studies, which is a huge contribution to my work. There is no doubt, without Svjetlana's help and

expertise, this project would have been near impossible to carry out. I cannot thank her enough for all her help, support and time.

I also want to thank my good friends and colleagues, Ernesto Hurtado and Dr. Plinio Hurtado, who I have worked with throughout the entirety of my postgraduate studies. They have both provided a high level of support and intellectual discussion that has helped me significantly throughout, as well as provided the much needed fun that is often require when undertaking a PhD. I am incredibly grateful for the memories that we have developed over the years. I also want to thank my friends, Francis Kette and Juewan Kim, for their support over the years and also their assistance with some of my work.

In more than one occasion, all of those in the renal laboratory have helped me during my studies. I would like to thank our laboratory head, Mr. Christopher Drogemuller and the staff, Mrs. Julie Johnston, Ms. Daniella Penko, Dr. Kisha Sivanathan and Mrs. Jodie Nitschke. They helped me with many aspects of my work and without them it would not have gone as smoothly as it did. They all offered their time and expertise and I appreciated them all immensely for that.

I was fortunate to have received the Playford Trust Alumni Scholarship in conjunction with the Cell Therapy Manufacturing Cooperative Research Centre (CTM CRC). This extra financial support provided me with the opportunity to travel extensively to international conferences in Boston, Hong Kong and Oxford, as well as several interstate conferences, to share my research with experts from all over the world.

Lastly, I would like to thank my partner Maddison Archer. She has been with me from the beginning and has offered her constant support through both the ups and downs of my PhD, all whilst undertaking her own. Maddison also assisted with my research, offering her skills and knowledge. She is a remarkable person and I am grateful to have had such a strong and amazing support with me through this time in my life.

LITERATURE REVIEW

Introduction

In recent studies, exploring alternative methods facilitating the transport of chemotherapeutics, genetic material and immune modulators has sparked the interest of many scientists. This has given rise to the emerging field of nanomedicine, aimed at exploring the use of nanoparticles (NP) for a range of different applications. Nanoparticles offer a unique medium, as the can be composed of a range of different materials, benefiting a range of application due to their customisability in size, shape and surface modifications, termed functionalisation. The functionalisation of particles with peptides, antibodies or genomic fragments, allows for specific targeting and directed NP content release both *in vitro* and *in vivo*. This can provide beneficial therapy to cancer patients receiving conventional chemotherapy. It also offers the medical professional and alternative way to treat their patients. The production of NP which have the ability to home in and target cancer cells specifically, allowing for localised release of chemotherapeutic drugs, decreases the amount of toxic drugs that may otherwise be administered to the patient (1, 2). This would reduce damage to healthy tissue and organs, increasing the well-being and quality of life of the patient. Research has shown that NP loaded with immune modulators possess the ability to enhance or suppress the immune system (3-7). As chronic administration of immunosuppression can lead to opportunistic infections, reactivation of latent pathogens and the development of tumours (8-10), this treatment also has particular benefit to organ transplant recipients.

This review will explore some of the commonly studied nanoparticles and their applications in drug delivery, cancer therapy and imaging. There will be a focus on transplant immunotherapy and how nanoparticles could be used for the induction of immunological tolerance. Some of the current limitations that exist within the field of nanomedicine, which may represent current roadblocks for the translation of nanoparticles into more commonly used clinical settings will also be discussed.

Nanoparticles

Nanoparticles are defined as, ultra-fine, microscopic structures a billionth of a meter in size. *Liposomes* were the first identified composite for NP experimentation. First described as the cellular membrane in 1965 (11), liposomes have developed into a platform for gene and drug delivery. The particle can be composed of a mono- or bilayer structures of self-assembling lipids (12). Liposomes offer several advantages for NP therapy, including their ability to encapsulate molecules, their tuneable biodegradability and biocompatibility (13). Their unique characteristics make them suitable as transfection reagents, transferring genetic materials into cells, promoted by lipofection, which utilised charge interactions between the cationic lipids to aggregate with the anionic material (13). Liposomes have been used as carriers for therapeutics, as their composition allows seamless interaction with the cellular lipid bilayer (11). The hydrophilic core and hydrophobic shell also offers a unique surface for the entrapment of different drug compounds. NP can undergo surface modifications, which can enhance or promote new functions of the NP. Polyethylene glycol (PEG) is a commonly used compound due to its biocompatibility with liposomes. PEG can be used to extend the half-life and stability of liposomes *in vivo* (12). Currently, there are 15 liposome-drug based therapies approved for clinical use (14).

Polymeric NP are derived from biocompatible and biodegradable natural polymers and have been comprehensively investigated as carriers of therapeutics (15). Polymeric NP are composed by block copolymer controlled polymerisations. The process involves control NP chain extension with monomers which permits a multifunction, multi-composite nanoparticle product. Once the copolymer is formed, they undergo spontaneous assembly into a core-shell micelle structure within an aqueous environment (16). Some of the most commonly used natural polymers include: chitosan, gelatin and sodium alginate (17-19). However, polymeric NP often respond to changes in pH by decreased stability (20) and because of this, synthetic polymers have been developed to overcome this limitation. Poly(D, L-Lactide), poly(lactide-co-glycolide) (PLA) or poly(lactic acid) are among the most commonly used. Although capable of overcoming stability issues, they increase NP biotoxicity. Polymeric NP have been used for the encapsulation of hydrophilic and hydrophobic small drugs and proteins and nucleic acid macromolecules (21).

Incorporating targeting ligands on the NP surface have also shown to increase cellular uptake and enhanced therapeutic outcomes.

Dendrimers are a subset of polymeric NP, defined by the branching 'tree-like' chemical structure. Again, these particles can be comprised of both natural and synthetic monomers such as amino acids, sugars and nucleotide (22). The dendrimers have a unique core which is comprised of several branched interior layers. This unique structure allows for the modifications of NP shape, size and stability (23, 24). Dendrimer surface modification allow for applications within medical imaging via chemical functional group modification (25).

Albumin-bound NP, abraxan, is a 130 nm complex bound to chemotherapeutic paclitaxel. It was clinically approved in 2005 for the treatment of breast cancer (26). Albumin based NP therapies exploit the natural, non-covalent, reversible binding ability of albumin to hydrophobic molecules. This mechanism bypasses the solvent-based toxicity for certain therapeutics (27). The albumin coating on the drug offers a type of drug functionalisation, as endothelial cells will concentrate the drug via albimun binding protein (gp60)-mediated transport, as well as SPARC (albumin secreted protein acidic and rich in cysteine), which is overexpressed in some cancers (28).

Quantum dots (QD) are unique particles which demonstrate side-dependant optical properties. Usually comprised of cadmium selenide (CdSe) and zinc selenide (ZnSe) core and shell respectively, these NP emit bright colours within a narrow wavelength band upon excitation. This unique property, along with their decreased photobleaching, long half-life and efficiency, gives them a significant advantage for diagnostic use, over the conventionally used organic fluorescent dyes for optical imaging, cell labelling and biomolecule tracking (29-31).

Iron oxide NP have been extensively studied as imaging agents, exploiting their superparamagnetic characteristic. Superparamagnetic iron oxide NP (SPION) can be composed of an iron oxide core, most commonly magnetite (Fe_3O_4) coated with dextran, chitosan or alginate (32-34). SPION have been used with T2 weighted magnetic resonance (MR) as contrast agents due to the ability to manipulate the core size, offering a size-dependant magnetic field strength. SPION have been especially useful in the monitoring of atherosclerosis (35, 36). Conventionally, gadolinium-chelated contrast agents are used for

MRI imaging. Ferumoxide and ferucarbotran are two clinically approved SPION based MRI imaging reagents (37), which have shown reduced toxic side effects whilst also having increased image sensitivity and specificity (38). *In* vivo, SPION are metabolised to iron which can be stored as ferritin and aid with erythropoiesis (38). SPION have also been functionalised with targeting ligands, allowing them to be use for both passive and active imaging agents (39).

Gold NP can be modified to alter size, shape, optical and chemical properties, display biocompatibility and permit surface modification (33). Gold interacts uniquely with free electrons within molecules and because of this, gold NP can enhance light absorption, scattering and fluorescence (40). These unique characteristics allow gold NP to be used for biochemical sensing, imaging, diagnostics and therapeutic applications. Colourmetric arrays, used to identify toxic industrial chemicals and surface-enhanced Ramen spectroscopy (SERS), commonly used to identify low abundance biomolecules, can be significantly enhanced when used in conjunction with gold NP (41).

Mesoporous Silica NP (MSN) were first reported in 2001 as a material for drug delivery (42). MSN have textural properties that make them excellent drug carriers, as their loading capacity and surface area is greatly increased, further enhanced by surface pores. This property of MSN can also be controlled during the manufacturing process by altering the functionalization of silanol groups, altering drug diffusion kinetics (43, 44). MSN have been unitised in various imaging applications by loading the particles pore with quantum dots or fluorescent dyes (45, 46). Surface modifications of MSN have been explored as an active target mechanism. NP have been coated with cancer specific targeting drugs and have displayed increased cancer cytotoxicity compared to controls (47).

Porous Silicon NP (pSiNP) offer an alternative to the above. Elemental silicon can be electrochemically etched to produces particles of varying size, shape and porosity. pSiNP display larger surface area to size characteristic as well as the ability to chemically modify the surface. This allows for loading with a huge variety of drugs, macromolecules and genomic materials, giving the pSiNP a myriad of applications. pSiNP are also highly biodegradable to non-toxic silicic acid, which is renally excreted (48). A majority of current research exploring nanoparticles as an improved therapy, study their use within a cancer setting. The role that nanoparticles could play within the suppression of the immune system, prevention transplant

rejections, is highly underrepresented. The applications of these nanoparticles will be explored further in this review. A summary of some common nanoparticles and their use can be seen in table 1 and figure 1.

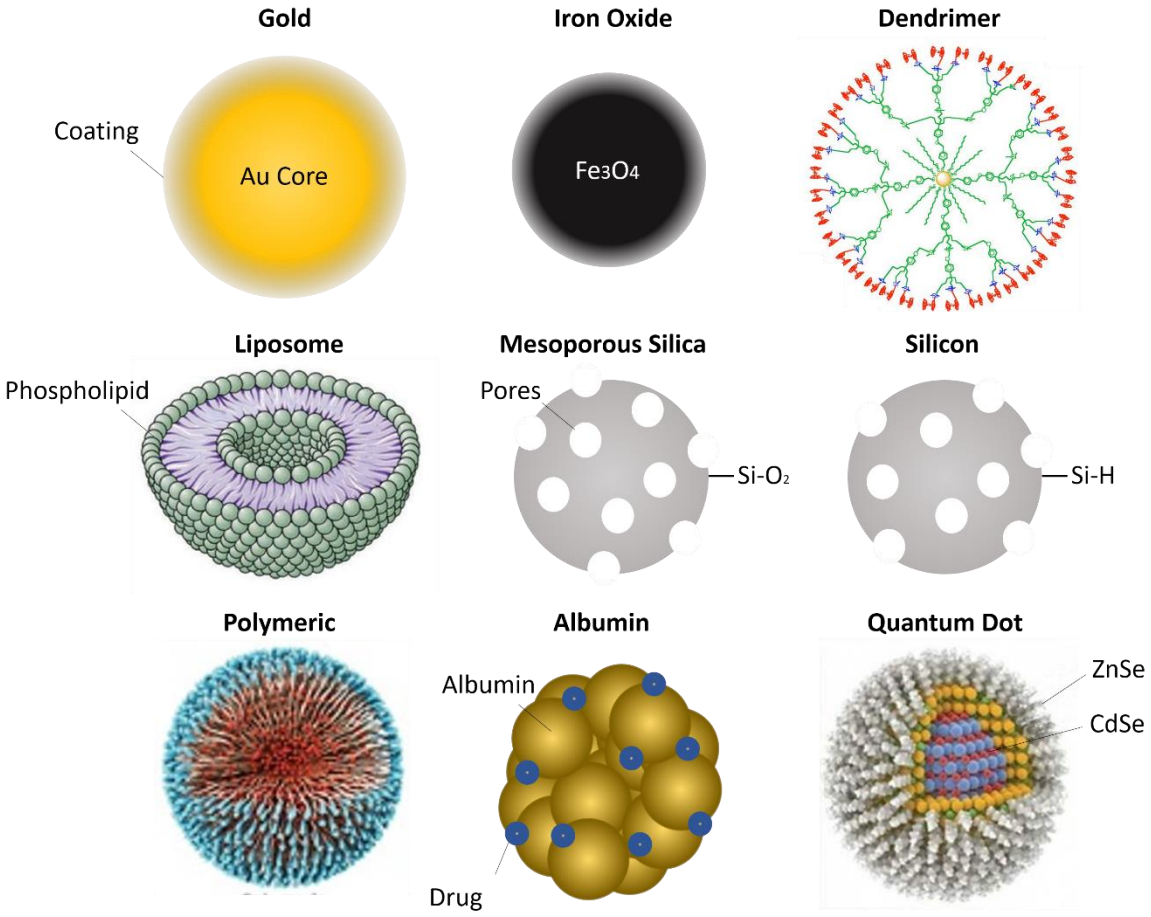

Figure 1. Cartoon depiction of the various nanoparticle compositions.

Table 1. Brief Summary of Nanoparticle Targets and Functionalisations

Nanoparticle	Functionalisation	Target/Use	Reference
liposomes	Amiloride hydrochloride	Cystic Fibrosis	(49)
	Budesonide	Asthma	(50)
	Doxorubicin + Verapamil	MDR-Leukaemia	(51)
	Insulin	Diabetes	(52)
	IL-2	Lung Cancer	(53)
	Irinotecan + Cisplatin	Small-Cell Lung Cancer	(54)
	Ketotifen	Asthma	(55)
	siRNA + Doxorubicin	MDR-Breast Cancer	(56)
	Tobramycin	Pulmonary Infections	(57)
	Vincrisine	Brain Cancer	(58)
	VEGF Gene	Pulmonary Hypertension	(59)
Albumin	Paclitaxel	Breast Cancer	(27)
Polymeric	RBITC	hAGP and hRGF	(60)
	Doxorubicin	ICAM-1	(61)
	Folate	HEC-1A Cancer Cells	(62)
	BSA	MCF-10A neo T-cells	(63)
Dendrimers	Boron	Neuron Capture Technology	(64)
	Doxorubicin	Colon Carcinoma	(65)
	Efavirenz	HIV	(66)
	Phosphorus	HIV-1	(67)
	Lamivudine	HIV	(68)
	siRNA	Lymphocytes	(69)
	G3. 5 PAMAM SN38	Hepatic Colorectal Cancer	(70)
	Sulphate Oligosaccharide	HIV	(71)
Iron Oxide	Lauric Acid SPION	Breast Cancer	(72)
	Maghemite	MRI	(73)
	Folic Acid	MRI	(74)
	EGF	Brain Tumour	(75)
	Poly-Dopamine	Stem Cells	(76)
Quantum Dots	5-Fluorouracil	Breast Cancer	(77)
	Doxorubicin	Ovarian Cancer	(78)
	Saquinavir	HIV-1	(79)
Gold	Methotrexate	Lung Cancer	(80)
	6-mercaptopurine	Leukaemia	(81)
	Tamoxifen-poly(ethylene glycol)-thiol	Breast Cancer	(82)
	Rhodamine 6G	Raman Imaging	(41)
Mesoporous Silica	Folic Acid	Pancreatic Cancer	(83)
	Camptothecin	Pancreatic Cancer	(83)
	Doxorubicin + Bcl-2 siRNA	HeLa Cells	(84)
	Galactose	Cancer	(85)
	γ-Secretase Inhibitor	Notch Therapy	(86)
	Polyethyleneimine	Cancer	(87)

Allo Immunity

Patients receiving allogeneic organs are required to take life-long immunosuppressive medications to prevent the development of graft versus host disease (GVHD) and organ rejection. The allo-immune response within a transplant patient is initiated by foreign antigens expressed on the donor organ or via passenger leukocytes. Without 'proper intervention', the immune system will begin to target the cells expressing foreign antigens, inevitably leading to decreased graft function and organ rejection. Patients require constant treatment to combat organ rejection and often necessitating secondary transplants, at immense cost on both a personal and financial level. Mechanistically, allo-immunity occurs when there is a genetic mismatch existing between the donor and patient genes, coding for the major histocompatibility complex (MHC) proteins (88).

There are two main forms of the MHC proteins relevant in transplantation, class I and class II (Figure 2). These proteins are responsible for the presentation of peptide fragments on the cell surface allowing for T-cells interaction. MHC class I can be further subdivided into human leukocyte antigens (HLA) A, B and C (89). HLAs are located on the short arm of chromosome 6, each parent providing a haplotype in Mendelian codominant inheritance to their progeny (90). HLA-A, B and C are expressed on all nucleated cells within the body and contain a polymorphic heavy α chain and non-polymorphic light β2 chain. Endogenous peptide fragments, approximately 9-11 amino acids, are expressed on HLA class I to cytotoxic $CD8^+$ T-lymphocytes (CTL). High affinity interactions with the T-cell receptor (TCR) expressed on CTL and the epitope within the MHC class I molecules trigger programmed death signals inducing apoptosis. This process is the initiation of cellular immunity and is the primary means that our body uses to combat intracellular pathogens such as bacteria and viruses (91). Cross presentation can also occur with $CD8^+$ T-cells. This is where extracellular antigen are presented on the surface of MHC class I proteins to naïve CTL. Strong TCR-MHC interactions added by costimulatory proteins CD28 on the T-cells and B7 receptors (CD80/CD86) on the antigen presenting cell (APC), lead to activation of the naïve CTL.

MHC class II can be subdivided into HLA-DR, DQ and DP and are primarily expressed on the surface of APC, such as macrophages, B cells and DC (90). Class II HLA contain both polymorphic α and β chains. Phagocytosis of extracellular debris, by APC undergoes processing and epitope presentation, usually between 12-28 amino acids. If strong interactions occur between the $CD4^+$ TCR receptors on naïve T-helper cells followed by co-stimulatory signalling by B7 and CD40 on APC interacting with CD28 and CD40L on T-cells, activation and clonal expansion of antigen specific $CD4^+$ lymphocyte will occur (92-94). The degree of HLA mismatch between donor and recipient is a determining factors of the degree of chronic organ rejection and graft loss (95). Traditionally, HLA A, B and DR are commonly typed and matched before kidney or pancreas transplants, with mismatches in HLA-DR being associated with poor patient-graft outcomes (96-98).

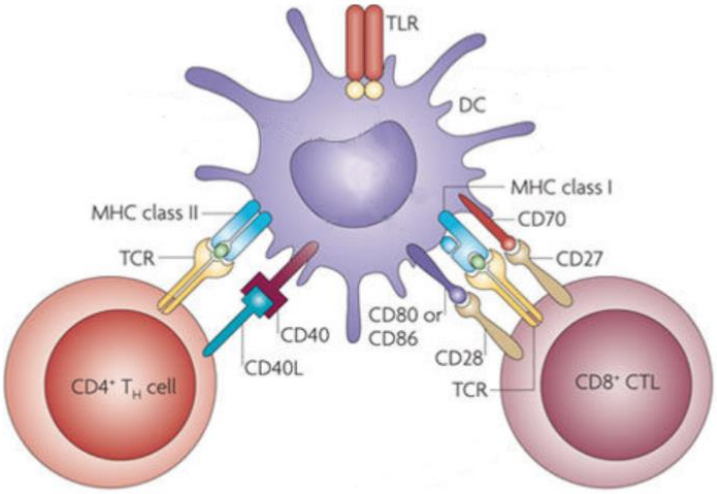

Figure 2. Dendritic cell (DC)– T-cell interaction. MHC Class I interacts with $CD8^+$ T-cells via the T-cell receptor (TCR) to present endogenous peptides leading to cytotoxic activation of the lymphocyte. MHC Class II is expressed on professional APC cells, presenting exogenous peptides to $CD4^+$ T-cell. Co-stimulatory markers CD40-CD40L provide signal 2 for complete lymphocyte activation. MHC Class I is expressed on all nucleated cells. Cytotoxic T-cells (CTL) interact with MHC Class I along with co-stimulatory markers CD80/CD86-CD28 promoting CTL activation and proliferation. Image adapted from Thaiss *et al.* (99)

In 1977 a review published by Lafferty *et al.* described the activation of allogeneic T-cells requiring three complimentary signals (100). More recent studies have expended on this hypothesis to identify some of the key mechanisms involved within the three signals. Signal one occurs during the interactions of the antigen presented on the MHC molecule to the TCR-CD3 complex. Signal two involves interactions between the costimulatory molecules. Several secondary signalling pathways have been described, however the best studied involves CD28-B7 and CD40L-CD40. Upon successful signals 1 and 2, the calcium-calcinurin, RAS-mitogen activated protein kinase and IKK-nuclear factor κB (NF-κB) pathways are activated. These pathways lead to the activation of transcription factors: nuclear factor of activated T-cells (NFAT), activation protein-1 (AP-1) and NF-κB respectively (101-103). T-cell also provide tertiary signals from secretion of IL-2 and IL-15 as well as upregulate CD25 (IL-2R) and CD40L (104-106), augmenting the cytokine environment around the interacting cells (107, 108) (Figure 3). IL-2 and IL-15 provide growth signals to the T-cells and NK cells via the mammalian target of rapamycin (mTOR), triggering T-cell cycle and proliferation (109, 110) . The T-cells will undergo clonal expansion coinciding with a burst of IL-2 release, promoting effector T-cell and $CD8^+$ T-cell mediated cytotoxicity.

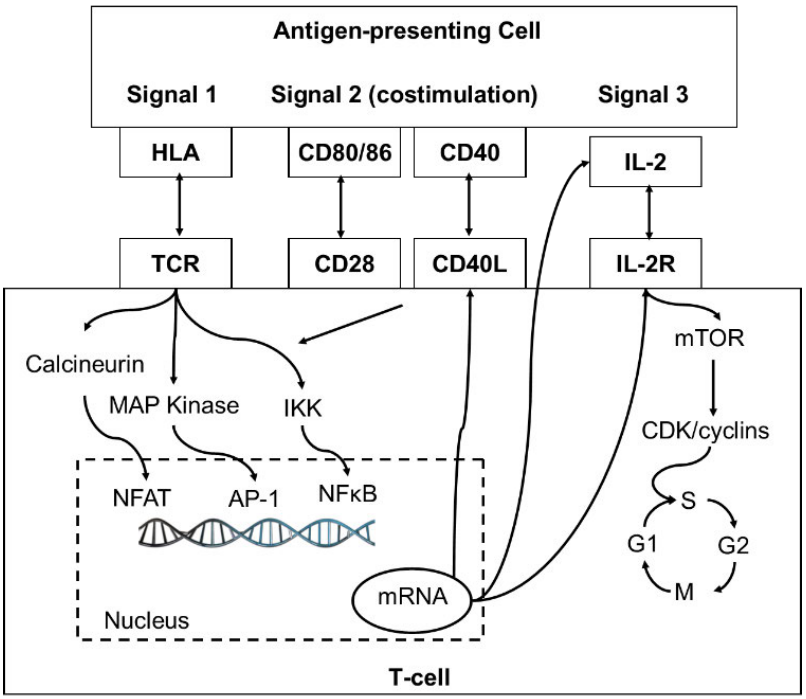

Figure 3. Three signals required for T-lymphocyte activations, leads to intracellular cascades activating transcription factors NFAT, AP-1 and NF-κB. Cytokine signalling via IL-2 activates mTOR pathway, leading to cell cycling and cell proliferation.

T-cell also respond to negative signals to decrease cellular activity. Program death ligands (PD-L), are transmembrane proteins part of the B7 receptor superfamily, expressed on APC and are responsible for immune system suppression. Two major types of PD-L exist, PD-L1 and PD-L2, which are capable of binding to receptor programmed cell death 1 (PD-1); on the surface of T- and B-cells. Activation of PD-1 inhibits T-cell proliferation, by inhibiting ζ-chain associated protein kinase 70 (ZAP-70) phosphorylation and T-cell surface glycoprotein CD3ζ reducing T-cell receptor (TCR) mediated activation. (111). This results in downstream inactivation of transcription factors NF-κB and AP-1 via decrease phosphorylation of protein kinase C theta's (PKC-θ) activation loop (112) (Figure 4).

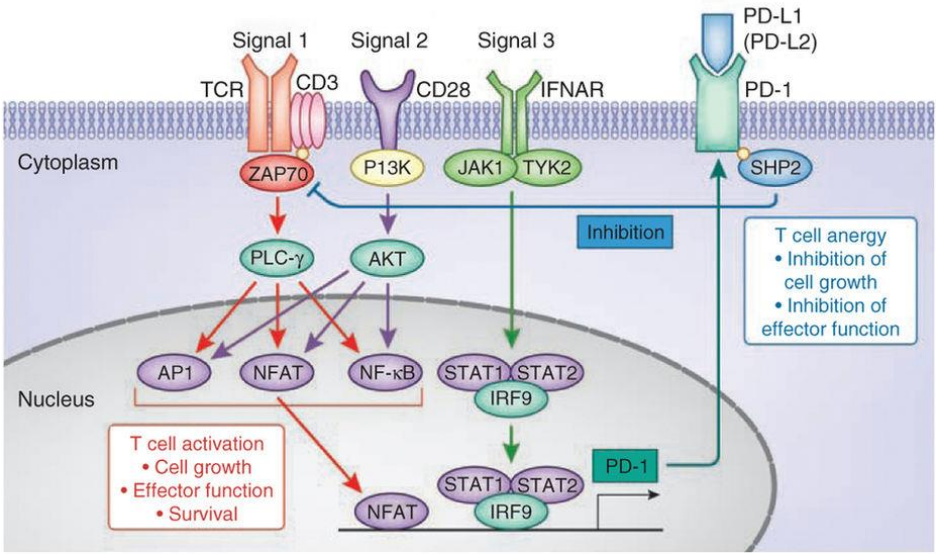

Figure 4. Programmed cell death (PD)-1 expression on T-lymphocytes inhibits T-cell receptor (TCR) signalling via tyrosine phosphatase, SHP-2. PD-1 activation by its ligands, PD-L1 or PD-L2, recruit SHP-2, promoting dephosphorylation of Zeta-chain-associated protein kinase 70 (Zap70). Zap70 dephosphorylation inhibits T-cell activation via CD3 (signal 1), preventing complete lymphocyte activation. Image is adapted from Okazaki *et al.* (113)

High affinity docking to the epitope presented on MHC class II molecules expressed on the APC resulting in the priming of the naïve T-helper cells, results in differentiation of the T-helper cells into several different subsets, including: memory T-cells, effector T-cells and T-regulatory cells (T_{regs}). The determinant for the differentiated subset is governed by the degree of co-stimulation and balance of cytokines expressed at those loci (114). Each population of $CD4^+$ T-helper cells have a unique set of functions, which will be discussed below.

Central memory T-cells are $CD45RO^+$ and expressed C-C chemokine receptor type 7 (CCR7) and CD62L, responsible for extravasation and migration to secondary lymphoid organs. The role of a memory T-cell is to respond to their cognate antigen upon repeat exposure. When exposed to their specific antigen, memory T-cells upregulate CD40L to a greater extent, resulting in more efficient activation of B-cells and DC and secretion of large quantities of IL-2 (115, 116).

Effector T-helper cells can differentiate into three main subtypes, T_h1, T_h2 and T_h17 (117). T_h1 cells are part of the cell mediated immunity and provide defence against intracellular micro-organisms, particularly in resistance to mycobacterial infections. The cytokine products of T_h1 cells are IL-2, lymphotoxin α (LTα) and Interferon γ (IFN-γ) (118). IFN-γ secreted by these cells plays a role in activating macrophages increasing microbicide activity and IL-2 is important for the establishment of $CD4^+$ T-cell memory and stimulation of cytotoxic $CD8^+$ T-cell proliferation.

T_h2 cells contribute to humoral immunity, protecting us against extracellular pathogens. Secretions from these cells include IL-4, IL-5, IL-9, IL-10, IL-13, IL-25 and amphiregulin. IL-4 contributes to the positive feedback for T_h2 cell differentiation and class switching in B cells (119, 120). Activated B-cells that interact with Th2 cells via CD40L or particular cytokines, such as IL-4, promote immunoglobulin (Ig) switching to produce IgG, IgE and IgA antibodies. IgE are more prominent within a hypersensitivity type I reactions (121). IgE production by B-cells, promotes the antibody uptake by high-affinity IgE receptor, FcεRI, on basophils and mast cells. Upon FcεRI cross-linking, the cells will degranulation, resulting in the secretion of histamine, serotonin, IL-4, IL-13 and tumour necrosis factor α (TNF-α) resulting in an inflammatory response. IL-5 secretions from T_h2 cells are important for the recruitment of eosinophil granulocytes (122).

IL-10 plays a role in suppressing T_h1 cell proliferation and has been shown to suppress the function of dendritic cells (123).

T_h17 plays an important role in the recruitment of neutrophils and macrophages to infected tissue, mediating a pro-inflammatory response. This cell subset secrets IL-17 which binds receptor IL-17 receptor A (IL-17RA), a receptor widely expressed on mesenchymal cells, such as endothelial cells, epithelial cells and fibroblasts (124). The binding of IL-17 activates transcription factor NF-κB and mitogen-activated protein kinase (MAPK) pathways (125, 126). A summary of the T-helper cells can be seen in figure 5.

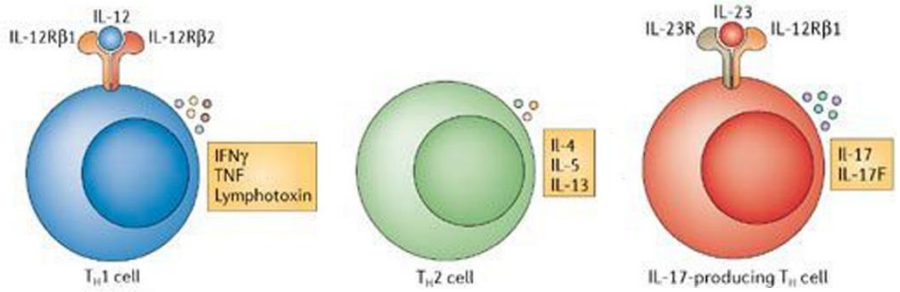

Figure 5. T-helper cell differentiation from $CD4^+$ naïve T-cells. $CD4^+$ T-cell activation by an APC with the addition of co-stimulation through CD28 and/or cytokines can lead to the differentiation into three main subsets of T-helper cells, T_h1, T_h2 and T_h17. T_h1 cells are major secretors of INF-γ, T_h2 mainly secrete IL-4 and IL-5 and T_h17 respond to IL-23 and secrete IL-17 cytokines. Image adapted from Dong *et al.(127)*.

Allo-recognition - Transplant rejection

Within a transplant setting, a patient can become sensitise to the donor HLA antigens, contributing to organ rejection. There are two main mechanisms by which this occurs, the direct and indirect pathways. The direct pathway involves the donor APC interacting directly with the recipients T-cells, whereas the indirect pathway is when the recipient APC presents an allo-peptide to a recipient T-cells (Figure 6). Activation via the direct pathway is clinically very important immediately post-transplant. If appropriate immunosuppression is not provided, a potent allo-response would follow resulting in acute cellular rejection. The indirect pathway is more responsible for the delayed immune reaction. Discrete populations

of effector T-cells and T-helper cells promote immunoglobulin class switching, memory B-cell and plasma cell production, leading to the development of the humoral immunity and production of donor specific antibodies (DSA) directed towards donor HLA.

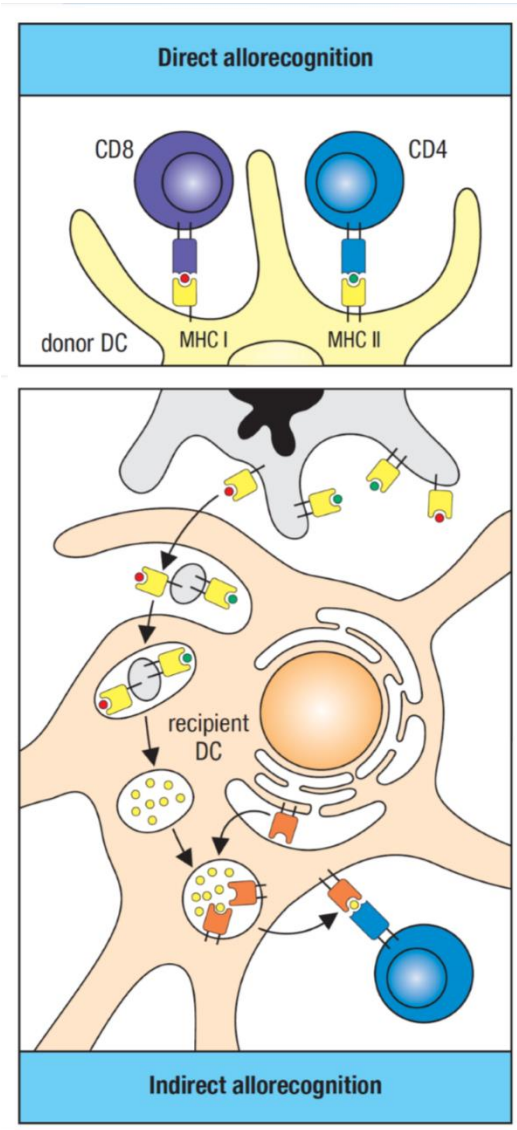

Figure 6. Direct and indirect pathways of allorecognition which contribute to allogeneic graft rejection. The direct pathway involves interactions of donor DC with recipient $CD4^+$ and $CD8^+$ T-cells. Indirect allorecognition is the processing and presentation of donor MHC via recipient APC. Image is adapted from Janeway's immunobiology (121).

Dendritic Cells – The Professional APC

Within humans, there are three major DC population lineages, myeloid, plasmacytoid and monocyte-related (128). Myeloid dendritic cells originate from $CD34^+$ myeloid haematopoietic stem cells within the bone marrow. These cells can differentiate into two lineages; $CD14^+$ $CD11c^+$ monocytes (129) and lineage negative (LIN^{neg}) $CD11c^-$ $IL3R\alpha^+$ precursor DC (130). Exposure to IL-2, IL-4 and granulocyte/macrophage colony stimulating factor (GM-CFS) induces the differentiation of the monocytes into immature DC (131). Dendritic cells are very rare, making up only 0.6-1.7% of the peripheral blood mononuclear cells (PBMC) within a human (132). Due to their rarity, DC are obtained by culturing monocytes with GM-CSF and IL-4 for *in vitro* and *in vivo* experimentation. The exact concentration of these cytokines vary within different laboratory centres and because of this the monocyte derive iDC can have a variances in levels of surface molecule expression. The consensus is that iDC have low expression of costimulatory markers CD40, CD80, CD86 and CD83 with high expression of MHC class II molecules. Human monocyte derived and

myeloid DC lineages express a unique receptor Dendritic Cell-Specific Intercellular adhesion molecule-3-Grabbing Non-integrin (DC-SIGN, CD209). DC-SIGN has been studied mainly because it is the binding receptor of both Hepatitis C and human immunodeficiency virus (HIV) (133-135). However, because of its unique expression it provides an optimal target for DC specific therapy. CD11c is another uniquely and highly expressed surface receptor found on dendritic cells, fitting the criterial as an alternative targeted for nanoparticle tracking, especially within a murine model. Mice possess several different DC subtypes within the myeloid and plasmacytoid lineages. The CD11c integrin, alpha X (ITGAX)$^{+}$, is expressed primarily on the murine conventional DC lineages, CD11c (High) CD4^{+} CD8a^{-}, CD4^{-} CD8a^{+} and CD4^{-} CD8a^{-} DC subsets (136). Murine CD11c offers a more analogous targeting receptor to human DC-SIGN compared to murine DC-SIGN. Comparatively, murine DC-SIGN in expressed on only the CD4^{+} and double negative myeloid DC lineages as well as plasmacytoid pre-DC (137), whereas murine CD11c is expressed on all the myeloid DC subsets and not plasmacytoid DC, similar to human DC-SIGN. Exploring the difference of nanoparticles targeting both CD11c and DC-SIGN could be highly beneficial in identifying an optimal receptor for myeloid DC uptake of nanocarriers for localised drug delivery.

Differentiation of monocytes into immature DC causes migration of the DC into the blood and to lymphoid tissue where they begin to phagocytose debris from apoptotic cells and present their antigens to T-cells. During a bacterial infection or the damaging of tissue due to transplantations, inflammatory mediators, such as lipopolysaccharides (LPS) or TNF-α respectively, are released. These mediators then act on immature DC to induce maturation into mature DC (mDCs).

Mature DC express high levels of co-stimulatory markers CD40, CD80 and CD86 as well as adhesion molecules ICAM1 (CD54) and CD58 and CCR7 chemokine receptor (92-94). Mature DC have decreased endocytic and phagocytic abilities and possess high levels of MHC II, increasing their antigen processing and presenting capacity. The phenotype of an mDC allows them to interact and activate naïve and memory CD4^{+} and CD8^{+} T-cells, mounting an immune response that can target specific pathogens or initiate allograft rejection.

Plasmacytoid DC (pDC) are among another subset of DC, characterised by lineage negative MHC II^{+} CD303 (BDCA-2)$^{+}$ surface expression. In an immature state, pDC are tolerogenic, where upon activation

can be either stimulatory or suppressive, which is dependent on the localised cytokine environment. pDC are known for their ability to secrete large amounts of Type I interferons (IFNs)-α and IFN-β, especially in response to viral infections.

Dendritic Cell Therapy for Cancer

As DC are capable of mounting an immune response directed towards single antigens, they have been explored as a novel form of cancer therapeutically termed, DC vaccines. Matured, HLA-A2 binding MUC1 pulsed human monocyte derived DC were used in a phase I trails in patients with metastiatic renal cell carcimona (RCC) (138). The aim was to use autologous matured DC to stimulate $CD4^+$ lymphocyte activation, reversing immune system senescence which is offen associated with cancer. During trials a group of patients receiving subcutanious injections of DC combanatorially with low-dose IL-2 demonstated tumour regression whilst also capable of producing a MUC1 peptide-specific T-cell response. Phase I/II trials were conducted using using Wilms' tumor1 protein (WT1) preconditioned DC as a cancer vaccine in individuals with acute myeloid leukaemia. DC administration was shown to induce complete remission in several patients who were in partial remission after chemotherapy (139). Furthermore, WT1 specific IFN-γ secreting $CD8^+$ T-cells were observed in vaccinated patients. The fussion of multiple myeloma (MM) cells to DC was also investigated as a novel cancer vaccine in patients who had received autologous stem cell transplantation (ASCT) treatement. A majority of the patients receiving the vaccine responded well to the treatement, with a reduction in their disease whilst also displaying both $CD4^+$ and $CD8^+$ myelma specific T-cell responses after ASCT (140).

Dendritic Cells and the Induction of Tolerance

Without DC-T-cell co-stimulatory interactions there is insufficient stimulation to activate T-cells but instead T-cell anergy is induced (114). DC which lack the necessary co-stimulatory molecules required for complete lymphocyte activation, not only have the ability to induce T-cell anergy but also promote the production of regulatory T-cells. Induced Treg (iT_{regs}), differentiate in peripheral lymphoid tissues under tolerogenic conditions (141). The *in vivo* expansion of this cell type, utilising *ex vivo* modified DC has

been explored within several studies and clinical trials, in order to promote immunological tolerance within transplant recipients.

The important role dendritic cells play within immune system was first recognised by Steinman *et al.* in 1983 but remarkable advances into the study of DC and their ability to induce tolerance were not thoroughly explored until the beginning of the 21st century (142, 143). The most common method for the production of tol-DC is culturing phenotypically immature DC with IL-10, TGFβ, hepatocyte growth factor and vasoactive intestinal peptide. Under these conditions the cells express low levels of MHC complexes, limited co-stimulatory molecules and decreased pro-inflammatory cytokines, allowing them to induce T-cell apoptosis and anergy (144).

DC have shown promising abilities to prevent allograft rejection. Morelli *et al.* and Wang *et al.*, (145, 146) experimented with intravenously infusing early apoptotic donor splenocytes in quiescent, prospective murine heart allograft recipients a week prior to transplantation and showed prolonged graft survival. Combining this treatment with a single, simultaneous injection of anti-CD40L monoclonal antibodies (mAb), indefinitely prolonged graft survival. A more recent study by Jian *et al.*, investigated the use of long non-coding RNA induced tol-DC to significantly prolong heart allograft survival. This study highlights the potential benefit of utilising genomic material as a method for tolerance induction (147). Tol-DC generated from vitamin D3 and IL-10 have been intravenously infused into rhesus macaque kidney allograft models. Preliminary DC infusions, concurrently with B7-CD28 co-stimulation locker (CTLA4Ig), demonstrated increase graft survival by approximately 3-fold whilst also regulating donor reacting memory CD95^{+} T-cells (148). The European consortium, the ONE Study is currently evaluating the safety and plausibility of cell therapy using autologous Tol-DC in living-donor kidney transplantation by phase I/II clinical trial (149). In 2016, Thomson *et al.*, proposed to perform phase I/II safety studies exploring the effects of donor-derived tol-DC in combination with conventional immunosuppression on kidney rejection (150).

Rapamycin

A common and well-studied immunosuppressive medication used for the prevention of organ rejection is rapamycin (Sirolimus). Rapamycin is a macrocyclic lactone product of *Streptomyces hygroscopicus* that causes disruption of the mammalian target of rapamycin (mTOR) pathway, inhibiting interleukin-2 (IL-2) signalling, suppressing B and T-cell activation (47, 151-154). Rapamycin is a potent inducer of tolerance in dendritic cells (DC), one of the most important immune cells with our body. DC possess the dichotomous function of immunostimulation and immunosuppression. They are the most potent of our antigen presenting cells (APC) (155) and are the key contributors to the development of graft versus host disease (GVHD), due to their specialised ability to process and present foreign peptides to T-cells. However, preconditioning DC with rapamycin, producing tolerogenic DC (tol-DC), promotes T-cell anergy and immunological tolerance (156-158). The ability to produce a functionalised NP, modified to express DC targeting antibody and secrete rapamycin, would provide a strong basis for the use of nanoparticles as a novel immunosuppressive therapy. *In* vivo, this could lead to prevention of allograft rejection in those who receive genetically mismatched donor organs and alleviate the necessity for chronic, systemic immune system suppression. Combining the interchangeable surface molecules and the ability to load a variety of drug cocktails or peptides, the use of nanoparticles for the treatment of multiple diseases is highly possible.

Although there are several compounds capable of inducing tol-DC, including vitamin D3, aspirin and even semen, rapamycin is of great interest because of its clinical relevance within the transplantation sector (159-161). Rapamycin is an immunophilin ligand and a macrocyclic-triene antibiotic produced by *Streptomyces hygroscopicus,* first described by Sehgal *et al. (152),* extracted from the mycelium within fungus identified on Easter Island. The drug binds the immunophilin FKBP-12 and acts as an inhibitor of RAPTOR-bound mTOR, preventing serine/threonine kinase autophosphorylation (162). mTOR inhibition causes the cell cycle to arrest at G1 and S phases and temporary inhibition of 4E-BP1, preventing growth factor driven proliferation of T-cells and other haematopoietic and non-haematopoietic cells and suppressed mRNA translation, effecting both secondary and tertiary signalling of T-cell activation (163, 164) (figure 7).

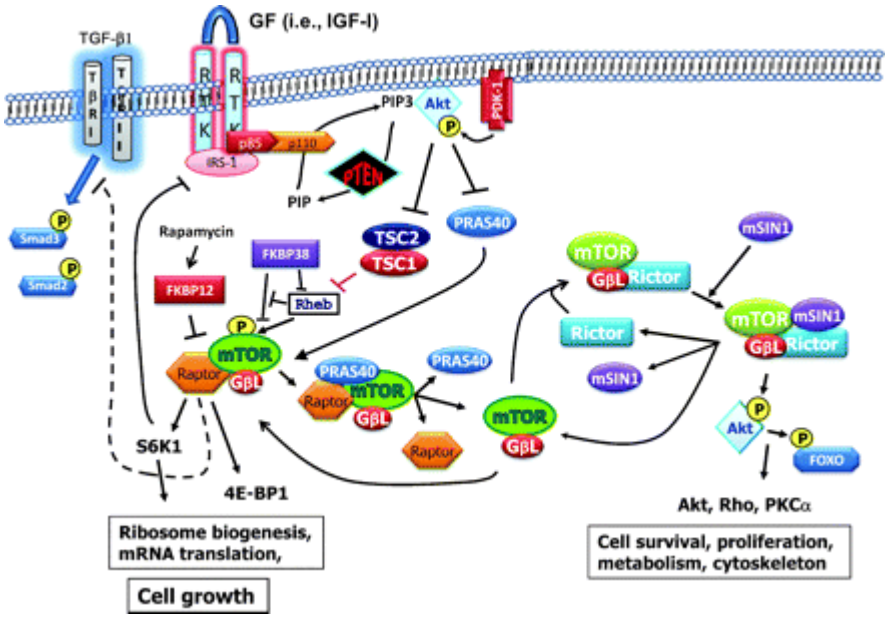

Figure 7. Rapamycin bind FKPB12, inhibiting mTOR1 and downstream activation of 4E-BP1 and S6K1. Rapamycin initiates cell cycle to arrest at G1 and S phases and the suppression of mRNA synthesis. Image is adapted from Garcia *et al.* (165)

Animal studies performed by Molano *et al.* on non-obese diabetic (NOD) mice receiving allogenic islet grafts and treated with rapamycin post transplantation, showed that rapamycin was able to prevent rejection and auto-immunity and hence prolong graft survival and insulin independence (166). It was reported by Toso *et al.* that converting from a cyclosporine-mycophenolate (MMF) combination to the Edmonton immunosuppressant regimen (Sirolimus and Tacrolimus), was highly beneficial to patients with borderline islet graft function (167). The extensive use of rapamycin has sparked debate over its efficacy and safety (168).

The detrimental effects of rapamycin have been well documents within pancreatic islet transplant settings. Pancreatic β-cell viability (169), glucose stimulate insulin release, pancreatic and duodenal homeobox 1 (PDX-1) and glucose transporter 2 (GLUT2) gene expression (170) were seen to decrease *in vitro*, when cultured with rapamycin. *In vivo*, rapamycin has been seen to impede islet cell engraftment and β-cell function (170, 171). Islet transplant animal models on rapamycin or rapamycin-tacrolimus combinatorial regimens demonstrated counterproductive effects, leading to the development of insulinemia, ergo hyperglycaemia within the animals. These results demonstrate that rapamycin has an effect on insulin

secretion pathways or can induce insulin hyporesponsiveness (172, 173). Studies have contradictory observations regarding the effects of rapamycin on β-cells function. This is most likely attributed to interspecific variation in animal models resulting in physiologically different responses to rapamycin treatments (174). Detrimental effects of rapamycin within humans have also been reported, however less extensively, in human islet cultures (175, 176). Studies which have demonstrated deleterious effects due to rapamycin, utilise extremely high concentrations, between 10-50 times higher than the clinically relevant dosage (175, 177-179). Studies by Laugharne et al., Zhang et al. and Bussiere et al., performed on rodent models have challenged the view of rapamycin's deleterious effects (169-171).

Rapamycin is not only a favourable immunosuppressant because of its ability to induce tolerance and drive T-cell anergy but compared to other immunosuppressants, rapamycin is not a calcinurin inhibitor, therefore it does not inhibit IL-2 transcription and secretion but instead the signalling effect IL-2 has on the cells. Rapamycin and its effect within transplant recipients has been extensively studied and well document and is regarded by many physicians as a favourable immunosuppressive medication, in combination with other drugs.

Tol-DC have been used to show prolonged graft survival in C3H/HeJ mice receiving a heart allograft (180). Dendritic cells were isolated from mouse bone marrow and treated with 10ng/ml of rapamycin, inducing their differentiation into tol-DC. Phenotypic analysis of rapamycin treated DC (Rapa-DC) showed resistance to maturation with lipopolysaccharide (LPS). Rapa-DC also demonstrated decreased co-stimulatory marker expression (CD80 and CD86) and MHC class II molecule as well as the ability to inhibit IL-2 and IFN-γ secretion from $CD4^+$ and $CD8^+$ T-cell respectively, when co-cultured at a ratio of 1:10 (Rapa-DC:T-cells). Taner *et al.*, showed that pulsing the Rapa-DC with allo-antigens prior to intravenous transfer into C3H heart graft recipients 7 days before receiving the transplant, graft survival could be prolonged significantly. Additionally, repetitive infusion with allo-antigen pulsed Rapa-DCs lead to indefinite graft survival (>100 days) in 40% of graft recipients.

Nanoparticle Therapy

Nanoparticle use within medicine has become a rapidly increasing research area which explores applications including imaging (181, 182), vaccination (183, 184), biomolecule detection (185) and drug delivery (186, 187). The ability to construct nanoparticles using different materials and fabrication techniques, permitting changes in pore size, shape, coating and overall dimensions, allows these particles to develop diverse functions, this allows them to be considered for use in a variety of fields.

The use of silicon for the manufacture of porous silicon nanoparticles (pSiNP) is a favourable element as its effect on cells has been well documented. As silicon is a trace element within humans and its degradation product is silicic acid, it poses no harmful effects *in* vitro or *in vivo* (188). The potential use of porous silicon nanoparticles for *in* vivo use was first published in 2009 by Park *et al*. The study showed biodegradability, low *in vivo* toxicity and homing of pSiNP when administered intravenously. It was shown that the particles accumulated within mononuclear phagocyte system (MPS) related organs, degrade within a few days and non-toxic by-products were removed via renal clearance, concluding that these particles have great potential for use in drug loading and delivery *in vivo.*

In terms of scientific progression, research into the drug loading of porous silicon nanoparticles is still in its infancy. The concept of loading a drug into a pSiNP is quite simple to grasp, unfortunately many potential problems can arise. Polarity of the drug is one of the major issues when it comes to loading. Identifying solutions which allow for the drug to be dissolved without affecting the structural integrity of the nanoparticle or altering its half-life and surface chemistry can be problematic. Once within the particles, selecting nanoparticles which show the desired characteristic (particle geometry and pore size) for optimal drug diffusion rate can be a laborious process. Manufacturing nanoparticles with surface antibodies for cell targeting can lead to issues with binding, degradation and specificity of targeting antibody, which need to be overcome.

In 2012, Gu *et al.,* identified the use of a porous silicon nanoparticle functionalised with agonistic antibody FGK45, used to target the CD40 receptor on APC (189). The nanoparticles were able to enhance the immune system via activation of antigen presenting cells. Their study showed that pSiNP functionalised with FGK45 were more readily taken up by APC compared to the unfunctionalised NP. Exposing APC to FGK45-pSiNP lead to a significantly enhanced response in B-cell activation. Furthermore, it was shown that the FGK45-pSiNP had a substantially higher activation potency than free FGK45 which required concentrations of 30-40 fold higher to produce the same level of B-cell activation. This experiment highlighted the importance of multivalency which is a significant advantage and feature of functionalised nanoparticles.

Secret *et al.,* (190) explored the use of functionalised porous silicon NP coated with several different cancer cell targeting antibodies and loaded with camptothecin. The study showed that the pSiNP were efficiently taken in by neuroblastoma cancer cells which express the corresponding receptor and release of camptothecin was significant to induce cancer cell death. Furthermore, they showed that pSiNP which were not functionalised were not absorbed by the cancer cells. These experiments confirmed the importance and specificity functionalisation can have, especially when the nanoparticles are loaded with potentially toxic chemotherapeutics.

The dichotomous function of DC and their remarkable plasticity makes them a prime target for use in non-conventional immunosuppressive therapy. A majority of the therapy currently explored involves *in vitro* manipulation of DC and infusion prior to transplantation or chronic, systemic immunosuppression administration, which can have detrimental effects, directed towards the patients lymphocytes. Utilising nanoparticles which are loaded with immuno-modulators and manufactured to target DC could permit *in vivo* manipulation of DC, as the NP will be infused directly into the recipient, and prevent the necessity for systemic immunosuppression as they will have targeted release directly affecting the cells of interest.

Finally, Maldonado *et al.,* (187) studied the use of biodegradable poly(lactide-co-glycan) (PLGA) nanoparticles which were loaded with rapamycin and ovalbumin (OVA) peptide or protein. The study explored the potential to induce immunological tolerance in Swiss Jack Lambert (SJL) mice which received OVA specific $CD4^+$ T-cells and immunised subcutaneously with $OVA_{323-339}$ admixed with TLR7/8 agonist.

It was observed that NP loaded with rapamycin and the OVA peptide could completely abrogate the proliferation of OVA specific $CD4^+$ T-cells as well as increase the number of $FoxP3^+$ T-regulatory cells. The studies also showed that they were capable of inducing B-cell tolerance, for at least 200 days, in mice that received the same nanoparticles. Interestingly, in order to induce tolerance, the nanoparticles needed to be loaded with both rapamycin and OVA. Free rapamycin or nanoparticles loaded with rapamycin only were unable to significantly decrease T-cell proliferation. Unfortunately this study did not assess the effect the nanoparticles had on dendritic cells but more the ability of NP to induces antigen specific T-cell tolerance and the humoral immune response. Therefore, the fate of these nanoparticles *in vivo* is a major gap in the knowledge. The nanoparticles may be directly acting on circulating T-cells or, more likely, track to the spleen, where they are taken in by dendritic cells. The rapamycin payload would then be released and this would promote the differentiation of immature DC into tolerogenic DC. Then with subsequent challenges with OVA, the protein would be processed and presented by the APC to OVA specific T-cells, promoting both T-cell anergy and $CD4^+$ Treg differentiation.

Conclusion

Exploring the work of targeted nanoparticles offers opportunity to develop a nanoparticle which has the ability to specifically target key immune cells to suppress the immune system. Loading a nanoparticle with rapamycin and peptides has the ability to induce the differentiation of immature dendritic cells into tol-DC and suppress antigen specific T-cells. Furthermore, as DC are an extremely rare cell population, exploring the functionalisation of nanoparticles with DC-SIGN, allowing them to specifically target DC may permit a localised release of their payload. This would provide an effective means for delivering immunosuppressive medications at concentrations significantly lower than currently implemented, preventing the need for chronic immunosuppression and hence lowering the detrimental side effects these medications have on patients.

Thesis Hypotheses

This thesis aims to develop on work carried out by Maldonado *et al.* (187), exploring nanoparticle mediated manipulation of the immune system, with a specific focus on dendritic cell (DC) induction of tolerance. Utilising a dendritic cell targeting, porous silicon nanoparticle, loaded with immunosuppressant, rapamycin we hypothesize:

1. DC will favour differentiation into a maturation resistant, tolerogenic state.
2. Furthermore, we expect these DC to elicit the differentiation of naive $CD4^+$ T-cells into suppressive, regulatory T-cells.

This thesis explores four main aims:

1. To develop DC targeting, porous silicon nanoparticles.
2. To show an enhanced targeting ability to DC compared to non-targeting nanoparticles.
3. To induce maturation resistant phenotype and function within DC preconditioned with rapamycin loaded nanoparticles and
4. To promote regulatory T-cell generation *in vivo* with rapamycin loaded nanoparticles.

STATEMENT OF AUTHORSHIP 1

Title of Paper	Manipulating human dendritic cell phenotype and function with targeted porous silicon nanoparticles
Publication Status	Published
Publication Details	Biomaterials – Elsevier Impact Factor 8.402 (2016) Accepted 16 November 2017

Principal Author

Name of Principal Author (Candidate)	Sebastian O. Stead		
Contribution to the Paper	Data analysis Project design Laboratory work Protocol optimisation		
Overall percentage (%)	75%		
Certification:	This paper reports on original research I conducted during the period of my Higher Degree by research candidature and is not subject to any obligations or contractual agreements with a third party that would constrain its inclusion in this thesis. I am the primary author of this paper		
Signature		Date	January 2018

Co-Author Contributions

Name of Co-Author	Steven J.P. McInnes		
Contribution to the Paper	Manufacture of nanoparticles training Assisted with particle degradation, functionalisation, IR spectrometry and Scanning electron microscopy		
Signature		Date	January 2018

Name of Co-Author	Svjetlana Kireta		
Contribution to the Paper	Responsible for training for DC and nanoparticle culture. Multi-colour flow cytometry training Responsible for data repeats in figure 1		
Signature		Date	January 2018

Name of Co-Author	Peter D. Rose		
Contribution to the Paper	Responsible for data in figure 1 and fundamental optimisation as part of honours project in 2014		
Signature		Date	January 2018

Name of Co-Author	Shilpanjali Jesudason		
Contribution to the Paper	Principal supervisor of Peter Rose and responsible for initial experimental design later continued by Prof. Toby Coates		
Signature		Date	January 2018

Name of Co-Author	Darling Rojas-Canales		
Contribution to the Paper	Intellectual contribution		
Signature		Date	January 2018

Name of Co-Author	David Warther		
Contribution to the Paper	Developer of functionalising chemical linker		
Signature		Date	January 2018

Name of Co-Author	Frederique Cunin		
Contribution to the Paper	Developer of functionalising chemical linker		
Signature		Date	January 2018

Name of Co-Author	Jean-Olivier Durand		
Contribution to the Paper	Developer of functionalising chemical linker		
Signature		Date	January 2018

Name of Co-Author	Christopher J. Drogemuller		
Contribution to the Paper	Intellectual contribution Assistance with data analysis		
Signature		Date	January 2018

Name of Co-Author	Robert P. Carroll		
Contribution to the Paper	Co-supervisor. Intellectual contribution. Assistance with data analysis.		
Signature		Date	January 2018

Name of Co-Author	P. Toby Coates		
Contribution to the Paper	Principal supervisor. Responsible for project funding. Intellectual contribution. Assistance with data analysis.		
Signature		Date	January 2018

Name of Co-Author	Nicolas H. Voelcker		
Contribution to the Paper	Co-supervisor. Provided laboratory space for nanoparticle manufacture Provided expertise for particle culture protocol optimisation Intellectual contribution Assistance with data analysis		
Signature		Date	January 2018

PUBLICATION 1

Manipulating Human Dendritic Cell Phenotype and Function with Targeted Porous Silicon Nanoparticles

Biomaterials 155 (2018) 92–102

Contents lists available at ScienceDirect

Biomaterials

journal homepage: www.elsevier.com/locate/biomaterials

Manipulating human dendritic cell phenotype and function with targeted porous silicon nanoparticles

Sebastian O. Stead [a], Steven J.P. McInnes [b], Svjetlana Kireta [c], Peter D. Rose [a], Shilpanjali Jesudason [a, c], Darling Rojas-Canales [c], David Warther [d], Frédérique Cunin [d], Jean-Olivier Durand [d], Christopher J. Drogemuller [a, c], Robert P. Carroll [a, c], P. Toby Coates [a, c, **, 1], Nicolas H. Voelcker [b, e, f, g, h, *, 1]

[a] University of Adelaide, Department of Medicine, Adelaide, Australia
[b] Future Industries Institute, University of South Australia, Adelaide, Australia
[c] Central Northern Adelaide Renal and Transplantation Service (CNARTS), The Royal Adelaide Hospital, Australia
[d] Institut Charles Gerhardt Montpellier, UMR 5253 CNRS -ENSCM-UM2-UM1, Ecole Nationale Supérieure de Chimie de Montpellier, 34296, Montpellier, France
[e] Drug Delivery, Disposition and Dynamics, Monash Institute of Pharmaceutical Sciences, Monash University, 381 Royal Parade, Parkville, Victoria, Australia
[f] Commonwealth Scientific and Industrial Research Organisation (CSIRO), Clayton, VIC, Australia
[g] Melbourne Centre for Nanofabrication, Victorian Node of the Australian National Fabrication Facility, Clayton, VIC, Australia
[h] Monash Institute of Medical Engineering, Monash University, Clayton, Victoria, Australia

ARTICLE INFO

Article history:
Received 29 September 2017
Received in revised form
13 November 2017
Accepted 16 November 2017
Available online 20 November 2017

Keywords:
Dendritic cells
Immunomodulation
Nanomedicine
Nanoparticles
Porous silicon
Rapamycin
Targeting

ABSTRACT

Dendritic cells (DC) are the most potent antigen presenting cells and are fundamental for the establishment of transplant tolerance. The Dendritic Cell Specific Intracellular adhesion molecule 3 Grabbing Non integrin (DC SIGN; CD209) receptor provides a target for dendritic cell therapy. Biodegradable and high surface area porous silicon (pSi) nanoparticles displaying anti DC SIGN antibodies and loaded with the immunosuppressant rapamycin (Sirolimus) serve as a fit for purpose platform to target and modify DC. Here, we describe the fabrication of rapamycin loaded DC SIGN displaying pSi nanoparticles, the uptake efficiency into DC and the extent of nanoparticle induced modulation of phenotype and function. DC SIGN antibody displaying pSi nanoparticles favourably targeted and were phagocytosed by monocyte derived and myeloid DC in whole human blood in a time and dose dependent manner. DC preconditioning with rapamycin loaded nanoparticles, resulted in a maturation resistant phenotype and significantly suppressed allogeneic T cell proliferation.

Nanoparticle based drug delivery platforms facilitating the transport of chemotherapeutics, genetic material and immune modulators are increasingly being recognised as efficient vehicles able to overcome limitations associated with pharmacokinetics of conventional drug formulations [1]. Nanoparticles for drug delivery can be fabricated with a variety of materials including liposomes [2], polymers such as polylactide co glycolide (PLGA) [3], poly γ glutamic acid [4], metals such as gold [5], mesoporous silica [6] and porous elemental silicon (pSi) [7]. The discovery of the enhanced permeability and retention (EPR) effect by Maeda et al., highlighted the potential for accumulation of nanoparticles in tumour tissues via extravasation through leaky blood vessels (passive targeting) [8] and has spurred research tempo into nanoparticle based drug delivery not only in cancer but also other pathologies including autoimmune conditions such as multiple sclerosis [9]. Antigen presenting cells (APC) are geared to capture and internalise nano scale species such as viruses, engineered nanoparticles are ideally poised to deliver antigens and drugs [10]. Recently, a study by Wang et al., identified that DC are capable of internalising cancer derived circulating miRNA (miR 410 5p), promoting angiogenesis and

* Corresponding author. Drug Delivery, Disposition and Dynamics, Monash Institute of Pharmaceutical Sciences, Monash University, Parkville, Australia.
** Corresponding author. University of Adelaide, Department of Medicine, Adelaide, Australia.
E-mail addresses: toby.coates@sa.gov.au (P.T. Coates), nicolas.voelcker@monash.edu (N.H. Voelcker).
[1] Co-Senior Authors.

https://doi.org/10.1016/j.biomaterials.2017.11.017
0142-9612/

tumour growth [11]. These realisations have led to an emerging research focus on the use of nanoparticles to target immune cells, including DC, for tolerogenicity in autoimmunity and cancer immunotherapy [12–16].

pSi based nanoparticles (pSiNP) are generated by anodisation or metal assisted chemical etching of single crystal silicon. They are particularly promising due to their biocompatibility and biodegradability, in contrast to the more frequently studied mesoporous silica [17,18]. The breakdown product of pSiNP is silicic acid, a nontoxic by product, which is filtered by the kidneys [19]. Furthermore, pSiNP also offer a very large surface area to volume ratio for drug loading. By altering the anodisation conditions, particle or pore size and shape, the loading and release of drug cargos can be optimised. Surface chemistry allows for straightforward covalent attachment of targeting ligands to the nanoparticle exterior, offering control over pore degradation and hence drug release kinetics [20–22].

Allogeneic graft tolerance without dependency on immunosuppressive medication has been referred to as the 'Holy Grail' of transplantation since the early 1950's [23]. The driving forces of tolerance involve several complex mechanisms, which involve the key player of immunomodulation, the professional antigen presenting cells (APC) [24–27]. DC are the most potent APC, interacting with $CD4^+$ and $CD8^+$ T cells by processing and presenting foreign peptides on MHC Class II and Class I proteins, respectively [28,29]. DC have specific pathogen receptors including a C type lectin called Dendritic Cell Specific Intercellular adhesion molecule 3 Grabbing Non integrin (DC SIGN) which plays an important role in peptide presentation and elicits T cell activation upon complement signalling by co stimulatory interactions and cytokine secretions. DC, depending on their co stimulatory molecule expression and their cytokine secretion profile, have been shown to possess dichotomous functions of immunostimulation and immunosuppression [30–32].

A common and well studied immunomodulatory medication is the macrolide molecule rapamycin (Sirolimus). Rapamycin is a macrocyclic lactone product of *Streptomyces hygroscopicus* that disrupts the mammalian target of rapamycin (mTOR) pathway. Rapamycin's disruption of the mTORC1 subunit inhibits raptor phosphorylation and downstream transcription factor activation [33]. Rapamycin's effect on DC decreases co stimulatory marker expression [14,34–37], preventing complete activation of interacting T cells, promoting T cell anergy and T regulatory (Treg) cell production.

In this work, we used a nanoparticle targeting DC via their uniquely expressed DC SIGN receptor for *ex vivo* immunomodulatory treatment. The expected key advantage of this approach is that targeted drug release reduces the total quantity of drug required to elicit a response whilst minimising harmful "off target" side effects. Phenotype and function of the DC were assessed by identifying expression levels of markers of DC maturation and the stimulatory capacity of allogeneic T cells by mixed lymphocyte reactions. In this study, we showed that displaying DC specific antibodies on the surface of pSiNP, enhanced uptake by the APC. Furthermore, we were able to induce maturation resistance in human monocyte derived DC when cultured with rapamycin loaded, targeting pSiNP.

1. Materials and methods

1.1. Fabrication and functionalisation of pSiNP

P^{++} type silicon (Si) wafers <100> with a resistivity of 0.8–1.2 mΩ/cm were electrochemically etched in a 3:1 mixture of 48% hydrofluoric acid (HF) to ethanol (EtOH). Silicon wafers were etched with a square wave format pattern, alternating between 50 mA/cm^2 for 7.3 s and 400 mA/cm^2 for 0.3 s for 1 h. The etched surface was electropolished in a 1:20 solution of HF to EtOH at 4 mA/cm^2 for 250 s. The porous layer was fractured by ultrasonication and filtered through a 0.22 μm nylon filter (Sartorius, Gφttingen, Germany). The resulting pSiNP underwent a hydrosilylation reaction by resuspension in 0.1 M of protected semicarbazide (tert butyl 2 [(allylamino)carbonyl] hydrazine carboxylate) [38] in tetrahydrofuran (THF) for 3 h at 85 °C under N_2 reflux (Fig. 7). pSiNP were rinsed twice in THF, twice in EtOH and stored at 4 °C. Boc group removal from the protected semicarbazide was performed by resuspending NP in a 2:3 solution of dichloromethane (CH_2Cl_2) and trifluoroacetic acid (TFA). pSiNP were agitated for 4 h at room temperature (RT) and washed once in CH_2Cl_2 and twice in EtOH.

1.2. Quantification of pSiNP concentration

A known volume of pSiNP in EtOH was placed in a 2 ml microcentrifuge tube (Eppendorf, Hamburg, German) of known mass. The tube was placed in a vacuum centrifuge to remove the EtOH and was re weighed to determine the NP mass per volume.

1.3. Drug loading

Rapamycin powder (LC Laboratories, Boston, USA) was dissolved in 100% undenatured EtOH at 2 mg/ml. Deprotected pSiNP were resuspended in rapamycin solution and agitated for 2 h at RT. The pSiNP were centrifuged at 22,000 × g for 10 min and washed twice in PBS. Drug loaded pSiNP (RAPA pSiNP) were analysed with a Hyperion 2000 microscope (Bruker, Massachusetts, USA) for infrared (IR) spectral analysis and cross referenced against pure rapamycin samples to confirm successful drug loading. Release kinetics was performed by loading pSiNP with C40 (glycyl 6 hexanoic (5(6) carboxamidofluorescien)) rapamycin (Tenova Pharmaceuticals, California, USA). pSiNP were resuspended in phosphate buffered saline (PBS) (pH 7.4) and placed in a 37 °C incubator. Released rapamycin was measured in the supernatant at various time points, using a FLUOstar Optima fluorescent plate reader (BMG Labtech, Ortenberg, Germany) with excitation at 485 nm and emission of 520 nm.

1.4. Antibody oxidation

Human DC SIGN antibody (BD Biosciences, California, USA. Clone DCN46) and Mouse IgG2κ isotype control (≈ 150,000 Da) (eBioscience, California, USA) antibody (0.5 mg/ml) were oxidised with a 0.1 M solution of sodium periodate ($NaIO_4$) at a 3000:1 M ratio ($NaIO_4$:antibody) and incubated on an orbital shaker in the dark for 30 min (RT, 60 rpm). Antibodies were purified through 10,000 Da molecular weight cut off (MWCO) purification columns (Sartorius) and washed three times in PBS (pH 7.4) by centrifugation at 12,000 × g for 10 min.

1.5. Antibody conjugation to pSiNP

Semicarbazide functionalised, RAPA pSiNP were resuspended in oxidised antibody. The solution was agitated in the dark for 30 min at RT. pSiNP were washed twice in PBS (22,000 × g for 2 min) and left pelleted for fluorophore conjugation or resuspended in media for immediate experimentation. Antibody binding was confirmed by measuring the UV absorbance at 280 nm (Nanodrop 2000, Thermo Scientific, Massachusetts, USA).

1.6. Fluorescent labelling of pSiNP

Fluorescein isothiocyanate powder (Sigma Aldrich. Missouri, USA) or XenoLight CF680 succinimidyl ester (SE) dye (Perkin Elmer, Massachusetts, USA) was dissolved in a 0.1 M solution of sodium carbonate buffer (Na_2CO_3, pH 9) to a concentration of 4 mg/ml. Stock dye (10 μl) was diluted 100 fold in PBS and added to each pelleted nanoparticle sample. Samples were placed on an orbital shaker in the dark for 1 h (RT, 60 rpm). pSiNP were washed several times in PBS (22,000 × g, 2 min) until the supernatant was col ourless. After the final wash, the pSiNP were resuspended in Ros well Park Memorial Institute (RPMI) medium (Invitrogen, Massachusetts, USA) supplemented with 10% foetal calf serum (FCS).

1.7. Monocyte derived dendritic cell culture

Peripheral blood mononuclear cells (PBMC) were isolated from 50 ml of buffy coat (ARCBS agreement 16 07SA 19) by underlying the blood with Ficoll hypaque (Lymphoprep, Stemcell Technologies, Vancouver, Canada). The blood was centrifuged at 600 × g for 20 min at RT (no break) to separate the blood and the PBMC. Monocytes were isolated from PBMC by negative selection using EasySep™ Human Monocyte enrichment kit (Stemcell Technolo gies. Vancouver, Canada) following the manufacturer's protocol. Briefly, cells (5×10^7 cells/ml) were treated with antibody enrich ment cocktail for 10 min at 4 °C, followed by incubation with magnetic beads for 5 min. Cells were placed in a magnet (Stemcell Technologies) for 2.5 min, allowing the purified $CD14^+$ monocytes to be poured off. Monocytes were resuspended in RPMI medium supplemented with 1% penicillin streptomycin, 1% glutamine, 10% FCS, 400 U/ml interleukin 4 (IL 4) (eBioscience) and 800 U/ml granulocyte macrophage colony stimulating factor (GM CSF) (kindly donated by Schering Plough) to a concentration of 1×10^6 cells/ml. At day 2, cells were treated with soluble rapamycin or RAPA pSiNP. At day 5, immature dendritic cells (iDC) were matured with 500 ng/ml of lipopolysaccharide (LPS) (Sigma Aldrich, Missouri, USA) for 48 h.

1.8. Transmission electron microscopy (TEM)

DC (1×10^6 cells) and pSiNP were processed for TEM as previ ously published [39]. Briefly, cells were fixed in EM fixative and osmium tetroxide, dehydrated via an increasing EtOH concentra tion gradient and embedded in resin before transferring to a Beem capsule (Ted Pella, California, USA) for later sectioning and imaging. Samples were imaged using a Philips CM100 TEM (Amsterdam, Netherlands).

1.9. Nanoparticle breakdown kinetics

One milligram of pSiNP was resuspended in 0.4 ml of PBS (pH 7.4) and briefly sonicated to disperse the pellet. Samples were resuspended to a final concentration of 0.25 mg/ml pSiNP in PBS. Aliquots of 10 μl were taken at various time points. Samples were diluted 1:1000 in MilliQ water and analysed for elemental silicon on an Agilent 8800 Triple Quadrupole inductively coupled plasma mass spectrometer (ICP MS) (Agilent, California, USA).

1.10. pSiNP targeting to dendritic cells

Non drug loaded, anti DC SIGN or non targeting isotype con trol antibody labelled pSiNP were resuspended in RPMI culture medium (2 mg/ml). pSiNP were added to a 24 well plate (BD Bio sciences) at 50 μg/ml containing 1×10^6 monocyte derived DC or 200 μl of whole blood. Cells were harvested at 30 min, 2 h and 24 h for uptake analysis. Whole blood samples were harvested and stained with Lineage cocktail, MHC class II (HLA DR), CD11c and BDCA 2 (CD303) antibodies (Table S1), for myeloid DC population gating. Red blood cells were lysed and cells fixed in FACS lysing solution (BD Biosciences) for 20 min at RT prior to analysis on FACSCanto II flow cytometer (BD Biosciences) and FSC Express (version 4) (DeNovo, California, USA).

1.11. Dendritic cell phenotyping

DC were harvested and resuspended in FACS wash buffer (PBS, 1% FCS, 20 mM sodium azide), and blocked in 10% heat inactivated rabbit serum, for 20 min at RT. Cells were then aliquoted into 5 ml FACS polypropylene tubes (BD Biosciences) containing antibodies: CD11c, CD14, CD40, CD80, CD83, CD86, CD209, MHC class I (pan HLA ABC) and MHC class II (HLA DR) (Table S2). Staining was per formed at 4 °C for 20 min. Cells were then analysed by flow cytometry.

1.12. Mixed lymphocyte reaction

RAPA pSiNP preconditioned DC were harvested and washed in RPMI, 10% FCS. Cells were resuspended to 1×10^5 cells/ml in culture medium and seeded in triplicate in a 96 well round bottom plate (BD Biosciences) at a ratio of 1:10 DC:T cells. $CD3^+$ T cells were isolated from allogeneic PBMC via magnetic bead enrichment (Stemcell Technologies) and CFDA SE (5 μM) (Thermo Scientific) or Violet proliferation dye (5 μM) (Life Technologies) stained prior to seeding. The plate was incubated (37 °C, 5% CO_2) for 4 days. Cells were harvested and washed with FACS washing buffer and stained at 4 °C for 20 min with CD3 (OKT3; eBioscience) and CD4 (MT310; Dako, California, USA) antibodies. Cells were fixed and analysed by flow cytometry to identify proliferation levels.

2. Results

pSiNP were generated by applying high current density steps periodically in between lower current density anodisation of silicon wafers to separate layers of desired porosity, thin 'sacrificial' sec tions of much higher porosity, followed by sonication and centri fugation [7,40]. Transmission electron microscopy (TEM) was used along with dynamic light scattering (DLS) to determine nano particle morphology and size distribution. Fig. S1 (A–C) shows three TEM micrographs of pSiNP (panel A top view, B and C size views). The etching method produced plate shaped pSiNP with pores running perpendicular through the plates' plane. DLS showed the pSiNP had an average size of 160 nm (±4 nm). Fig. S1 D shows the kinetics of nanoparticle degradation at physiological pH 7.4 obtained by quantifying elemental silicon with inductively coupled plasma mass spectrometry (ICP MS). Particles exhibited a rapid initial break down and within approximately 24 h, pSiNP were completely degraded. These degradation kinetics were acceptable for the *in vitro* testing as initial tracking experiments confirmed that a majority of the pSiNP binding occurred within 24 h. The pSiNP were functionalised with a protected semicarbazide linker via hydrosilylation. Upon removal of the protective Boc group, the particle surface was reacted with periodate oxidised monoclonal antibodies, DC SIGN or Isotype control IgG after loading with immunosuppressant, rapamycin (Fig. 1).

DC SIGN modified pSiNP were rapidly taken up by human monocyte derived DC at 37 °C, indicating that pSiNP were phago cytosed in a time and dose dependent manner. Fig. 2A shows a TEM of untreated DC. DC cultured with anti DC SIGN antibody conjugated to pSiNP (DC SIGN pSiNP) (100 μg/ml) for 30 min

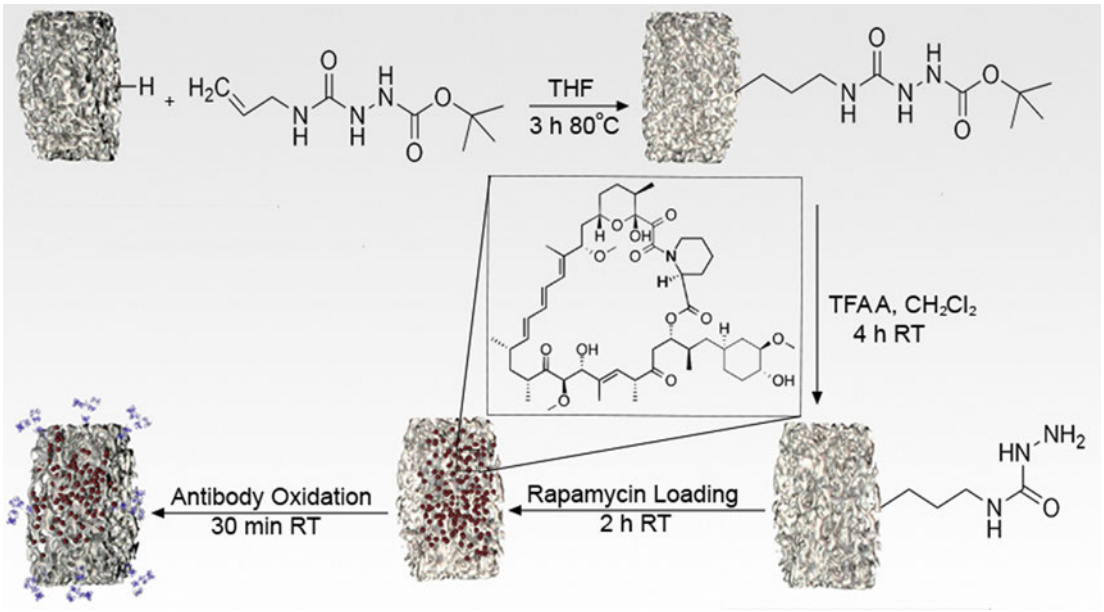

Fig. 1. Reaction for functionalisation, drug loading and antibody immobilisation on pSiNP surface. Silicon hydride terminated pSiNP undergo hydrosilylation with protected semicarbazide in a solution of tetrahydrofuran (THF). pSiNP are deprotected in trifluoroacetic anhydride (TFAA) and dichloromethane (CH_2Cl_2) prior to drug loading and conjugation of periodate-oxidised antibodies.

showed low levels of binding to the DC surface (Fig. 2B). DC binding and lysosomal internalisation of the pSiNP increased at 2 h and showed further increase at 24 h (Fig. 2C and D respectively). Using FITC labelled pSiNP, DC cultured with non targeting, isotype con trol antibody displaying pSiNP (isotype pSiNP) (Fig. 2F) showed lower FITC staining after 2 h incubation when compared to cells incubated with anti DC SIGN pSiNP (Fig. 2G). Fig. 2H shows that 20 μg/ml and 50 μg/ml of DC SIGN pSiNP were phagocytosed more rapidly compared to the isotype pSiNP control at all time points. Incubating DC with pSiNP at a concentration of 20 μg/ml for 30 min showed a 73% positivity for the targeting DC SIGN pSiNP compared to 17% for the non targeting isotype pSiNP. Increasing the nano particle concentration to 50 μg/ml showed an increased uptake of DC SIGN pSiNP to 91% compared to 46% of the isotype pSiNP (Fig. 2H). At 24 h, >94% of the human monocyte derived DC pop ulation was positive for either isotype or DC SIGN pSiNP at both 20 and 50 μg/ml. However, as indicated by the mean fluorescence intensity (MFI), DC phagocytosed approximately 2 fold more pSiNP when they displayed the DC SIGN antibody. Isotype pSiNP were non specifically taken up by the DC and were seen to not bind the DC SIGN receptor, indicated by the high level of DC SIGN surface staining with the fluorescently labelled antibody CD209. In contrast, DC cultured with DC SIGN pSiNP had decreased receptor tagging due to the competitive binding of the DC SIGN pSiNP to the same receptor epitope, which did not permit the binding of the fluorescent antibody (Fig. S2). The decrease in CD209 staining on the DC cultured with DC SIGN pSiNP confirmed that oxidation of the conjugated antibodies did not impair their function.

Myeloid DC were assessed for their nanoparticle uptake effi ciency in a whole blood assay. FITC expression (proportional to pSiNP uptake) was measured within the lineage negative, MHC class II positive, CD11c positive ($Lin^{-}HLA\ DR^{+}CD11c^{+}$) DC popula tion (Fig. 3A). After 24 h incubation, approximately 42% of the myeloid DC population was positive for DC SIGN pSiNP compared to only 11% of the DC cultured with isotype pSiNP (Fig. 3B). Fig. 3C is a graphical representation of the MFI of DC cultured with fluo rescently labelled pSiNP displaying monoclonal antibodies. A sta tistically significant difference between MFI ($p < 0.001$) was observed between DC cultured with isotype (1751 ± 83) and DC SIGN (3065 ± 109) pSiNP after 24 h confirming that DC SIGN pSiNP were taken up approximately 2 fold more effectively than the control isotype pSiNP.

pSiNP were incubated in a 2 mg/ml solution of rapamycin for 2 h at RT followed by washing in PBS. As the functional groups of rapamycin possess infrared spectral features distinct from pSi, infrared spectroscopy was employed to confirm successful rapa mycin loading within the pSiNP. RAPA pSiNP's IR spectrum showed bands corresponding to the macrocyclic groups at 1452, 2875, 2911 and 2964 cm^{-1}, the triene portion of the rapamycin molecule at 1643 and 3026 cm^{-1} and a peak at 1720 $cm^{-1,}$ corresponding to the carbonyl groups present (Fig. 4Aa). The peaks were also seen in IR spectrum from pure rapamycin crystals (Fig. 4Ab). pSiNP not loaded with drug showed no peaks at these positions (Fig. 4Ac). Nano particle release kinetics were determined by quantification of fluorescent rapamycin ($\lambda_{emission}$ 520 nm) detected in the super natant of the release buffer (PBS, pH 7.4) (Fig. 4B). The particles followed a sigmoidal regression (r^2 0.98), with 50% of the drug being released within the first 4 h. From the maximum value, it was calculated that RAPA pSiNP released a total of 5% w/w (rapamycin/ pSiNP). Therefore, subsequent experiments utilised 183 ng of RAPA pSiNP per ml to deliver an equivalent of 10 nM rapamycin. This concentration was also used in the free rapamycin control group.

DC treated with free rapamycin showed maturation resistant characteristics after stimulation with LPS with approximately a 1.5 fold lower expression of co stimulatory marker CD40 and MHC class II, a 2 fold reduction in CD80, MHC class I and maturation marker CD83 and an approximate 4 fold reduction in CD86 compared to mature DC (Fig. 5B). DC preconditioned with DC SIGN RAPA pSiNP showed maturation resistance upon LPS stimulation, with comparable surface marker expression levels to the free rapamycin control. Increases in the mean surface expression of co stimulatory markers CD40, CD83, MHC class I and MHC class II were seen for DC treated with rapamycin loaded isotype pSiNP compared to DC SIGN RAPA pSiNP (Fig. 5). Culturing DC with either isotype or DC SIGN pSiNP at low concentrations in the absence of rapamycin resulted in insignificant receptor expression change

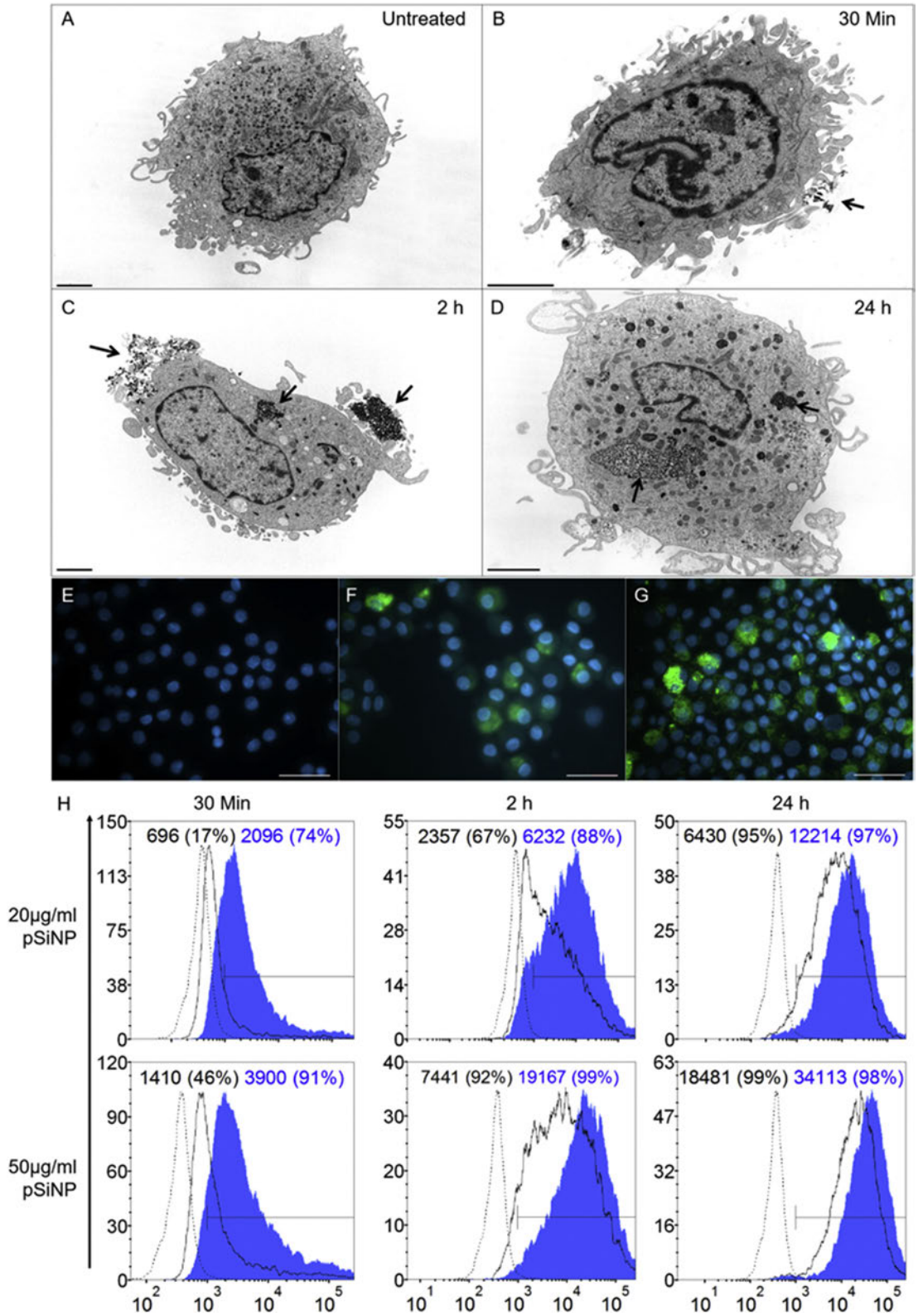

Fig. 2. (A D) TEM micrographs of mature DC (mDC). (A) Untreated mDC. (B, C, D) mDC treated with 100 µg/ml of DC-SIGN pSiNP and cultured for 30 min, 2 h and 24 h. Arrows indicate surface binding and internalisation of pSiNP. Scale bar represents 2 µm. (E G) Fluorescence microscopy of mDC. (E) Untreated mDC. mDC cultured with 100 µg/ml of FITC-labelled isotype pSiNP (F) or DC-SIGN pSiNP (G) taken at 24 h. Scale bar represents 40 µm at 40× magnification. (H) Flow cytometry histograms representing nanoparticle uptake was dependent on DC-SIGN display. Monocyte-derived DC treated with 20 µg/ml or 50 µg/ml of isotype pSiNP (Black line) or DC-SIGN pSiNP (Blue shaded) at 30 min, 2 h and 24 h (n 9, data is representative of one blood donor). Dashed line represents untreated DC control. Histograms show mean fluorescence intensity (MFI) and % positivity in parentheses. (For interpretation of the references to colour in this figure legend, the reader is referred to the web version of this article.)

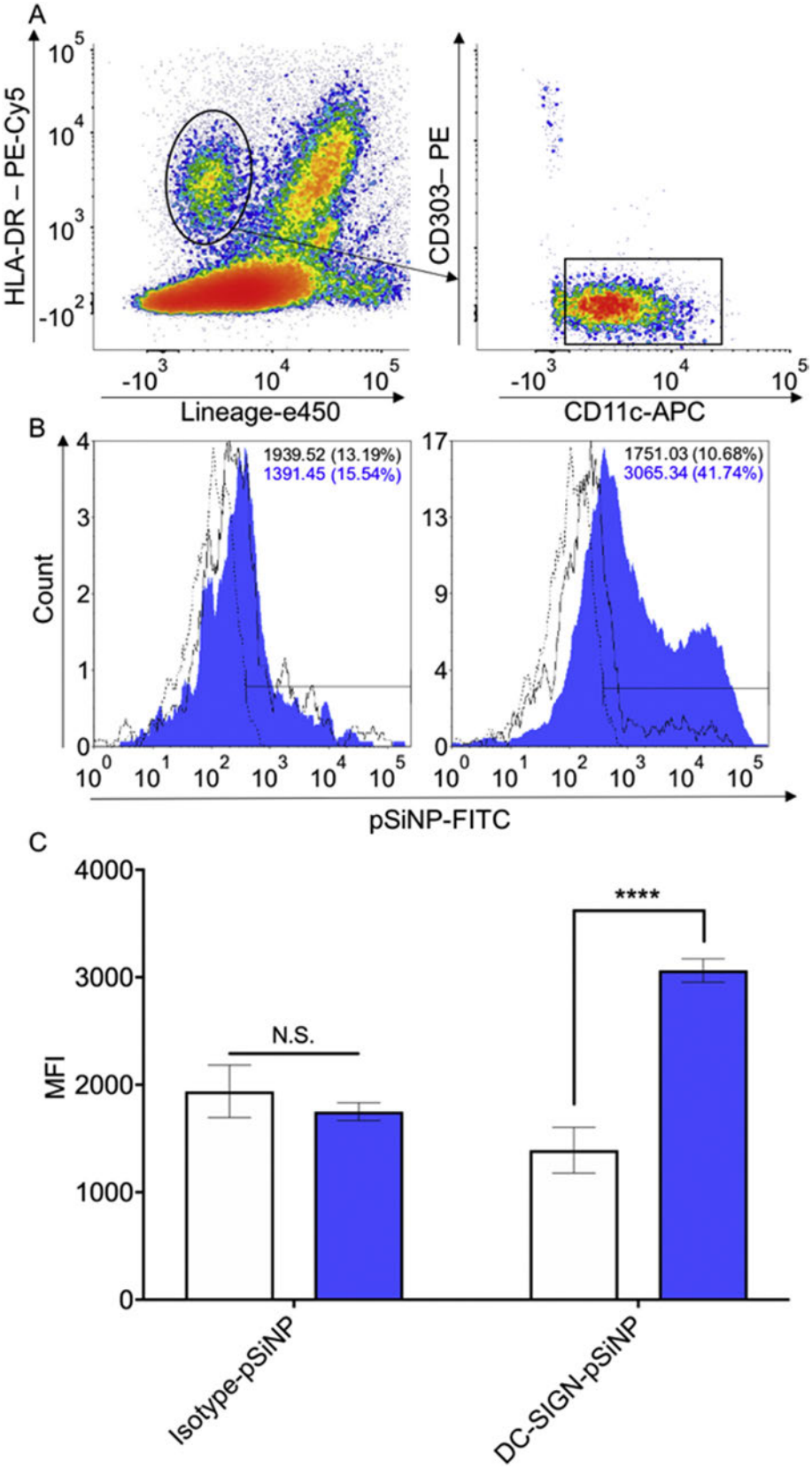

Fig. 3. DC-SIGN pSiNP were favourably phagocytosed compared to isotype pSiNP (A) Gating strategy for myeloid DC population in whole blood samples. Peripheral blood from healthy donors was incubated with pSiNP. Myeloid DC population was gated as lineage (CD2 , CD3 , CD14 , CD16 , CD19 , CD56 and CD235a), HLA-DR^{+} (oval) and CD11c^{+} (rectangle). The level of FITC expression within the population was used to determine pSiNP uptake by myeloid DC. (B) pSiNP target myeloid DC population in whole blood. Flow cytometric analysis confirmed the uptake of isotype pSiNP (Black line) and DC-SIGN pSiNP (Blue shaded) within myeloid DC at 2 h and 24 h, compared to untreated DC (Dashed line). The nanoparticle concentration used was 50 μg/ml. (C) MFI was approximately 2-fold higher in myeloid DC incubated with DC-SIGN pSiNP (Blue column) compared to isotype pSiNP (white column) at 24 h. This indicated a greater uptake of DC-SIGN functionalised pSiNP compared to the non-targeting control isotype pSiNP in a whole blood setting. Data are representative of one blood donor out of three independent experiments (n 3), statistical significance identified by unpaired *t*-test, ****$p < 0.0001$. (For interpretation of the references to colour in this figure legend, the reader is referred to the web version of this article.)

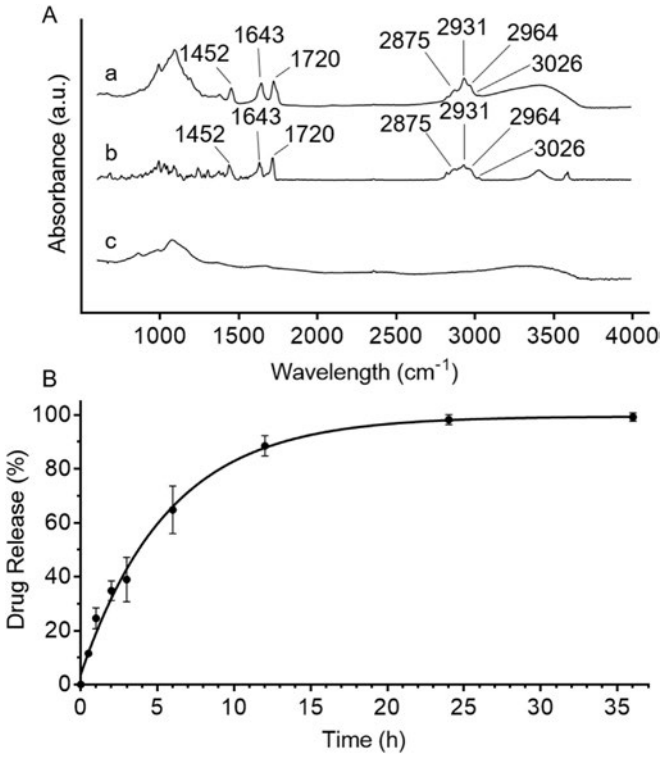

Fig. 4. (A) FTIR spectra of (a) rapamycin-loaded pSiNP (b) pure rapamycin crystals and (c) unloaded pSiNP. Characteristic peaks of pure rapamycin at 1452, 1643, 1720, 2875, 2931, 2965 and 3026 cm ^{1} were present within the RAPA-pSiNP and absent in the unloaded samples, confirming successful drug loading. (B) Release kinetics of fluorescent rapamycin from pSiNP in PBS (pH 7.4) over 36 h. 50% of rapamycin is released within the first 4 h. Data represented as mean ± SEM, n 3.

compared to untreated immature DC, at low concentrations. A significant increase of 1.6 fold was seen for maturation marker CD83, only when DC were exposed to pSiNP concentrations 500 fold higher (i.e. 100 μg/ml) than what we used in this study when loaded with rapamycin (≈200 ng/ml) (Fig. 6).

Immature DC were an important negative control in this study, due to their poor ability to stimulate allogeneic T cell proliferation, therefore serving as an optimal comparison to show maturation resistance in the matured, rapamycin treated DC. The immature DC were poor allogeneic T cell stimulators, producing an average T cell proliferative response of 13%. In contrast, mature DC were more potent T cell stimulators, up regulating 26% of allogeneic T cells. Matured, rapamycin preconditioned DC either receiving free rapamycin or isotype and DC SIGN RAPA pSiNP, maintained poor T cell stimulatory abilities *in vitro* (Fig. 6). The treatment of DC with these rapamycin formulations, even for matured cells, resulted in an average proliferation of 14%, a reduction of approximately 50% in proliferating allogeneic T cells, compared to mature DC not treated with rapamycin.

3. Discussion

In this study, we used biodegradable pSiNP, which we have recently characterised [41], of 160 nm size which were functionalised by a semicarbazide linker (Fig. 7). These pSiNP enabled the direct conjugation of periodate oxidised cell targeting antibodies to their surface. Exploiting this principle, we have recently described the vectorisation of a hydrophobic anticancer drug using antibody functionalised pSiNP to cancer cells [7,42,43]. We explored camptothecin loaded, p75NTR antibody functionalised pSiNP for targeting to neuroblastoma cells. When compared to their non targeting control nanoparticles, anti p75NTR pSiNP decreased neuroblastoma cell viability by approximately 80%. The porous nature of pSiNP creates a reservoir for the loading of small molecule drugs. The introduction of foreign materials into a homeostatic environment can induce an inflammatory response, leading to the maturation of immature DC, potentially diminishing the immunosuppressive effectiveness of the drug. pSiNP were shown not to stimulate immature DC at low concentrations (Fig. 5), preserving the immunosuppressive potency of rapamycin.

Immunomodulators such as azathioprine, prednisolone, and mycophenolic acid have all been shown to play a role in the suppression of the immune system [44–46]. With long term use, most of these drugs result in severe cytotoxic side effects and increased susceptibility of developing opportunistic infections and cancer [47]. The macrolide compound rapamycin disrupts the IL 2 pathway by the formation of a rapamycin FKBP12 complex, which acts as an allosteric inhibitor of mammalian target of rapamycin (mTOR), preventing downstream signalling [48,49]. The extensive research into the maturation resistant effects of rapamycin on DC and its clinical relevance made it the drug of interest for immunomodulation. Rapamycin was loaded into the pSiNP by passive diffusion with the antibody being directly conjugated to the surface by a chemical linker. When placed in culture, rapamycin was seen to diffuse from the particles with a standard sigmoidal drug release kinetic profile; with 50% of the drug released within the first 4 h. This was determined by measuring the relative fluorescence intensity of the fluorescent rapamycin analogy present within the culture medium. We have shown consistent results in the production of a maturation resistant DC when treated with RAPA pSiNP, similar to the free rapamycin control and other studies [34,50,51]. Myeloid DC representing less than 1% of total peripheral blood leukocytes [52] play a major role in the stimulation of T cells via complement signalling and IL 12 secretion [53]. IL 12 contributes to the differentiation of naïve $CD4^+$ T cells into T helper 1 (Th1) cells, and promoting interferon gamma (IFN γ), tumour necrosis factor alpha (TNF α) secretion and natural killer (NK) T cell production [54–56]. Recruitment of macrophages to a transplanted site via mature myeloid DC stimulation contributes to the overall foreign organ destruction, inevitably leading to graft rejection [57]. Inducing maturation resistance within the myeloid DC population has the potential to prevent foreign organ rejection; and this could be achieved by *ex vivo* targeting and preconditioning of myeloid DC with rapamycin. Therefore, promoting T cell anergy and $CD4^+$ T_{reg} cell production. T_{reg} cells can lead to the secretion of IL 10 contributing to the suppression of DC, as shown by Fassbender et al. [58]. Furthermore, due to rapamycin's unique ability to promote T_{reg} cells, this could induce a tolerogenic state within the immune system promoting indefinite allo graft survival devoid of immunosuppression. We surmised that if we found a way to deliver rapamycin via a nanocarrier, normal cell processes would be unaffected, preventing systemic suppression of the immune system; and that implementing a nanoparticle based delivery strategy for rapamycin, we could provide a means of enhanced and localised delivery. We were encouraged by the results of Das et al. and Jhunjhunwala et al. [59,60]. who showed that utilising PLGA nanoparticles for the intracellular delivery of rapamycin to DC had a more potent effect than conventional systemic administration. Since DC SIGN is highly expressed on immature myeloid DC and on a small population of $BDCA2^+$ precursor placmacytoid DC in the blood [61], it is a prime candidate for specific cell targeting. Here, we achieved this by covalent conjugation of DC SIGN antibody to the surface of pSiNP. This approach allowed us to investigate actively targeted rapamycin delivery to DC to induce a maturation resistant phenotype. With the identification of unique cell markers,

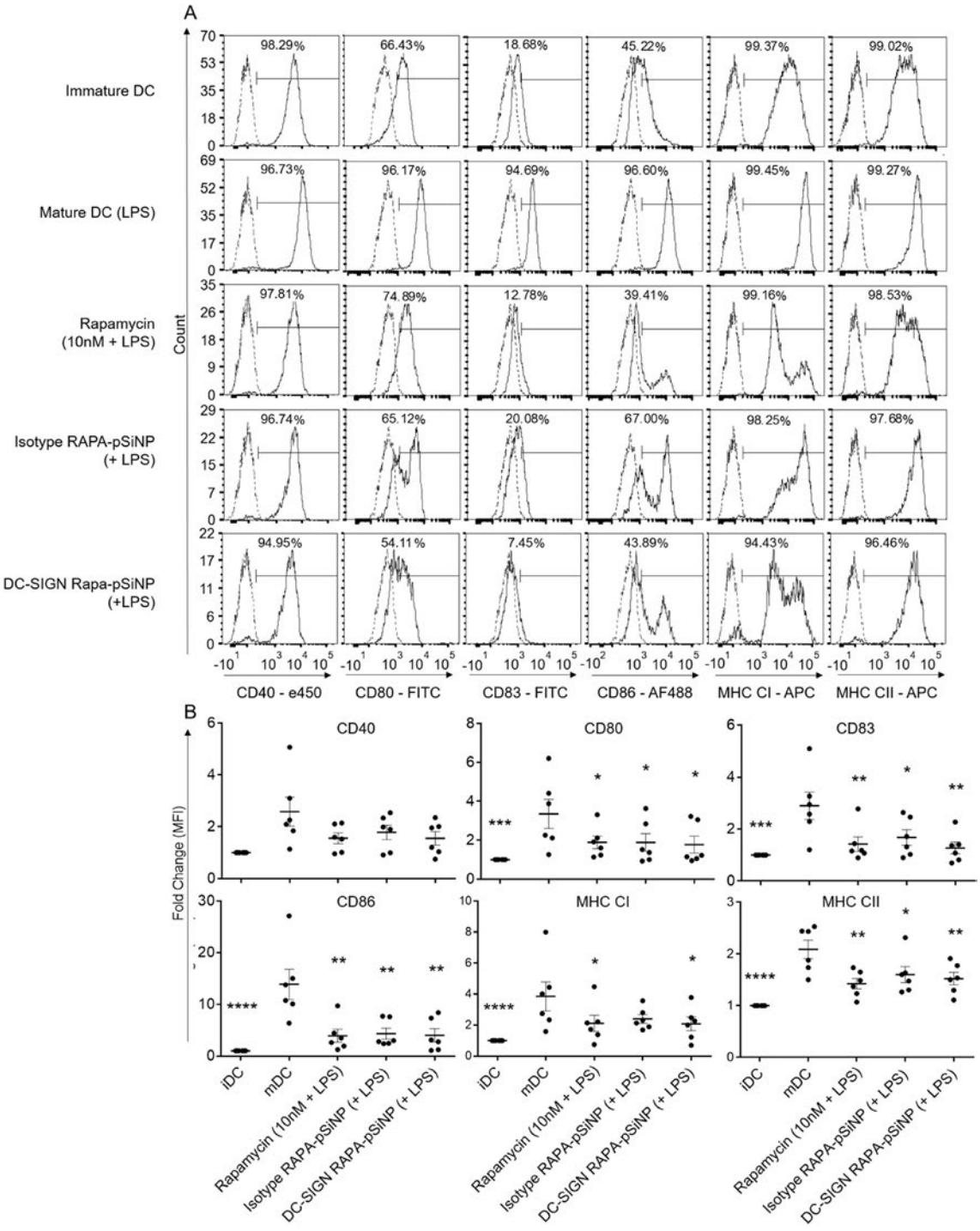

Fig. 5. (A) Flow cytometric histograms of DC preconditioned with rapamycin. Monocyte-derived immature DC were treated with 10 nM of rapamycin at day 2, added directly to the supernatant (free rapamycin) or delivered via pSiNP. Maturation resistant phenotype was seen in DC preconditioned with free rapamycin and RAPA-pSiNP, panel is representative of one donor. (B) Graphs represent the MFI fold change compared to immature DC of co-stimulatory markers CD40, CD80 and CD86 along with DC maturation marker CD83 and major histocompatibility complexes I and II; Data represented as mean ± SEM n 6, statistical significance identified by One-way ANOVA *p < 0.05, **p < 0.01, ***p < 0.001, ****p < 0.0001.

such as cell specific surface expressed macromolecules [62], these nanoparticles could be adapted to carry a range of drugs to target a wide range of cells both *ex vivo* and *in vivo*.

Due to the phagocytic nature of DC, non specific uptake was observed with isotype pSiNP when cultured for 24 h. Therefore, isotype RAPA pSiNP induced similar maturation resistant pheno types of human monocyte derived DC compared to DC SIGN pSiNP. However, when placed in a more complex *ex vivo* setting such as whole blood, the benefits of displaying DC SIGN were evident: uptake of DC SIGN pSiNP was up to 4 fold greater compared to isotype pSiNP over the same time frame of 24 h. When nano particles are placed in a whole blood setting, corona formation occurs from plasma protein binding the surface [63]. These coronas have been well studied, and have shown to impede uptake

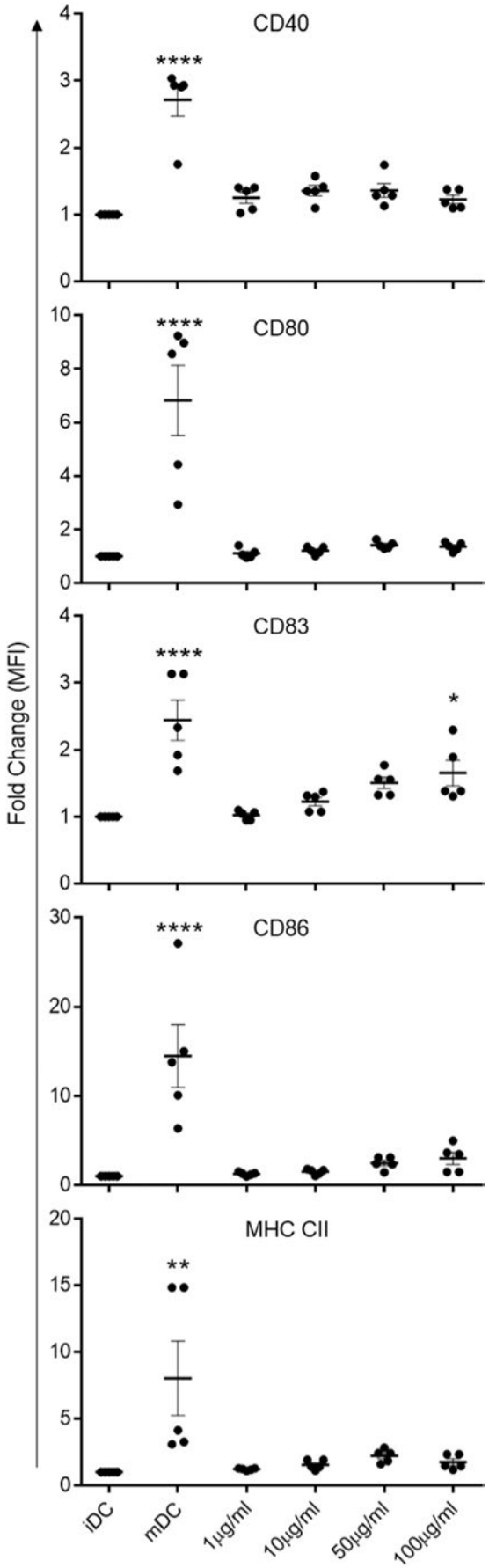

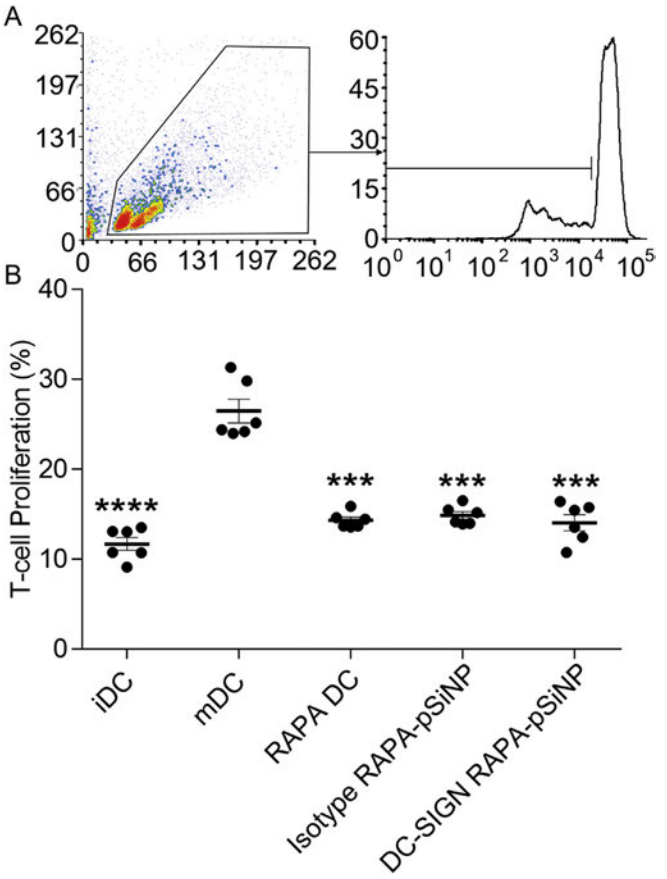

Fig. 7. Gating strategy for T-cell mixed lymphocyte reaction. T-cells were stained with violet proliferation dye. Violet stain dilution was used to determine total proliferation levels of purified $CD3^+$ T-cells when co-cultured with preconditioned matured DC at a 10:1 ratio. DC preconditioned with rapamycin either via pSiNP or addition of free drug (10 nM) directly in the supernatant were both poor stimulators of T-cells proliferation when compared to untreated mDC. Statistical significance indicated by an *, compared to mature DC. n 6. ***p < 0.001, ****p < 0.0001.

efficiency, affect nanoparticle bio distribution and drug release kinetics [64–67]. Therefore, within a *ex vivo* setting with large volumes of whole blood, it may be theorised that DC SIGN pSiNP will require longer incubation times or higher dosage to adequately target low abundance cell populations, such as the DC.

Due to the non specific uptake of the isotype RAPA pSiNP over the 24 h co culture, enough rapamycin was released which resulted in DC with poor allogeneic stimulatory abilities (Fig. 7B). Within a single cell culture setting this is expected, due to the inability to remove the unbound nanoparticles after a short incubation time. During this time, DC SIGN RAPA pSiNP bound significantly more than the isotype pSiNP based on the tracking data. As the particles were internalised in a time dependant manner, in both a single cell culture and within whole blood, it was hypothesised that in an *ex vivo* setting, less rapamycin would diffuse out of the DC SIGN RAPA pSiNP before reaching its targeted cell. Whereas utilising an isotype pSiNP would result in a lower delivery of rapamycin to the DC, as the time to target the cells would be longer. This would result

Fig. 6. Immunogenicity of immature human monocyte-derived dendritic cells co-cultured with isotype or DC-SIGN pSiNP over 48 h pSiNP treated DC maintained immature phenotype with concentrations <100 μg/ml. At concentration ≥100 μg/ml of either isotype or DC-SIGN pSiNP a 1.7-fold increase in maturation marker CD83 was seen compared to immature DC. Data represented as mean ± SEM n 5, statistical significance identified by One-way ANOVA, *p < 0.05, ****p < 0.001.

in more rapamycin diffusing from the pSiNP which would dilute in the circulation. The end effect would be that a considerably lower mass of DC SIGN RAPA pSiNP would be required compared to a non targeted formulation.

A limitation of our study was the extended culture period of monocyte derived DC with the drug loaded nanoparticles. The non specific uptake and diffusion kinetics of the particles inevi tably lead to the lack of dichotomy between DC phenotype and function when treated with targeting or non targeting pSiNP (Fig. 5B). However, the initial *in vitro* tracking experiments showed that within the first 2 h, functionalisation of pSiNP with targeting monoclonal antibody (DC SIGN) was highly beneficial for rapid uptake by DC (Fig. 2H). Future experiments will focus on using flow cytometric sorting to remove unbound pSiNP after short incubation times as well as an *in vivo* tracking model to identify the bio distribution of the DC targeting pSiNP compared to non targeting pSiNP.

4. Conclusion

Here we report an immunomodulatory approach utilising RAPA pSiNP targeting DC via their uniquely expressed receptor, human DC SIGN. Human monocyte derived DC cultured with DC SIGN pSiNP showed approximately a 3 fold increased uptake efficiency compared to isotype pSiNP within the first 30 min and at 24 h approximately a 2 fold greater uptake amount of DC SIGN pSiNP indicated by the MFI. Furthermore, within whole blood, DC SIGN antibody functionalisation permitted a 4 fold greater uptake by myeloid DC, one of the least abundant cell populations in the hu man body. Preconditioning DC with RAPA pSiNP resulted in phenotypically immature DC upon maturation, which displayed poor allogeneic T cell stimulatory capabilities compared to the mature DC. DC SIGN pSiNP therefore provide an effective means for delivering immunosuppressive medications directly to a DC pop ulation *ex vivo* with an increased capacity and in a reduced amount of time compared to non targeting pSiNP.

Acknowledgements

We thank J. Brealey, Senior Scientist, SA Pathology, for his assistance with the electron microscopy experiments. This research was supported in part by the Cooperative Research Centre for Cell Therapies Manufacturing (CRC CTM).

Appendix A. Supplementary data

Supplementary data related to this article can be found at https://doi.org/10.1016/j.biomaterials.2017.11.017.

References

[1] E. Blanco, H. Shen, M. Ferrari, Principles of nanoparticle design for overcoming biological barriers to drug delivery, Nat. Biotech. 33 (9) (2015) 941 951.
[2] V.P. Torchilin, Recent advances with liposomes as pharmaceutical carriers, Nat. Rev. Drug Discov. 4 (2) (2005) 145 160.
[3] P. Elamanchili, et al., Characterization of poly(D,L-lactic-co-glycolic acid) based nanoparticulate system for enhanced delivery of antigens to dendritic cells, Vaccine 22 (19) (2004) 2406 2412.
[4] T. Uto, et al., Targeting of antigen to dendritic cells with poly(gamma-glutamic acid) nanoparticles induces antigen-specific humoral and cellular immunity, J. Immunol. 178 (5) (2007) 2979 2986.
[5] F. Kikuchi, et al., Formation of gold nanoparticles by glycolipids of Lactobacillus casei, Sci. Rep. 6 (2016) 34626.
[6] M. Gary-Bobo, et al., Multifunctionalized mesoporous silica nanoparticles for the in vitro treatment of retinoblastoma: drug delivery, one and two-photon photodynamic therapy, Int. J. Pharm. 432 (1 2) (2012) 99 104.
[7] E. Secret, et al., Antibody-functionalized porous silicon nanoparticles for vectorization of hydrophobic drugs, Adv. Healthc. Mater. 2 (5) (2013) 718 727.
[8] H. Maeda, H. Nakamura, J. Fang, The EPR effect for macromolecular drug delivery to solid tumors: improvement of tumor uptake, lowering of systemic toxicity, and distinct tumor imaging in vivo, Adv. Drug Deliv. Rev. 65 (1) (2013) 71 79.
[9] L. Zhang, et al., Nanoparticles in medicine: therapeutic applications and developments, Clin. Pharmacol. Ther. 83 (5) (2008) 761 769.
[10] J.A. Hubbell, S.N. Thomas, M.A. Swartz, Materials engineering for immunomodulation, Nature 462 (7272) (2009) 449 460.
[11] J. Wang, et al., Cancer-derived circulating MicroRNAs promote tumor angiogenesis by entering dendritic cells to degrade highly complementary MicroRNAs, Theranostics 7 (6) (2017) 1407.
[12] L.M. Kranz, et al., Systemic RNA delivery to dendritic cells exploits antiviral defence for cancer immunotherapy, Nature 534 (7607) (2016) 396 401.
[13] T.K. Kishimoto, et al., Improving the efficacy and safety of biologic drugs with tolerogenic nanoparticles, Nat. Nano 11 (10) (2016) 890 899.
[14] R.A. Maldonado, et al., Polymeric synthetic nanoparticles for the induction of antigen-specific immunological tolerance, Proc. Natl. Acad. Sci. U. S. A. (2) (2015) 112. E156 E165.
[15] A. Yeste, et al., Tolerogenic nanoparticles inhibit T cell mediated autoimmunity through SOCS2, Sci. Signal. 9 (433) (2016) ra61.
[16] M.D. McHugh, et al., Paracrine co-delivery of TGF-beta and IL-2 using CD4-targeted nanoparticles for induction and maintenance of regulatory T cells, Biomaterials 59 (2015) 172 181.
[17] S.M. Haidary, E.P. Córcoles, N.K. Ali, Nanoporous silicon as drug delivery systems for cancer Therapies, J. Nanomater. 2012 (2012) 15.
[18] M.H. Kafshgari, N.H. Voelcker, F.J. Harding, Applications of zero-valent silicon nanostructures in biomedicine, Nanomed. Lond. 10 (16) (2015) 2553 2571.
[19] D.M. Reffitt, et al., Silicic acid: its gastrointestinal uptake and urinary excretion in man and effects on aluminium excretion, J. Inorg. Biochem. 76 (2) (1999) 141 147.
[20] R. Misra, S.K. Sahoo, Intracellular trafficking of nuclear localization signal conjugated nanoparticles for cancer therapy, Eur. J. Pharm. Sci. 39 (1 3) (2010) 152 163.
[21] H.S. Choi, et al., Design considerations for tumour-targeted nanoparticles, Nat. Nanotechnol. 5 (1) (2010) 42 47.
[22] S.J. McInnes, N.H. Voelcker, Silicon-polymer hybrid materials for drug delivery, Future Med. Chem. 1 (6) (2009) 1051 1074.
[23] N.L. Tilney, TRANSPLANT from Myth to Reality, Yale University Press, 2003.
[24] R.M. Steinman, M.C. Nussenzweig, Avoiding horror autotoxicus: the importance of dendritic cells in peripheral T cell tolerance, Proc. Natl. Acad. Sci. U. S. A. 99 (1) (2002) 351 358.
[25] N. Garbi, et al., Tonic T cell signalling and T cell tolerance as opposite effects of self-recognition on dendritic cells, Curr. Opin. Immunol. 22 (5) (2010) 601 608.
[26] F.X. Hubert, et al., Aire regulates the transfer of antigen from mTECs to dendritic cells for induction of thymic tolerance, Blood 118 (9) (2011) 2462 2472.
[27] Y. Lei, et al., Aire-dependent production of XCL1 mediates medullary accumulation of thymic dendritic cells and contributes to regulatory T cell development, J. Exp. Med. 208 (2) (2011) 383 394.
[28] K. Hochweller, et al., Dendritic cells control T cell tonic signaling required for responsiveness to foreign antigen, Proc. Natl. Acad. Sci. U. S. A. 107 (13) (2010) 5931 5936.
[29] M. Lambotin, et al., A look behind closed doors: interaction of persistent viruses with dendritic cells, Nat. Rev. Microbiol. 8 (5) (2010) 350 360.
[30] J.M. Curtsinger, et al., Inflammatory cytokines provide a third signal for activation of naive CD4+ and CD8+ T cells, J. Immunol. 162 (6) (1999) 3256 3262.
[31] Y. Liu, C.A. Janeway Jr., Microbial induction of co-stimulatory activity for CD4 T-cell growth, Int. Immunol. 3 (4) (1991) 323 332.
[32] J.M. Curtsinger, D.C. Lins, M.F. Mescher, Signal 3 determines tolerance versus full activation of naive CD8 T cells: dissociating proliferation and development of effector function, J. Exp. Med. 197 (9) (2003) 1141 1151.
[33] T. Weichhart, M. Hengstschlager, M. Linke, Regulation of innate immune cell function by mTOR, Nat. Rev. Immunol. 15 (10) (2015) 599 614.
[34] T. Taner, et al., Rapamycin-treated, alloantigen-pulsed host dendritic cells induce ag-specific T cell regulation and prolong graft survival, Am. J. Transpl. 5 (2) (2005) 228 236.
[35] K.L. Pothoven, et al., Rapamycin-conditioned donor dendritic cells differentiate CD4CD25Foxp3 T cells in vitro with TGF-beta1 for islet transplantation, Am. J. Transpl. 10 (8) (2010) 1774 1784.
[36] H.R. Turnquist, et al., Rapamycin-conditioned dendritic cells are poor stimulators of allogeneic CD4+ T cells, but enrich for antigen-specific Foxp3+ T regulatory cells and promote organ transplant tolerance, J. Immunol. 178 (11) (2007) 7018 7031.
[37] K.M. Silk, et al., Rapamycin conditioning of dendritic cells differentiated from human ES cells promotes a tolerogenic phenotype, J. Biomed. Biotechnol. 2012 (2012) 172420.
[38] Y. Coffinier, et al., Semicarbazide-functionalized Si(111) surfaces for the site-specific immobilization of peptides, Langmuir 21 (4) (2005) 1489 1496.
[39] J.K. Brealey, Ultrastructural observations in a case of BK virus nephropathy with viruses in glomerular subepithelial humps, Ultrastruct. Pathol. 31 (1) (2007) 1 7.
[40] Z. Qin, et al., Size control of porous silicon nanoparticles by electrochemical perforation etching, Part. Part. Syst. Charact. 31 (2) (2014) 252 256.
[41] A. Cifuentes-Rius, et al., Dual-action cancer therapy with targeted porous

silicon nanovectors, Small (29) (2017) 13.
[42] H. Alhmoud, et al., Porous silicon nanodiscs for targeted drug delivery, Adv. Funct. Mater. 25 (7) (2015) 1137 1145.
[43] M. Alba, et al., Silica nanopills for targeted anticancer drug delivery, Small 11 (36) (2015) 4626 4631.
[44] I. Tiede, et al., CD28-dependent Rac1 activation is the molecular target of azathioprine in primary human CD4+ T lymphocytes, J. Clin. Investig. 111 (8) (2003) 1133 1145.
[45] L.J. Langman, et al., Pharmacodynamic assessment of mycophenolic acid-induced immunosuppression in renal transplant recipients, Transplantation 62 (5) (1996) 666 672.
[46] A.M. Woltman, et al., The effect of calcineurin inhibitors and corticosteroids on the differentiation of human dendritic cells, Eur. J. Immunol. 30 (7) (2000) 1807 1812.
[47] H. Chatrath, et al., De novo malignancy post-liver transplantation: a single center, population controlled study, Clin. Transpl. 27 (4) (2013) 582 590.
[48] L.A. Banaszynski, C.W. Liu, T.J. Wandless, Characterization of the FKBP.rapamycin.FRB ternary complex, J. Am. Chem. Soc. 127 (13) (2005) 4715 4721.
[49] J. Chung, et al., Rapamycin-FKBP specifically blocks growth-dependent activation of and signaling by the 70 kd S6 protein kinases, Cell 69 (7) (1992) 1227 1236.
[50] R. Fischer, et al., Use of rapamycin in the induction of tolerogenic dendritic cells, Handb. Exp. Pharmacol. (188) (2009) 215 232.
[51] G.Y. Wang, et al., Rapamycin-treated mature dendritic cells have a unique cytokine secretion profile and impaired allostimulatory capacity, Transpl. Int. 22 (10) (2009) 1005 1016.
[52] J. Haller Hasskamp, J.L. Zapas, E.G. Elias, Dendritic cell counts in the peripheral blood of healthy adults, Am. J. Hematol. 78 (4) (2005) 314 315.
[53] P. Blanco, et al., Dendritic cells and cytokines in human inflammatory and autoimmune diseases, Cytokine Growth Factor Rev. 19 (1) (2008) 41 52.
[54] L. Ziegler-Heitbrock, The CD14+ CD16+ blood monocytes: their role in infection and inflammation, J. Leukoc. Biol. 81 (3) (2007) 584 592.
[55] B. Alberts, A. Johnson, J. Lewis, Microbiology of the Cell, fourth ed., Carland Science, New York, 2002.
[56] G. Schreibelt, et al., Toll-like receptor expression and function in human dendritic cell subsets: implications for dendritic cell-based anti-cancer immunotherapy, Cancer Immunol. Immunother. 59 (10) (2010) 1573 1582.
[57] K.R. Wyburn, et al., The role of macrophages in allograft rejection, Transplantation 80 (12) (2005) 1641 1647.
[58] M. Fassbender, et al., Cyclic adenosine monophosphate and IL-10 coordinately contribute to nTreg cell-mediated suppression of dendritic cell activation, Cell Immunol. 265 (2) (2010) 91 96.
[59] S. Das, et al., Delivery of rapamycin-loaded nanoparticle down regulates ICAM-1 expression and maintains an immunosuppressive profile in human CD34+ progenitor-derived dendritic cells, J. Biomed. Mater. Res. A 85 (4) (2008) 983 992.
[60] S. Jhunjhunwala, et al., Delivery of rapamycin to dendritic cells using degradable microparticles, J. Control Release 133 (3) (2009) 191 197.
[61] E.J. Soilleux, et al., Constitutive and induced expression of DC-SIGN on dendritic cell and macrophage subpopulations in situ and in vitro, J. Leukoc. Biol. 71 (3) (2002) 445 457.
[62] B.P. Gray, K.C. Brown, Combinatorial peptide libraries: mining for cell-binding peptides, Chem. Rev. 114 (2) (2013) 1020 1081.
[63] V. Mirshafiee, et al., Impact of protein pre-coating on the protein corona composition and nanoparticle cellular uptake, Biomaterials 75 (2016) 295 304.
[64] A. Lesniak, et al., Effects of the presence or absence of a protein corona on silica nanoparticle uptake and impact on cells, ACS Nano 6 (7) (2012) 5845 5857.
[65] L. Zhu, et al., Analysis of the effects of 17beta-oestradiol and serum deprivation on the contents of proteins in breast cancer cells by isobaric tags for relative and absolute quantification and two-dimensional liquid chromatography-tandem mass spectrometry, Se Pu 27 (3) (2009) 270 278.
[66] S. Nagayama, et al., Time-dependent changes in opsonin amount associated on nanoparticles alter their hepatic uptake characteristics, Int. J. Pharm. 342 (1 2) (2007) 215 221.
[67] A. Cifuentes-Rius, et al., Optimizing the properties of the protein corona surrounding nanoparticles for tuning payload release, ACS Nano 7 (11) (2013) 10066 10074.

STATEMENT OF AUTHORSHIP 2

Title of Paper	Murine and Non-Human Primate Dendritic Cell Targeting Nanoparticles for *In Vivo* Generation of Regulatory T-cells
Publication Status	Published
Publication Details	ACS Nano Impact Factor13.942 (2016) Accepted June 2018

Principal Author

Name of Principal Author (Candidate)	Sebastian O. Stead		
Contribution to the Paper	Data analysis Project design Laboratory/murine work Particle manufacture Murine injection Protocol optimisation		
Overall percentage (%)	75%		
Certification:	This paper reports on original research I conducted during the period of my Higher Degree by research candidature and is not subject to any obligations or contractual agreements with a third party that would constrain its inclusion in this thesis. I am the primary author of this paper		
Signature		Date	January 2018

Co-Author Contributions

Name of Co-Author	Svjetlana Kireta		
Contribution to the Paper	Handling, injections and autopsies of non-human primates		
Signature		Date	January 2018

Name of Co-Author	Steven J.P. McInnes		
Contribution to the Paper	Mass Spectrometry Nanoparticle manufacture Intellectual contribution		
Signature		Date	January 2018

Name of Co-Author	Francis D. Kette		
Contribution to the Paper	Assisted with animal autopsy and processing		
Signature		Date	January 2018

Name of Co-Author	Kisha Sivanathan		
Contribution to the Paper	Regulatory T-cell flow cytometry staining assistance		
Signature		Date	January 2018

Name of Co-Author	Juewan Kim		
Contribution to the Paper	Stimulation assay and confocal microscopy assistance		
Signature		Date	January 2018

Name of Co-Author	David Warther		
Contribution to the Paper	Developer of functionalising chemical linker		
Signature		Date	January 2018

Name of Co-Author	Frederique Cunin		
Contribution to the Paper	Developer of functionalising chemical linker		
Signature		Date	January 2018

Name of Co-Author	Jean-Olivier Durand		
Contribution to the Paper	Developer of functionalising chemical linker		
Signature		Date	January 2018

Name of Co-Author	Christopher J. Drogemuller		
Contribution to the Paper	Intellectual contribution Assistance with data analysis and experimental design		
Signature		Date	January 2018

Name of Co-Author	Robert P. Carroll		
Contribution to the Paper	Co-supervisor. Intellectual contribution. Assistance with data analysis.		
Signature		Date	January 2018

Name of Co-Author	Nicolas H. Voelcker		
Contribution to the Paper	Co-supervisor. Provided laboratory space for nanoparticle manufacture Intellectual contribution. Assistance with data analysis.		
Signature		Date	January 2018

Name of Co-Author	P. Toby Coates		
Contribution to the Paper	Principal supervisor Provided project funding Intellectual contribution Assistance with data analysis		
Signature		Date	January 2018

PUBLICATION 2

Murine and Non-Human Primate Dendritic Cell Targeting Nanoparticles for *In Vivo* Generation of Regulatory T-cells

ACS NANO
Cite This: ACS Nano 2018, 12, 6637 6647
www.acsnano.org

ARTICLE

Murine and Non-Human Primate Dendritic Cell Targeting Nanoparticles for *in Vivo* Generation of Regulatory T-Cells

Sebastian O. Stead,[†] Svjetlana Kireta,[‡] Steve J. P. McInnes,[§] Francis D. Kette,[†] Kisha N. Sivanathan,[†] Juewan Kim,[†] Eduardo J. Cueto-Diaz,[∥] Frederique Cunin,[∥] Jean-Olivier Durand,[∥] Christopher J. Drogemuller,[†,‡] Robert P. Carroll,[†,‡] Nicolas H. Voelcker,*[,⊥,#,∇,○] and Patrick T. Coates*[,†,‡]

[†]Department of Medicine, University of Adelaide, Adelaide 5000, Australia
[‡]Central Northern Adelaide Renal and Transplantation Service (CNARTS), The Royal Adelaide Hospital, Adelaide 5000, Australia
[§]Future Industries Institute, University of South Australia, Adelaide 5095, Australia
[∥]Case 1701, UMR 5253 CNRS ENSCM UM, Institut Charles Gerhardt Montpellier, 34095 Montpellier, cedex 5, France
[⊥]Drug Delivery, Disposition, and Dynamics, Monash Institute of Pharmaceutical Sciences, Monash University, 381 Royal Parade, Parkville, Victoria 3052, Australia
[#]Commonwealth Scientific and Industrial Research Organization (CSIRO), Clayton, Victoria 3169, Australia
[∇]Melbourne Center for Nanofabrication, Victorian Node of the Australian National Fabrication Facility, Clayton, Victoria 3168, Australia
[○]Monash Institute of Medical Engineering, Monash University, Clayton, Victoria 3800, Australia

Supporting Information

ABSTRACT: Porous silicon nanoparticles (pSiNP), modified to target dendritic cells (DC), provide an alternate strategy for the delivery of immunosuppressive drugs. Here, we aimed to develop a DC targeting pSiNP displaying c type lectin, dendritic cell specific intercellular adhesion molecule 3 grabbing non integrin (DC SIGN), and CD11c monoclonal antibodies. The *in vivo* tracking of these fluorescent DC targeting nanoparticles was assessed in both C57BL/6 mice and common marmosets (*Callithrix jacchus*) by intravenous injection (20 mg/kg). Rapamycin and ovalbumin $(OVA)_{323-339}$ peptide loaded pSiNP were employed to evaluate their ability to generate murine $CD4^+CD25^+FoxP3^+$ regulatory T cells *in vivo* within OVA sensitized mice. *In vivo*, pSiNP migrated to the liver, kidneys, lungs, and spleen in both mice and marmosets. Flow cytometry confirmed pSiNP uptake by splenic and peripheral blood DC when functionalized with targeting antibodies. C57BL/6 OVA sensitized mice injected with CD11c pSiNP loaded with rapamycin + $OVA_{323-339}$ produced a 5 fold higher number of splenic regulatory T cells compared to control mice, at 40 days post pSiNP injection. These results demonstrate the importance of the immobilized targeting antibodies to enhance cellular uptake and enable the *in vivo* generation of splenic regulatory T cells.

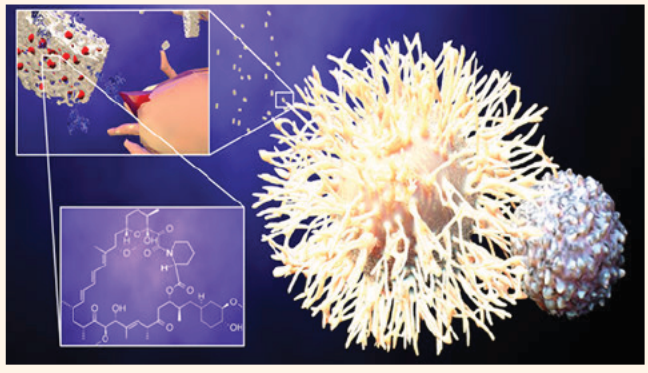

KEYWORDS: *rapamycin, regulatory T cells, nanoparticles, porous silicon, nanomedicine, tolerance, DC SIGN*

Long term transplant survival is significantly hindered by chronic graft rejection. However, increased susceptibility to infection and malignancies are major complications of prolonged immunosuppression.[1] Ideally, patients could maintain a functional organ devoid of immunosuppressive medication, by promoting donor specific immune hypo responsiveness or "immune tolerance", significantly reducing the risk of developing cancer and infection. This has been termed the "holy grail" of transplantation since first proposed in the 1950s.[2]

Received: March 1, 2018
Accepted: July 6, 2018
Published: July 6, 2018

DOI: 10.1021/acsnano.8b01625
ACS Nano 2018, 12, 6637–6647

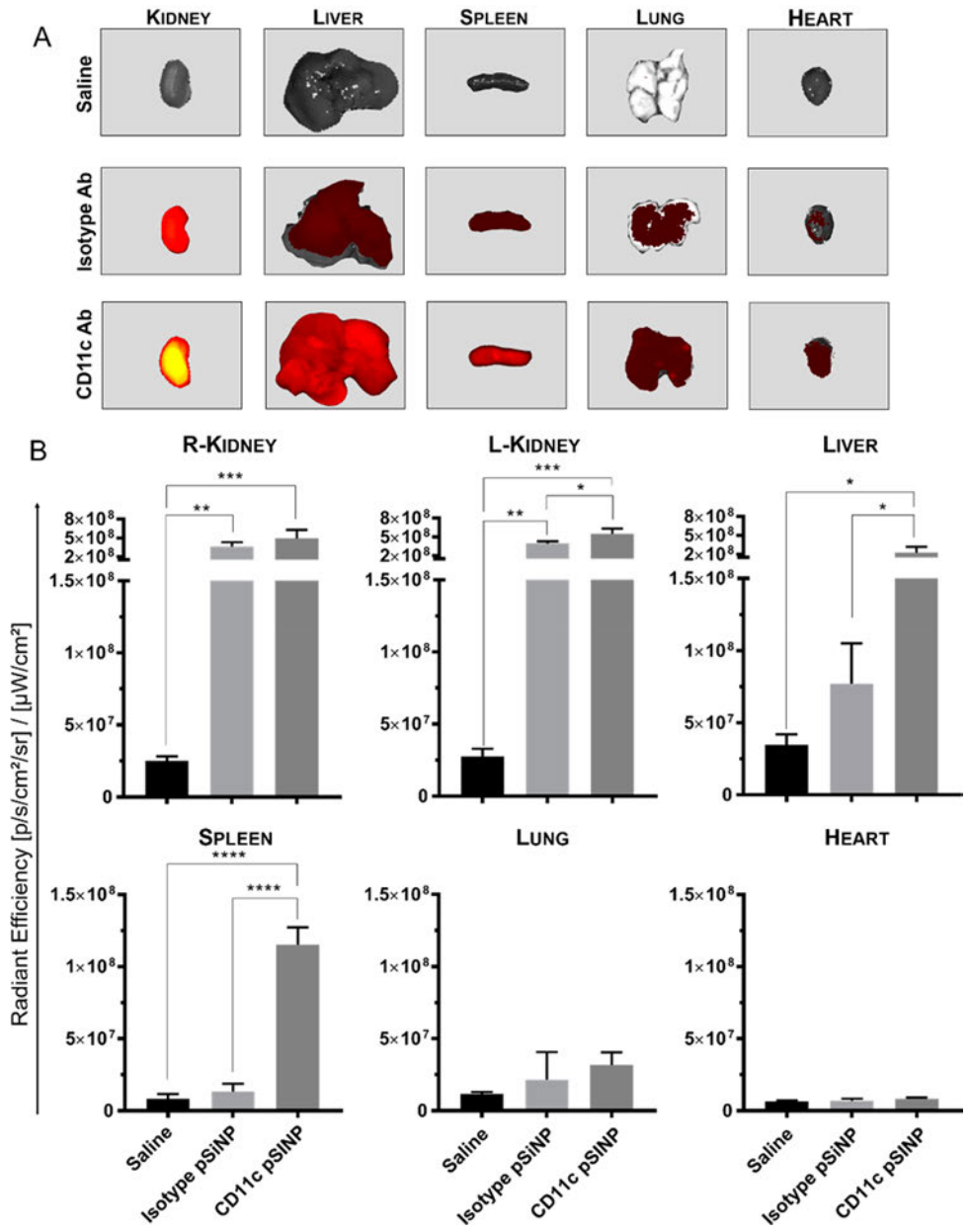

Figure 1. CD11c pSiNP track predominately to the kidneys, followed by the liver, spleen, lungs, and heart. (A) Individual organs taken from the mice at 24 h post injection (i.v.) with fluorescent pSiNP. Heat map (red to yellow) indicates presence of pSiNP. (B) Quantification of total fluorescence as radiant efficiencies of each of the organs at 24 h. Mice injected with CD11c pSiNP had approximately 10 fold higher levels in the spleen compared to isotype pSiNP. CD11c pSiNP tracked significantly more to the kidneys and lungs of the mice compared to isotype pSiNP. Insignificant presence of pSiNP was seen within the lungs and heart. (Data are represented as mean ± SD, $n = 3$ per group, significance determined by one way ANOVA, * $p < 0.05$, ** $p < 0.01$, *** $p < 0.001$, **** $p < 0.0001$).

Dendritic cells (DC) within the immune system are responsible for processing and presenting foreign peptides, inducing an immune response toward an allogeneic transplant. DC are the most potent of the antigen presenting cells (APC), capable both of immunostimulation and immunosuppression and drive antigen specific tolerance by promoting regulatory T cell (Treg) production.[3,4] One promising approach is the induction of tolerance to allogeneic grafts *via* targeting DC with drug loaded nanoparticles designed to dampen immune responsiveness and generate "tolerogenic DC" (tol DC). The use of tol DC in transplantation, as an immune therapy, has developed significant traction in recent years, with several clinical trials investigating the benefits of *in vivo* DC therapy.[5,6]

Rapamycin is a commonly used immunosuppressive medication that promotes formation of tol DC.[7] Precondition ing DC with rapamycin induces a maturation resistant phenotype, characterized by decreased co stimulatory and maturation markers expression,[8−10] which can induce T cell anergy and promote Treg generation.[11] DC also express specific surface molecules including the c type lectin, dendritic cell specific intercellular adhesion molecule 3 grabbing non integrin (DC SIGN; CD209). Coupling DC SIGN mono clonal antibodies to porous silicon drug loaded nanoparticles creates a method to specifically target DC *in vivo*. Utilizing targeting, drug loaded nanocarriers that deliver therapeutics specifically to these key immune cells, has the potential to

DOI: 10.1021/acsnano.8b01625
ACS Nano 2018, 12, 6637−6647

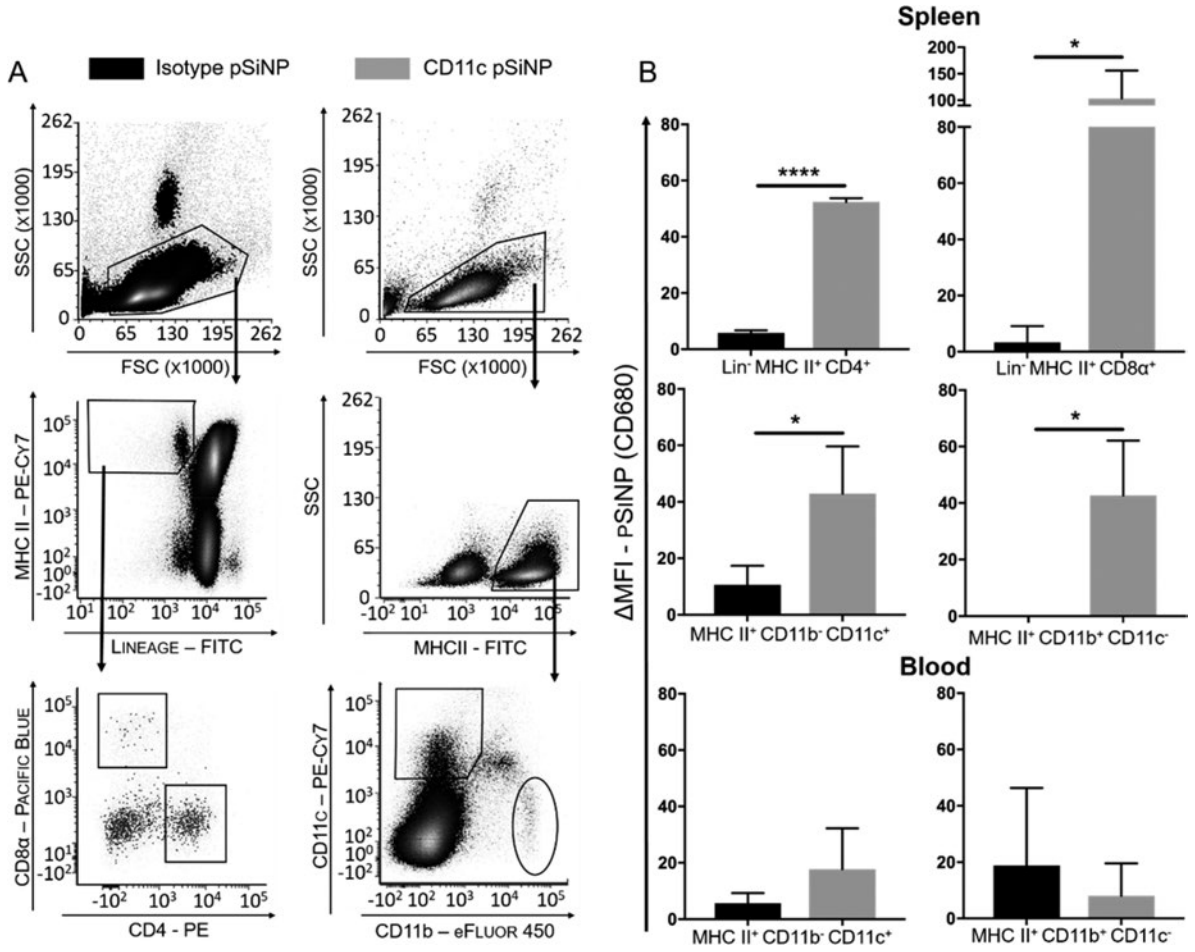

Figure 2. CD11c pSiNP track to murine splenic myeloid CD4$^+$ and CD8α^+DC *in vivo*. (A) Gating strategy of lineage negative MHC II$^+$CD4$^+$ or CD8α^+DC, MHC II$^+$CD11b$^-$CD11c$^+$DC, and MHC II$^+$CD11b$^+$CD11c$^-$ macrophages. (B) Quantification of the mean fluorescence intensity (MFI), representative of pSiNP accumulation, within splenic and blood DC and macrophage populations. CD4$^+$ and CD8α^+ DC showed approximately 9 fold and 31 fold higher levels of CD11c pSiNP, respectively, in the spleen at 24 h. Data are presented as delta (Δ) MFI ± SD, normalized to the baseline fluorescence levels in saline injected control animals (n = 3 per group, statistical significance determined by two tailed t test, * $p < 0.05$, **** $p < 0.0001$).

reduce off targeted drug effects. Here, we studied the uptake of DC targeting porous silicon nanoparticles (pSiNP), function alized with antibodies to murine CD11c and human/non human primate (NHP) DC SIGN *in vivo*. Rapamycin loaded pSiNP were also assessed in their ability to generate Treg *in vivo* in an ovalbumin (OVA) sensitized murine model. We utilized both a murine and a NHP model to investigate the hypothesis that displaying DC targeting antibodies on pSiNP would permit a higher level of cell targeting *in vivo* compared to their non targeting counterparts.

RESULTS

Murine DC Targeting with CD11c-pSiNP. Porous silicon nanoparticles (pSiNP), <200 nm in size, manufactured by alternating high and low current density anodization of silicon wafers, were functionalized with a protected semicarbazide linker *via* hydrosilylation.[12] Boc group removal from the pSiNP surface permitted reaction with periodate oxidized mAb and fluorescent tag, CF680, both of which covalently link directly to the NP. Murine CD11c integrin has been used extensively to categorize myeloid lineage negative, MHC class II$^+$CD4$^+$CD8α^- and MHC class II$^+$CD4$^-$CD8α^+ DC subsets.[13] Due to the highly unique expression of CD11c on myeloid DC subsets, it served as a prime target for pSiNP within a murine model. Isotype and CD11c pSiNP were administered intravenous (i.v.) to mice. Whole body images showed nanoparticle accumulation within the kidney of mice injected with either isotype or CD11c pSINP, most prominent within the first hour. The fluorescence was seen to dissipate in a time dependent manner (Figure S1A). However, quantifica tion of organ fluorescence (Figure 1A,B) as radiant efficiencies (RE), the fluorescence emission radiance per incident excitation irradiance, showed both isotype and CD11c pSiNP accumulation was time dependent. Isotype pSiNP mice showed a maximum pSiNP accumulation in the liver (1.2×10^8 RE), spleen (2.2×10^7 RE), and kidneys (4.2×10^8 RE) at 6 h and lungs (2.1×10^7 RE) at 12 h (Figure S1) with no significant heart uptake. Kidney fluorescence was 14 fold higher than the saline control at 6 and 24 h (Figure S1 and Figure 1). CD11c pSiNP mice had significantly higher pSiNP accumulation in the liver, lungs, heart, spleen and kidneys compared to both the saline and isotype pSiNP control mice. Maximum fluorescence was seen in the liver (2.3×10^8 RE) and spleen (1.2×10^8 RE) at 24 h (Figure 1), and the lungs (4.3×10^7 RE), kidneys (1.2×10^9 RE), and heart (1.6×10^7 RE) at 12 h (Figure S1). CD11c pSiNP accumulated 10 fold

DOI: 10.1021/acsnano.8b01625
ACS Nano 2018, 12, 6637–6647

higher than isotype pSiNP in the spleen at 6 and 24 h (Figure 1). CD11c pSiNP mice splenic fluorescence decreased by approximately 60% from 6 to 12 h, accompanied by increased presence in the heart and kidneys at 12 h (Figure S1).

The flow cytometric gating strategy utilized the lineage negative population to remove T cells, B cells, and NK cells while focusing on the MHC II$^+$ population (Figure 2A, middle left panel). This population contains both myeloid and conventional DC and is therefore further divided into both CD4$^+$ and CD8α^+ subsets (Figure 2A, bottom left panel). These populations within the spleen identified accumulation of pSiNP in mice injected with either CD11c or isotype pSiNP. Both CD4$^+$ and CD8α^+ conventional DC subsets were positive for CD11c pSiNP at 24 h. CD4$^+$ and CD8α^+ DC had approximately a 9 fold and 31 fold higher uptake of CD11c pSiNP, respectively, compared to isotype pSiNP (Figure 2). The MHC II population was also divided into CD11b$^-$CD11c$^+$ and CD11b$^+$CD11c$^-$ (Figure 2A, right lower panel) to highlight the total nanoparticle accumulation within the CD11c$^+$ DC and CD11b$^+$ macrophage populations. MHC II$^+$CD11b$^-$CD11c$^+$ splenic DC showed positivity for CD11c pSiNP and no detectable levels of isotype pSiNP (Figure 2). Splenic MHC II$^+$CD11b$^+$CD11c$^-$ macrophages[14] accumulated CD11c pSiNP 4 fold higher than isotype pSiNP after 24 h (Figure 2). CD11c pSiNP were preferentially taken up by the MHC II$^+$ CD11b$^-$CD11c$^+$ population within the peripheral blood, at 12 and 24 h, with no detectable uptake of isotype pSiNP (Figure S2 and Figure 2, respectively). Blood macrophages were positive for isotype pSiNP at 1, 12, and 24 h, however, blood DC and macrophage populations indicated no significance uptake between isotype or CD11c pSiNP (Figure S2 and Figure 2). Injecting mice with dye conjugated directly to the antibody in the absence of nanoparticles allowed us to identify differences in biodistribition compared to functionalized pSiNP (Figure S3). Quantification of organ fluorescence in mice injected with isotype or CD11c antibodies only was markedly different to antibodies conjugation to fluorescent pSiNP. Significant differences between isotype and CD11c Ab mice were only observed in the left kidney and the heart, but not the liver or the spleen (Figure S3B). Neither of the splenic and blood DC populations displayed any significant difference between isotype and CD11c antibody injected animals (Figure S3C).

Histological sections displayed brown aggregates in the liver and spleen of CD11c pSiNP and isotype pSiNP mice, respectively (Figure S4). No large aggregates were observed in the heart, lungs, or kidneys. The organs appeared healthy compared to the control animals, with no detectable inflammation. CD11c (PE) and MHC II (FITC) splenic staining confirmed co localization of CD11c and pSiNP supporting observations from flow cytometry (Figure S4).

Murine Regulatory T-Cell Generation with pSiNP. The pSiNP pores (21 ± 11 nm diameter) allow them to be loaded with drugs and peptides.[12] We recently showed consistent rapamycin loading (5% w/w) *via* passive diffusion into the pSiNP pores. This loading regime equated to 1 mg/kg of rapamycin per 20 mg/kg of pSiNP.[15] The cytometric gating highlights the total lymphocyte population. Focusing on this, we isolated CD4 and FoxP3 expressing cells, then further expanding this population to identify the proportion expressing high levels of CD25, obtaining CD4$^+$ CD25$^+$ FoxP3$^+$ Treg (Figure 3A, left to right). Staining of the splenic Treg, 40 days following final intravenous injection, was approximately 5 fold

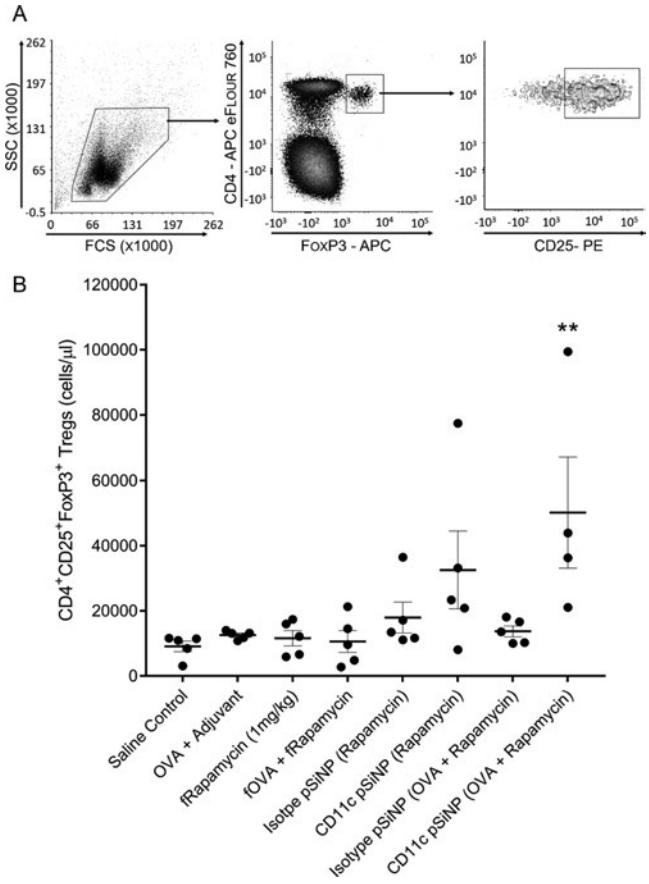

Figure 3. Injections of rapamycin and peptide loaded CD11c pSiNP promote Treg production *in vivo* up to 40 days post injection. (A) Gating strategy of murine splenic CD4$^+$FoxP3$^+$CD25$^+$ Treg. (B) Treg were counted using flow cytometer counting beads to determine the concentration of Treg in OVA sensitized mice spleen. Mice which received CD11c pSiNP (i.v.) loaded with OVA$_{323-339}$ peptide and rapamycin showed an approximate 5 fold increase in the number of splenic Treg compared to the untreated control mice and mice receiving free rapamycin and/or peptide (fRapamycin ± fOVA) with or without pSiNP delivery. (Data are represented as mean ± SEM, n = 5 per group with the exception of CD11c pSiNP (OVA + rapamycin) n = 4, statistical significance determined by one way ANOVA, ** p < 0.01).

higher (p < 0.01) in mice receiving CD11c pSiNP loaded with OVA$_{323-339}$ and rapamycin compared to the saline control, positive control, fRapamycin, (±OVA$_{323-339}$), and isotype pSiNP (OVA + rapamycin) mice (Figure 3). Mice receiving CD11c pSiNP loaded with only rapamycin displayed an increase of approximately 2.5 fold in total splenic Treg concentrations, although not significant (p = 0.1).

Nonhuman Primate DC Targeting DC-SIGN-pSiNP. DC specific receptor DC SIGN is expressed on non human primate and human DC.[16] Isotype and DC SIGN pSiNP accumulated predominantly in the kidneys and liver, with DC SIGN pSiNP also showing up in the lungs of the marmosets (Figure 4). Isotype pSiNP marmoset organs displayed high fluorescence in the kidneys (3.0 × 10^8 RE), liver (1.8 × 10^8 RE), and spleen (1.4 × 10^8 RE), with small amounts of fluorescence detected in the lungs (2.5 × 10^7 RE) and heart (2.5 × 10^7 RE). DC SIGN pSiNP tracked mostly to the kidneys (5.0 × 10^8 RE), followed by the liver (6.5 × 10^7 RE),

DOI: 10.1021/acsnano.8b01625
ACS Nano 2018, 12, 6637–6647

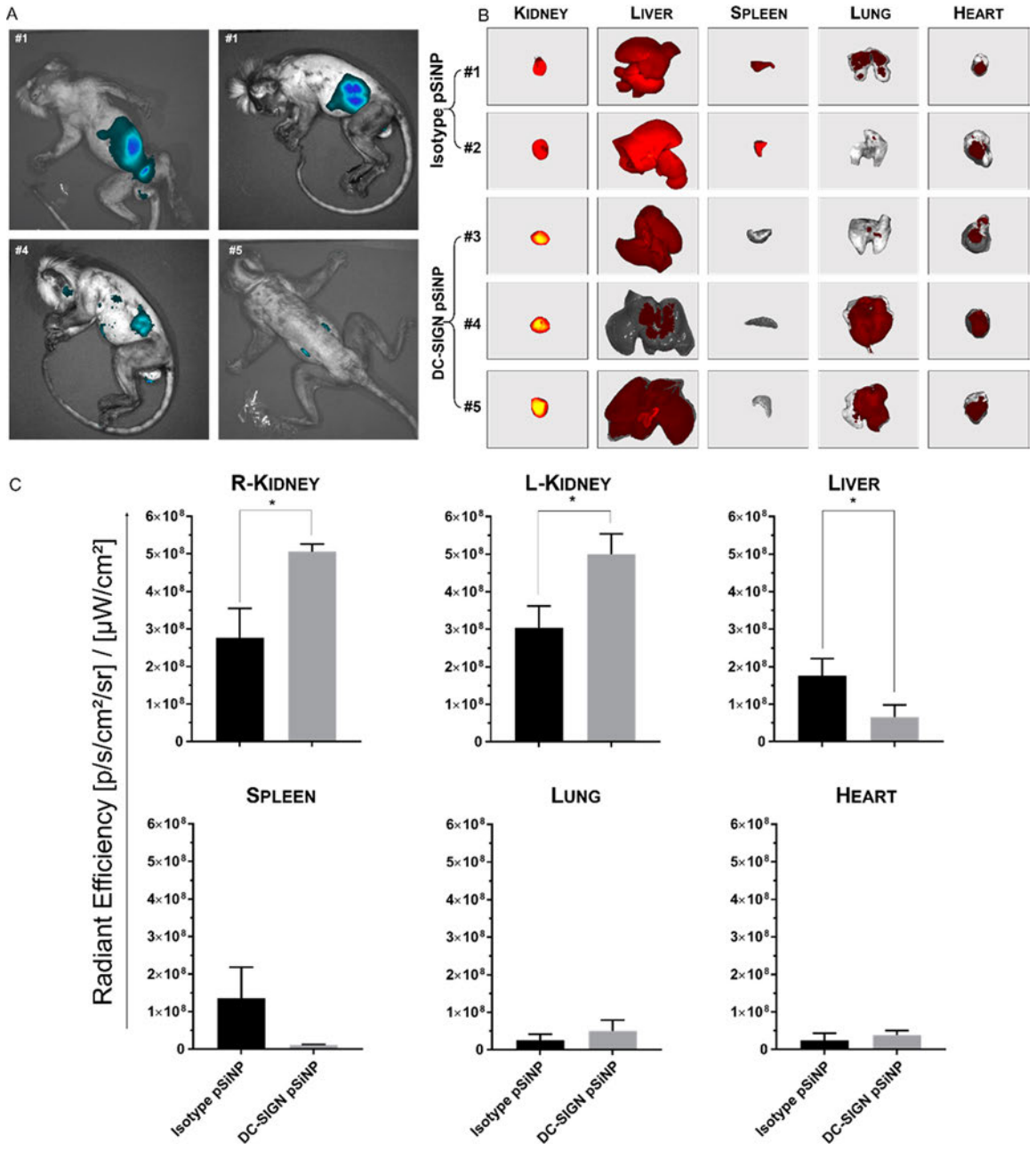

Figure 4. CD SIGN pSiNP track predominately to the kidneys, followed by the liver, spleen, lungs, and heart. (A) Topographical distribution of fluorescent pSiNP in marmosets at 24 h indicated by blue color. Isotype pSiNP (top) accumulated around kidneys and liver; DC SIGN pSiNP (bottom), present in the kidneys and lungs of marmosets. (B) Individual organs taken from the marmosets at 24 h post injection (i.v.) with fluorescent pSiNP. Heat map (red to yellow) indicates presence of pSiNP. (C) Quantification of total fluorescence as radiant efficiencies of each of the organs at 24 h. Marmosets injected with CD11c pSiNP showed a higher level in the kidneys compared to marmosets which received isotype pSiNP. DC SIGN pSiNP tracked highly to the lungs of the animals. DC SIGN pSiNP has significantly greater deposition within the kidneys compared to isotype pSiNP, which were seen to accumulate significantly more within the livers of the marmosets. (Data are represented as mean ± SD, isotype pSiNP $n = 2$, DC SIGN pSiNP $n = 3$, significance determined by two tailed t test, * $p < 0.05$).

lungs (5.0×10^7 RE), heart (3.9×10^7), and spleen (1.0×10^7 RE) within 24 h.

The lineage negative, MHC II$^+$CD11c$^+$ splenic myeloid DC population indicated a 3.5 fold uptake increase of the isotype pSiNP compared to the DC SIGN pSiNP. Blood myeloid DC had detectable levels of DC SIGN pSiNP in one of the three marmosets, whereas isotype pSiNP was not seen in blood myeloid DC (Figure 5). Splenic CD14$^+$ monocytes showed an uptake of DC SIGN pSiNP with no detectable levels of isotype pSiNP. Blood monocytes accumulated isotype pSiNP approximately 2 fold more than DC SIGN pSiNP, although no significant difference was observed (Figure 5). Splenic CD20$^+$ B cells showed a 7 fold greater positivity for isotype pSiNP compared to DC SIGN pSiNP. No off targeting uptake of pSiNP was observed by CD3$^+$ T cells and CD56$^+$ natural killer cells.

Urine analyzed by inductive coupled plasma mass spectrom etry (ICP MS) quantified boron and silicon deposits within

DOI: 10.1021/acsnano.8b01625
ACS Nano 2018, 12, 6637–6647

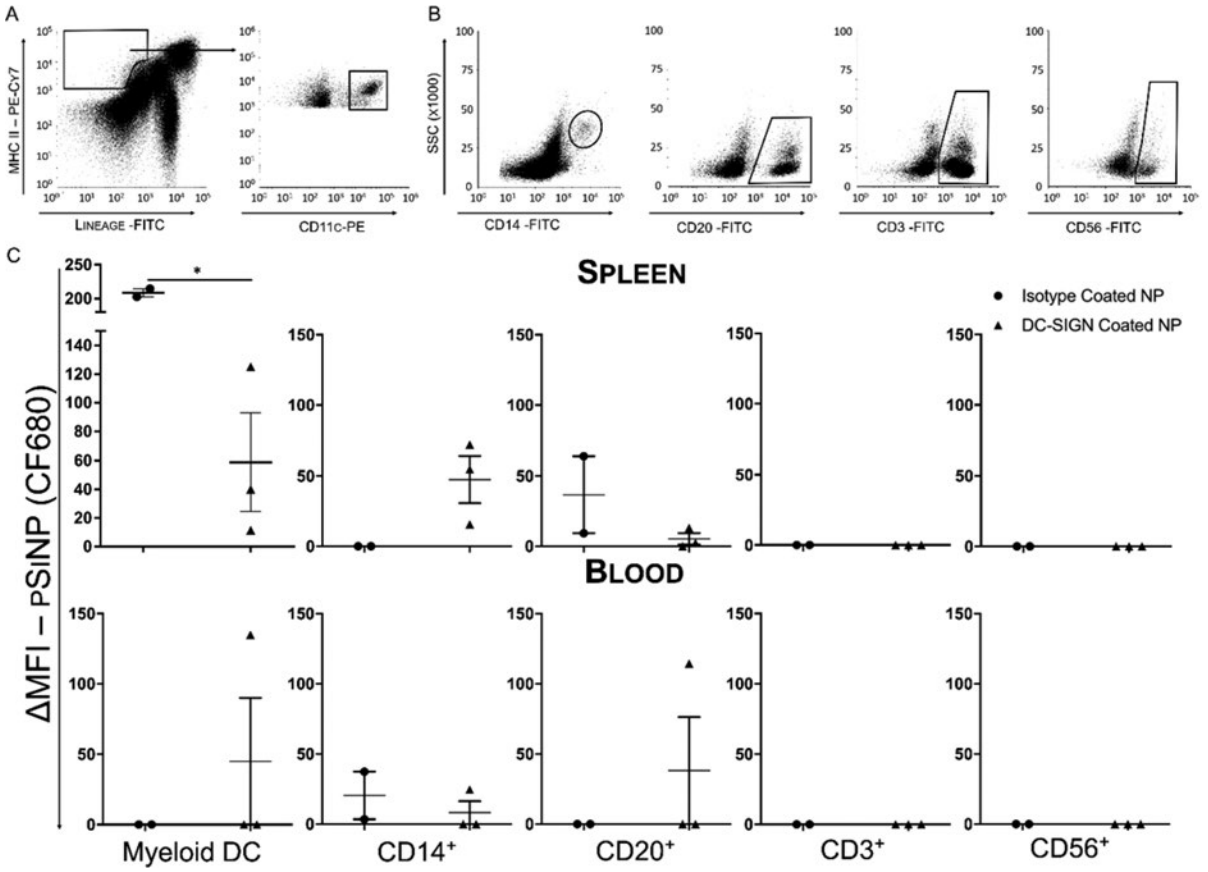

Figure 5. Flow cytometric of marmoset cellular uptake of pSiNP. (A) Marmoset gating strategy of lineage negative MHC II$^+$CD11c$^+$ myeloid DC. (B) Gating of monocytes (CD14), B cells (CD20), T cells (CD3), and natural killer cell (CD56) populations for flow cytometry. (C) Splenic and peripheral blood cell populations nanoparticle uptake. A higher proportion of isotype pSiNP were phagocytosed by splenic myeloid DC compared to DC SIGN pSiNP. (Data are presented as ΔMFI ± SEM. Isotype pSiNP n = 2, DC SIGN pSiNP n = 3, statistical significance determined by two tailed t test, * $p < 0.05$).

the urine. Isotype pSiNP marmosets displayed a 10 fold (6 ppm) and 7 fold (103 ppm) higher concentration of boron and silicon in the urine, respectively, compared to DC SIGN pSiNP marmosets (Figure 6).

pSiNP were detected within the liver, heart, lungs, and kidneys of the marmosets, with few detectable clusters present in the spleen (Figure S5). DC SIGN pSiNP marmoset lungs showed aggregates ranging from 1 to 10 μm in size and were more dispersed throughout the tissue compared to the isotype pSiNP marmosets (≤8 μm). Ten μm clusters in livers from pSiNP DC SIGN pSiNP marmoset could be seen, with isotype pSiNP marmoset clusters generally smaller (≤4.5 μm).

DISCUSSION

In this study, DC targeted pSiNP were functionalized with anti CD11c or anti DC SIGN antibodies to investigate biodistribution *in vivo*. The nanoparticles, <200 nm in size and functionalized with a semicarbazide linker, allowed for the direct conjugation of antibody and fluorescent dye to their surface. We have comprehensively characterized these pSiNP recently in Cifuentes Rius *et al.*[12] As DC play a major role in both immunostimulation and immunosuppression within the immune system, they are the most potent of the antigen presenting cells and are responsible for the phagocytosis and presentation of foreign peptides as well as the maintenance of immunological self tolerance. Foreign peptides are processed and presented on MHC classes I and II which bind complementary receptors expressed on CD8$^+$ and CD4$^+$ T lymphocytes, respectively.[17] If appropriate signaling occurs *via* the binding of co stimulatory proteins CD80/CD86 and CD40 on DC interacting with CD28 and CD40L expressed on T lymphocytes, an inflammatory response promotes the clonal expansion of T lymphocytes with the aid of pro inflammatory cytokines.[18,19] Clonal expansion of antigen specific CD4$^+$ T cells promotes B lymphocyte differentiation into antibody producing plasma cells, contributing to the humoral immunity.[20] However, a lack of co stimulatory marker expression by DC may promote T cell anergy and immune system senescence.[11] These DC are termed tol DC by their ability to induce CD4$^+$FoxP3$^+$ Tregs that promote immuno logical tolerance toward foreign antigens, such as those seen in allogeneic organ transplantation. DC are key immune cells, and there is significant benefit to targeting them *in vivo* to treat cancer, induce tolerance, and develop new vaccines. Phase 1 clinical trials utilizing DC therapy to treat metastatic renal cell carcinoma (RCC) have been explored by Wierecky *et al.*[21] HLA A2 binding MUC1 peptide pulsed autologous mature DC, derived from peripheral blood monocytes, were subcutaneously injected into patients with RCC. This study found a proportion of patients demonstrated tumor regression when treated with peptide pulsed DC. Intravenous delivery of *ex vivo* modified tol DC, preconditioned with vitamin D3 and IL 10, has also prolonged allogeneic kidney graft survival in NHP.[22] These methods utilized *ex vivo* modification of DC

DOI: 10.1021/acsnano.8b01625
ACS Nano 2018, 12, 6637–6647

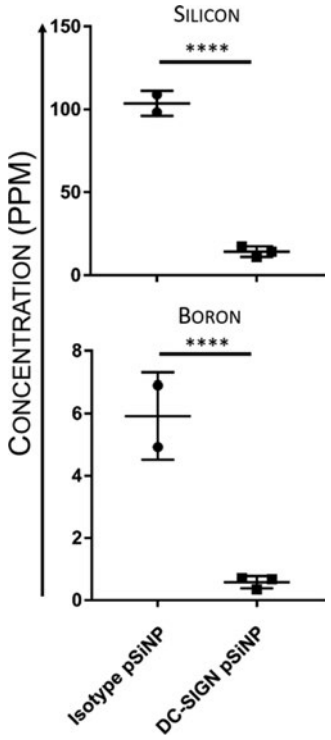

Figure 6. Isotype pSiNP are secreted more readily than DC SIGN pSiNP in NHP. The pSiNP injected into the marmosets were produced from wafers doped with boron to produce optimal resistivity for pSiNP etching. Due to this process, silicon and boron are the two major degradation products of the pSiNP and can hence be used to measure particle secretion. Marmosets injected with DC SIGN pSiNP had an approximately 7 fold and 10 fold lower concentration of silicon and boron in their urine, respectively. (Data are representative of mean ± SD, $n = 2$ (isotype pSiNP) $n = 3$ (DC SIGN pSINP). Statistical significance was determined by two tailed t test, **** $p < 0.0001$).

prior to infusion. The emerging field of nanomedicine can bypass this modification by their targeted therapeutic delivery mechanisms.[23] We successfully targeted DC populations within murine and NHP animal models. OVA sensitized mice demonstrated a significant 5 fold increase in Treg, maintained for up to 40 days postinjections. We have established an alternative method of drug delivery to induce Treg generation completely *in vivo* while reducing off targeting effects shown by enhanced delivery with DC targeting antigen functionalized pSiNP.

Neither mice nor NHP showed adverse reaction to intravenous administration of pSiNP. DC targeting pSiNP in both models showed systemic distribution to the kidneys, liver, spleen, and lungs. Large nanoparticles (≈ 200 nm) have been shown to aggregate *in vivo* by activating the intrinsic coagulation system.[24] Clot formation promotes fibrinogen and globulin binding to nanoparticle surface, known as corona formation.[25] These proteins unfold, linking to adjacent nanoparticles causing aggregates.[26] Furthermore, nanoparticle induced unfolding of fibrinogen promotes macrophage activation by Mac 1 (CD11b) binding.[27] This phenomenon could explain the observed pSiNP aggregation within some of the tissues. Intravenous pSiNP administration in mice traveled *via* the vena cava to the heart. Large pSiNP aggregates would travel unencumbered through larger atrial and ventricular spaces, resulting in minimal accumulation, which was consistent in both animal models and evident from the low organ fluorescence (Figures 1 and 4). The pulmonary circulation offers a site of restricted movement, due to alveolar capillaries, providing an optimal location for pSiNP aggregation, indicative of increase lung fluorescence. This accumulation may be enhanced by the presence of pulmonary macrophages.[28] Arterial circulation carries pSiNP to the liver, spleen, and kidneys. pSiNP uptake in the liver could be attributed to the non specific phagocytic nature of liver Kupffer cells,[29] one of the most abundant populations of macrophages, resulting in the increased fluorescence (Figure 1). We observed CD11c pSiNP preferentially tracked to the spleen compared to isotype pSiNP as well as accumulated significantly in the kidneys compared to all other organs. These pSiNP degrade by 90% within 24 h.[15] Once broken down, these nanoparticles are renally excreted as non toxic silicic acid.[30]

The NHP circulation is identical to mice, with the femoral vein traveling to the inferior vena cava *via* the iliac vein. However, distribution of pSiNP was markedly different. Marmosets displayed high levels of pSiNP accumulation within the lungs. This phenomenon was augmented in marmosets injected with DC SIGN pSiNP, potentially reducing the levels of DC SIGN pSiNP in the liver compared to the isotype pSiNP (Figure 4). The undiagnosed, histologically indicative, chronic lung disease in the marmosets (average age 13 years) compared to juvenile (6−8 weeks) mice, may explain this finding. Splenic deposition was also different compared to the mice. Isotype pSiNP accumulated in the spleen more than the DC SIGN pSiNP. In accordance with the murine model, kidney fluorescence intensity was significantly higher in DC targeting pSiNP marmosets. Urine analysis showed that although marmosets had a larger accumulation of DC SIGN pSiNP within the kidneys, isotype pSiNP marmosets secreted 7 fold higher silicon concentrations, suggesting prolonged DC SIGN pSiNP retention.

Cytometric analysis of murine and marmoset splenic DC subsets reflected the total splenic fluorescence. CD11c pSiNP mice had significantly greater fluorescence within the spleens and significantly higher uptake by lineage negative, MHC CII^+CD4^+ and $CD8\alpha^+$ conventional DC populations. $CD4^+$ and $CD8\alpha^+$ DC had 9 fold and 31 fold higher fluorescence intensities in CD11c pSiNP mice, respectively, highlighting the importance of nanoparticle functionalization with antibodies to preferentially target some of the least abundant cells. A higher concentration of CD11c pSiNP in the spleen increases the chance of non specific uptake, indicated by CD11c pSiNP fluorescence in $CD11b^+CD11b^-$ macrophages (Figure 2). The uptake of pSiNP within $CD11c^+$ blood DC was significantly reduced compared to the spleen with little fluorescence observed. Blood $CD11b^+$ macrophages were more positive for isotype pSiNP compared to CD11c pSiNP, potentially due to the increased targeting and uptake of CD11c pSiNP by DC, resulting in fewer circulating CD11c pSiNP remaining for macrophage phagocytosis. Confocal microscopy of the spleen showed that CD11c pSiNP were more abundant and highly distributed throughout, compared to isotype pSiNP (Figure S2).

pSiNP tracking to marmoset splenic myeloid DC produced contrary results. Isotype pSiNP were phagocytosed 3.5 fold more by the lineage negative, MHC CII^+CD11c^+ myeloid DC, while DC SIGN pSiNP were taken up predominately by $CD14^+$ monocytes. One DC SIGN pSiNP marmoset showed a high level of pSiNP uptake by blood $CD11c^+$ DC. This

DOI: 10.1021/acsnano.8b01625
ACS Nano 2018, 12, 6637−6647

particular marmoset also displayed minimal fluorescence in the lungs compared to the other two injected with DC SIGN pSiNP. Since pSiNP were not trapped within the pulmonary circulation in that marmoset, they could remain in the circulation until they reached the spleen. The remaining two DC SIGN pSiNP marmosets had significantly higher lung accumulation of pSiNP, which would decrease circulating mass. Primate histology revealed chronic lung damage and inflammation, best characterized as chronic airways disease, potentially due to their age. The pathology seen in the lung may have promoted alveolar macrophage recruitment,[31,32] resulting in a higher degree of non specific phagocytosis of pSiNP. Alternatively, pulmonary DC within the lungs may have been targeted by the particles.

The different tracking ability of DC targeting pSiNP in murine and NHP models may also be explained by the difference in targeting antigens and animal species. These data showed that CD11c pSiNP promoted DC specific targeting to a greater extent than DC SIGN pSiNP. Murine DC SIGN was not utilized due to its expression on only $CD4^+$ conventional DC as well as placmacytoid pre DC lineages.[33] Therefore, CD11c was more analogous to human DC SIGN, being expressed on only murine myeloid DC lineages. We have also established the use of this cross reactive human DC SIGN antibody clone to classify marmoset monocyte derived DC.[34]

Tol DC lack the necessary co stimulatory markers required for naïve T cell activation. Instead, tol DC differentiate naïve T cells into Treg or enhance the function of pre existing Treg. Rapamycin induced selective expansion of murine $CD4^+CD25^+FoxP3^+$ Treg has been well documented by Battaglia *et al.*[35] Upon repeated stimulation with the OVA protein on days 33, 47, and 61, the rapamycin and $OVA_{323-339}$ peptide preconditioned DC would continue to phagocytose and process the OVA protein for continued promotion of the discrete pool of OVA reactive regulatory T cells. OVA sensitized CD11c pSiNP (rapamycin + $OVA_{323-339}$) mice showed a significantly (5 fold) higher level of Treg compared to the mice treated with i.v. rapamycin or isotype pSiNP. This finding demonstrates the importance of nanoparticle functionalization with cell targeting antibodies. We have expanded on our *in vitro* work where we induced tol DC with rapamycin loaded pSiNP[15] by promoting Treg expansion completely *in vivo*. Future experiments utilizing these pSiNP should explore longer time points to follow Treg fate. We previously demonstrated the ability to produce camptothecin loaded silicon nanoparticles, nanodiscs, and silica nanopills for the targeted killing of neuroblastoma cancer cells.[36−38] We have now explored the potential of these pSiNP within a transplant immunology setting. Translation of this protocol into a transplantation model to induce graft tolerance without *ex vivo* DC modification would be highly beneficial in exploring the full extent of these nanoparticles.

Pathological changes, potentially due to age related illness, may have resulted in the high pSiNP tracking variability within the DC SIGN pSiNP animal test group, potentially skewing the *in vivo* tracking abilities and is a main limitation within this study. The lack of a completely identical targeting antigen between the murine and NHP animal models also made it difficult to compare pSiNP uptake between the two species. Potential future directions include functionalizing pSiNP with marmoset reactive CD11c antibody, identifying if this promotes DC uptake within the spleen. Younger marmosets should also be utilized for these experiments, as it was seen that one of the DC SIGN pSiNP marmosets did display tracking abilities to both splenic and blood DC *in vivo,* suggesting a potentially highly beneficial method for targeting both populations of DC.

CONCLUSION

In conclusion, pSiNP displaying DC targeting mAb were well tolerated in mice and in NHP. The animals showed no adverse side effects or embolus formation from particle aggregation. Effective targeting to blood and tissue DC was demonstrated. pSiNP loaded with rapamycin, targeting CD11c promoted the generation of Treg *in vivo* without the more commonly used preliminary *ex vivo* modification of DC. An unexpected and interesting finding was the enhanced kidney targeting ability of DC targeting pSiNP, demonstrating a significantly higher renal tracking capability in murine and NHP models, compared to isotype pSiNP. Identifying this enhanced pSiNP tracking to the kidneys offers a potential route to treat rare conditions such as Fanconi syndrome, cystinuria, and even renal cell cancer. This is enhanced by the ability of pSiNP to be loaded with a variety of medications, chemotherapeutics, or even genomic payloads, providing a more localized, targeted delivery. In conjunction with our recent findings, that pSiNP can modify DC function *in vitro*, this study provides further *in vivo* validation for the potential of targeted nanomedicine for future drug delivery in transplantation and other immune mediated diseases.

MATERIALS AND METHODS

Mice. Male C57BL/6 mice 7−8 weeks old were purchased from Animal Resources Center, Western Australia. Mice received intravenous (i.v.) injections of pSiNP (20 mg/kg) coated with purified Armenian hamster isotype control monoclonal antibody (mAb) (BD Biosciences, California, USA. Clone G94−56) or purified Hamster antimouse CD11c mAb (BD Biosciences. Clone HL3). Animals were imaged at 1, 6, 12, and 24 h. Mice were maintained in the University of Adelaide Animal Facility in accordance with Australian animal ethics guidelines, applications 20123 and 31951.

Marmosets. Common marmoset (*Callithrix jacchus*) monkeys were housed at The Queen Elizabeth Hospital Animal house. Marmosets received i.v. injections *via* left femoral vein, of pSiNP (20 mg/kg) coated in purified isotype control (eBioscience, California, USA, Clone eBMG2b) or DC SIGN mAb (BD Biosciences, Clone DCN46). Animals were euthanized 24 h post injection. Prior to the autopsy, marmosets were imaged to obtain a topographic distribution of pSiNP. Marmosets were maintained at the Queen Elizabeth Hospital Animal Facility in accordance with the NHMRC Australian guidelines for the holding and use of non human primates for medical research. CALHN animal ethics committee approval number 55 15.

Immunization Protocol. C57BL/6 mice immunization protocol was adapted from Maldonado *et al.*[39] Mice were subcutaneously injected with 100 μg of OVA protein (Grade V, Sigma. Missouri, USA) admixed 1:1 (v/v) in saline and Alhydrogel adjuvant (*Invivo*Gen, California, USA), to a final volume of 100 μL on days 0, 14, and 28. Concurrently, mice received a 100 μL i.v. injection of saline, free rapamycin (fRapamycin, 1 mg/kg), 100 μg fluorescently labeled free $OVA_{323-339}$ peptide (FITC βAla ISQAVHAAHAEI NEAGR OH, Auspep, Victoria, Australia) (fOVA) and fRapamycin, or isotype or CD11c pSiNP loaded with rapamycin and/or $OVA_{323-339}$. Challenges of 100 μg of OVA protein were given on days 33, 47, and 61 subcutaneously. Mice were humanely euthanized on day 68.

Preparation of pSiNP. pSiNP were prepared as previously described.[15] Silicon wafers were electrochemically etched and polished in aqueous hydrofluoric acid. The porous layer was fractured

DOI: 10.1021/acsnano.8b01625
ACS Nano 2018, 12, 6637−6647

by ultrasonication and filtered. Filtrate was resuspended in a 0.1 M solution of protected semicarbazide (*tert* butyl 2 [(allylamino) carbonyl] hydrazine carboxylate)[40] in tetrahydrofuran for 3 h at 85 °C under N_2 reflux. Nanoparticles were rinsed twice in tetrahydrofuran and twice in ethanol (EtOH) and stored at 4 °C.

Drug and Peptide Loading of pSiNP. Boc group was removed from the protected semicarbazide by resuspending pSiNP in a 2:3 solution of dichloromethane and trifluoroacetic acid and agitated (4 h, room temperature (RT)) and washed once in dichloromethane, twice in EtOH and twice in saline (22,000*g*, 10 min).[15] pSiNP were loaded with rapamycin, with or without fluorescently labeled $OVA_{323-339}$ peptide. Deprotected pSiNP were resuspended in a solution of rapamycin dissolved in EtOH (2 mg/mL) and incubated for 2 h at RT. The pSiNP were washed once in saline and resuspended in a solution of $OVA_{323-339}$ (1:5 ratio of peptide to pSiNP) in saline (10 min, RT) before the addition of the oxidized antibody.

Antibody and Fluorophore Coating of pSiNP. Antibody attachment to pSiNP was as previously described.[15] Antibodies and appropriate isotype matched controls were admixed with sodium periodate and placed on an orbital shaker in the dark for 30 min (RT, 60 rpm). Antibodies were washed in PBS with centrifugal concentrators (Sartorius, Germany). Nanoparticles were resuspended in oxidized antibody for 30 min and agitated. Antibody binding was confirmed by measuring the UV absorbance (280 nm) (Nanodrop 2000, Thermo Scientific, Massachusetts, USA). For the tracking experiments, antibody labeled pSiNP were pelleted and resuspended in a solution of XenoLight CF680 succinimidyl ester (SE) dye (PerkinElmer. Massachusetts, USA) dissolved in a 1 mM solution of sodium carbonate buffer (pH = 9). Samples were placed in the dark on an orbital shaker for 1 h (RT, 60 rpm). Nanoparticles were washed several times in saline (22,000*g*, 2 min) until the supernatant was colorless and resuspended in saline and sonicated thoroughly immediately prior to injection.

***In Vivo* and *ex Vivo* Fluorescence Imaging.** Animals or their kidneys, livers, hearts, lungs, and spleens were placed in an IVIS Lumina Series III Imaging System (Caliper Life Sciences, Massacutests, USA). The charge coupled device camera obtained fluorescence images utilizing the appropriate filter combinations (excitation 660 nm, emission 680−700 nm). Reflected light photographs were overlaid with fluorescent images and analyzed using Living Images 4.5.5 software. Signal intensity was assessed by radiant efficiencies (RE) ($[p/s/cm^2/sr]/[\mu W/cm^2]$).

Murine and Non-Human Primate Splenocyte Processing. Harvested spleens were kept at 4 °C in RPMI 1640 (Invitrogen, Massachusetts, USA). Spleens were homogenized through a 70 μm filter and resuspended in 50 mL in PBS. Filtrate was centrifuged, 450*g* for 7 min at RT. The supernatant was discarded, and the pellet resuspended in 10−30 mL of red blood cell lysis buffer (155 mM NH_4Cl, 5 mM $NaHCO_3$, 127 μM EDTA) and incubated at 37 °C for 10 min. Cells were washed in PBS (1% heat inactivated fetal calf serum (FCS)). Splenocytes were resuspended in FACS wash buffer (phosphate buffered saline (PBS), 1% FCS, 20 mM sodium azide) containing 10% heat inactivated rabbit serum to a concentration of 1×10^6 cell/ml and blocked for 20 min (RT) before flow cytometry staining.

***In Vivo* Tracking Flow Cytometry Staining.** Whole blood or splenocytes were stained with antibodies (Tables S1 and S2) and incubated at 4 °C for 30 min. After incubation, FACS lysing solution (BD Biosciences) was added to the splenocytes and the whole blood, 1 or 2 mL, respectively, and vortexed. The cells were washed in wash buffer until supernatants were clear and resuspended in 200 μL wash buffer before acquisition on a FACSCanto II (BD Biosciences) and analysis with FCS Express v6 (*De Novo* Software, Glendale, CA).

Regulatory T-Cell Staining. Murine splenic Treg were stained as per manufacturer's instructions (Treg detection kit, Miltenyi Biotec. Bergisch Gladbach, Germany). Briefly, 2×10^6 splenocytes were resuspended in 100 μL of wash buffer with the addition of CD4 (clone GK1.5, eBioscience) and CD25 (clone 7D4, Miltenyi Biotec) antibodies. The cells were incubated in the dark (10 min, 4 °C). Splenocytes were washed in wash buffer (300*g* for 5 min) and resuspended in fix/perm buffer (30 min, 4 °C). Splenocytes were washed in wash buffer and permeabilization buffer before the addition of FoxP3 antibody (30 min, 4 °C). Prior to acquisition on a FACSCanto II, APC Calibrite counting beads (BD Biosciences) were added.

Scanning Electron Microscopy (SEM). Tissue sections were gradient dehydrated (70−90% 10 min, RT) and 100% (2×, 10 min, RT) in undenatured EtOH devoid of silicon. Samples were allowed to air dry and placed on an aluminum SEM mounting stub (Ted Pella, California, USA) and splutter coated (Quorum Q150T ES, Quorum Technologies. Lewes, UK) with carbon. Samples were imaged with a XL30 SEM (Philips Electrical Company, Amsterdam, Netherlands).

Histopathological Analyses. Organs were fixed in 10% formaldehyde for light microscopic examination. Following routine dehydration and transparency procedures, the tissues were embedded in paraffin blocks. Five μm sections were melted onto Superfrost microscope slides (Thermo Scientific). Sections were stained with hematoxylin and eosin (H&E).

Immunofluorescence. Optimal cutting temperature (OCT) compound (Agar Scientific. Essex, United Kingdom) embedded murine tissues were sectioned and transferred to slides. Unfixed tissues were stained *via* direct immunofluorescence. Sections were equilibrated to RT and washed in PBS for 5 min. Sections were then incubated at RT for 30 min in 10% blocking buffer before primary conjugated antibody was added for 1 h, in the dark. Sections were washed in PBS (2 × 5 min) before the addition of 4′,6′ diamidino 2 phenylindole (DAPI) (Biolegend, California, USA) for nucleus staining and mounting with fluorescent mounting media (Dako, Glostrup Municipality, Denmark).

Inductively-Coupled Plasma Mass Spectrometry (ICP-MS). Urine samples taken from the marmosets were diluted in ICP MS buffer (2% 1 butanol, 0.05% EDTA, 0.05% Triton X 100, and 1% NH_4OH in water) and run on an Agilent 8800 Triple Quadrupole ICP MS (Agilent Technologies, California, USA).

ASSOCIATED CONTENT

Supporting Information

The Supporting Information is available free of charge on the ACS Publications website at DOI: 10.1021/acsnano.8b01625.

Additional figures and tables (PDF)

AUTHOR INFORMATION

Corresponding Authors

*E mail: toby.coates@sa.gov.au.

*E mail: nicolas.voelcker@monash.edu.

ORCID

Sebastian O. Stead: 0000 0001 8567 7042

Jean-Olivier Durand: 0000 0003 4606 2576

Nicolas H. Voelcker: 0000 0002 1536 7804

Notes

The authors declare no competing financial interest.

ACKNOWLEDGMENTS

We would like to acknowledge Ms. M. Archer and Ms. L. Hodson for their assistance with tissue processing. Mr. M. Smith, facility manager of the Queen Elizabeth Hospital animal house, and Dr. D. Noonan and Dr. T. Kuchel for their assistance with animal procedures. We would also like to acknowledge the University of Adelaide, Adelaide Microscopy (AM) and the Australian Microscopy Microanalysis Research Facility (AMMRF). This work was performed in part at the Melbourne Center for Nanofabrication (MCN) in the Victorian Node of the Australian National Fabrication Facility (ANFF).

DOI: 10.1021/acsnano.8b01625
ACS Nano 2018, 12, 6637−6647

REFERENCES

(1) Chatrath, H.; Berman, K.; Vuppalanchi, R.; Slaven, J.; Kwo, P.; Tector, A. J.; Chalasani, N.; Ghabril, M. *De Novo* Malignancy Post−Liver Transplantation: A Single Center, Population Controlled Study. *Clin. Transplant.* **2013**, *27*, 582−590.

(2) Tilney, N. L. *Transplant: From Myth to Reality*; Yale University Press: New Haven, CT, 2003; p 116.

(3) Maldonado, R. A.; von Andrian, U. H. How Tolerogenic Dendritic Cells Induce Regulatory T *Cells*. *Adv. Immunol.* **2010**, *108*, 111−165.

(4) Coates, P. T. H.; Thomson, A. W. Dendritic Cells, Tolerance Induction and Transplant Outcome. *Am. J. Transplant.* **2002**, *2*, 299−307.

(5) Coates, P. T. H.; Barratt Boyes, S. M.; Donnenberg, A. D.; Morelli, A. E.; Murphey Corb, M.; Thomson, A. W. Strategies for Preclinical Evaluation of Dendritic Cell Subsets for Promotion of Transplant Tolerance in the Non Human Primate. *Hum. Immunol.* **2002**, *63*, 955−965.

(6) Thomson, A. W.; Zahorchak, A. F.; Ezzelarab, M. B.; Butterfield, L. H.; Lakkis, F. G.; Metes, D. M. Prospective Clinical Testing of Regulatory Dendritic Cells in Organ Transplantation. *Front. Immunol.* **2016**, *7*, 1−11.

(7) Sehgal, S. N. Rapamune®(Rapa, Rapamycin, Sirolimus): Mechanism of Action Immunosuppressive Effect Results from Blockade of Signal Transduction and Inhibition of Cell Cycle Progression. *Clin. Biochem.* **1998**, *31*, 335−340.

(8) Silk, K. M.; Leishman, A. J.; Nishimoto, K. P.; Reddy, A.; Fairchild, P. J. Rapamycin Conditioning of Dendritic Cells Differ entiated from Human ES Cells Promotes a Tolerogenic Phenotype. *J. Biomed. Biotechnol.* **2012**, *2012*, 1−11.

(9) Taner, T.; Hackstein, H.; Wang, Z.; Morelli, A. E.; Thomson, A. W. Rapamycin Treated, Alloantigen Pulsed Host Dendritic Cells Induce Ag Specific T Cell Regulation and Prolong Graft Survival. *Am. J. Transplant.* **2005**, *5*, 228−236.

(10) Turnquist, H. R.; Raimondi, G.; Zahorchak, A. F.; Fischer, R. T.; Wang, Z.; Thomson, A. W. Rapamycin Conditioned Dendritic Cells Are Poor Stimulators of Allogeneic CD4+ T Cells, but Enrich for Antigen Specific FoxP3+ T Regulatory Cells and Promote Organ Transplant Tolerance. *J. Immunol.* **2007**, *178*, 7018−7031.

(11) Pothoven, K.; Kheradmand, T.; Yang, Q.; Houlihan, J.; Zhang, H.; Degutes, M.; Miller, S.; Luo, X. Rapamycin Conditioned Donor Dendritic Cells Differentiate CD4+ CD25+ FoxP3+ T Cells *In Vitro* with TGF B1 for Islet Transplantation. *Am. J. Transplant.* **2010**, *10*, 1774−1784.

(12) Cifuentes Rius, A.; Ivask, A.; Sporleder, E.; Kaur, I.; Assan, Y.; Rao, S.; Warther, D.; Prestidge, C. A.; Durand, J. O.; Voelcker, N. H. Dual Action Cancer Therapy with Targeted Porous Silicon Nano vectors. *Small* **2017**, *13*, 1701201.

(13) Edwards, A. D.; Chaussabel, D.; Tomlinson, S.; Schulz, O.; Sher, A.; Reis e Sousa, C. Relationships among Murine CD11c(high) Dendritic Cell Subsets as Revealed by Baseline Gene Expression Patterns. *J. Immunol.* **2003**, *171*, 47−60.

(14) Gonçalves, R.; Mosser, D. M. The Isolation and Character ization of Murine Macrophages. *Curr. Protoc. Immunol.* **2015**, *83*, 14.1.1−14.1.16.

(15) Stead, S. O.; McInnes, S. J.; Kireta, S.; Rose, P. D.; Jesudason, S.; Rojas Canales, D.; Warther, D.; Cunin, F.; Durand, J. O.; Drogemuller, C. J.; Carroll, R. P.; Coates, P. T.; Voelcker, N. H. Manipulating Human Dendritic Cell Phenotype and Function with Targeted Porous Silicon Nanoparticles. *Biomaterials* **2018**, *155*, 92−102.

(16) Jesudason, S.; Collins, M. G.; Rogers, N. M.; Kireta, S.; Coates, P. T. H. Non Human Primate Dendritic Cells. *J. Leukocyte Biol.* **2012**, *91*, 217−228.

(17) Hochweller, K.; Wabnitz, G. H.; Samstag, Y.; Suffner, J.; Hämmerling, G. J.; Garbi, N. Dendritic Cells Control T Cell Tonic Signaling Required for Responsiveness to Foreign Antigen. *Proc. Natl. Acad. Sci. U. S. A.* **2010**, *107*, 5931−5936.

(18) McLellan, A.; Heiser, A.; Hart, D. Induction of Dendritic Cell Costimulator Molecule Expression Is Suppressed by T Cells in the Absence of Antigen Specific Signalling: Role of Cluster Formation, CD40 and HLA Class II for Dendritic Cell Activation. *Immunology* **1999**, *98*, 171.

(19) Thompson, C. B.; Lindsten, T.; Ledbetter, J. A.; Kunkel, S. L.; Young, H. A.; Emerson, S. G.; Leiden, J. M.; June, C. H. CD28 Activation Pathway Regulates the Production of Multiple T Cell Derived Lymphokines/Cytokines. *Proc. Natl. Acad. Sci. U. S. A.* **1989**, *86*, 1333−1337.

(20) Alberts, B.; Johnson, A.; Lewis, J.; Raff, M.; Roberts, K.; Walter, P. *Mol. Biol. Cell.*, 4th ed.; Garland Science: New York; 2002; pp 3486−3490.

(21) Wierecky, J.; Müller, M. R.; Wirths, S.; Halder Oehler, E.; Dörfel, D.; Schmidt, S. M.; Häntschel, M.; Brugger, W.; Schröder, S.; Horger, M. S.; Kanz, L.; Brossart, P. Immunologic and Clinical Responses After Vaccinations with Peptide Pulsed Dendritic Cells in Metastatic Renal Cancer Patients. *Cancer Res.* **2006**, *66*, 5910−5918.

(22) Ezzelarab, M.; Zahorchak, A.; Lu, L.; Morelli, A.; Chalasani, G.; Demetris, A.; Lakkis, F.; Wijkstrom, M.; Murase, N.; Humar, A.; Shapiro, R.; Cooper, D. K.; Thomson, A. W. Regulatory Dendritic Cell Infusion Prolongs Kidney Allograft Survival in Nonhuman Primates. *Am. J. Transplant.* **2013**, *13*, 1989−2005.

(23) Fan, Y.; Moon, J. J. Nanoparticle Drug Delivery Systems Designed to Improve Cancer Vaccines and Immunotherapy. *Vaccines* **2015**, *3*, 662−685.

(24) Ilinskaya, A. N.; Dobrovolskaia, M. A. Nanoparticles and the Blood Coagulation System. Part II: Safety Concerns. *Nanomedicine* **2013**, *8*, 969−981.

(25) Ajdari, N.; Vyas, C.; Bogan, S. L.; Lwaleed, B. A.; Cousins, B. G. Gold Nanoparticle Interactions in Human Blood: A Model Evaluation. *Nanomedicine* **2017**, *13*, 1531−1542.

(26) Dominguez Medina, S.; Kisley, L.; Tauzin, L. J.; Hoggard, A.; Shuang, B.; Indrasekara, A. S. D. S.; Chen, S.; Wang, L. Y.; Derry, P. J.; Liopo, A.; et al. Adsorption and Unfolding of a Single Protein Triggers Nanoparticle Aggregation. *ACS Nano* **2016**, *10*, 2103−2112.

(27) Deng, Z. J.; Liang, M.; Monteiro, M.; Toth, I.; Minchin, R. F. Nanoparticle Induced Unfolding of Fibrinogen Promotes Mac 1 Receptor Activation and Inflammation. *Nat. Nanotechnol.* **2011**, *6*, 39−44.

(28) van Oud Alblas, A. B.; Van Furth, R. Origin, Kinetics, and Characteristics of Pulmonary Macrophages in the Normal Steady State. *J. Exp. Med.* **1979**, *149*, 1504−1518.

(29) Kawada, N.; Parola, M. In *Satellate Cells in Health and Disease*; Gandhi, C. R., Pinzani, M.; Academic Press: London, 2015; pp 185−207.

(30) Reffitt, D. M.; Jugdaohsingh, R.; Thompson, R. P.; Powell, J. J. Silicic Acid: Its Gastrointestinal Uptake and Urinary Excretion in Man and Effects on Aluminium Excretion. *J. Inorg. Biochem.* **1999**, *76*, 141−147.

(31) de Boer, W. I.; van Schadewijk, A.; Sont, J. K.; Sharma, H. S.; Stolk, J.; Hiemstra, P. S.; van Krieken, J. H. J. Transforming Growth Factor B1 and Recruitment of Macrophages and Mast Cells in Airways in Chronic Obstructive Pulmonary Disease. *Am. J. Respir. Crit. Care Med.* **1998**, *158*, 1951−1957.

(32) Woodruff, P. G.; Ellwanger, A.; Solon, M.; Cambier, C. J.; Pinkerton, K. E.; Koth, L. L. Alveolar Macrophage Recruitment and Activation by Chronic Second Hand Smoke Exposure in Mice. *Int. J. Chronic Obstruct Pulm. Dis.* **2009**, *6*, 86−94.

(33) Caminschi, I.; Corbett, A. J.; Zahra, C.; Lahoud, M.; Lucas, K. M.; Sofi, M.; Vremec, D.; Gramberg, T.; Pöhlmann, S.; Curtis, J.; Handman, E.; van Dommelen, S. L.; Flaming, P.; Degli Esposti, M. A.; Shortman, K.; Wright, M. D. Functional Comparison of Mouse Cire/Mouse DC SIGN and Human DC SIGN. *Int. Immunol.* **2006**, *18*, 741−753.

(34) Prasad, S.; Kireta, S.; Leedham, E.; Russ, G. R.; Coates, P. T. H. Propagation and Characterization of Dendritic Cells from G CSF Mobilized Peripheral Blood Monocytes and Stem Cells in Common Marmoset Monkeys. *J. Immunol. Methods* **2010**, *352*, 59−70.

DOI: 10.1021/acsnano.8b01625
ACS Nano 2018, 12, 6637−6647

(35) Battaglia, M.; Stabilini, A.; Roncarolo, M. G. Rapamycin Selectively Expands CD4+ CD25+ FoxP3+ Regulatory T Cells. *Blood* **2005**, *105*, 4743−4748.
(36) Secret, E.; Smith, K.; Dubljevic, V.; Moore, E.; Macardle, P.; Delalat, B.; Rogers, M. L.; Johns, T. G.; Durand, J. O.; Cunin, F.; Voelcker, N. H. Antibody Functionalized Porous Silicon Nanoparticles for Vectorization of Hydrophobic Drugs. *Adv. Healthcare Mater.* **2013**, *2*, 718−727.
(37) Alhmoud, H.; Delalat, B.; Elnathan, R.; Cifuentes Rius, A.; Chaix, A.; Rogers, M. L.; Durand, J. O.; Voelcker, N. H. Porous Silicon Nanodiscs for Targeted Drug Delivery. *Adv. Funct. Mater.* **2015**, *25*, 1137−1145.
(38) Alba, M.; Delalat, B.; Formentín, P.; Rogers, M. L.; Marsal, L. F.; Voelcker, N. H. Silica Nanopills for Targeted Anticancer Drug Delivery. *Small* **2015**, *11*, 4626−4631.
(39) Maldonado, R. A.; LaMothe, R. A.; Ferrari, J. D.; Zhang, A. H.; Rossi, R. J.; Kolte, P. N.; Griset, A. P.; O'Neil, C.; Altreuter, D. H.; Browning, E.; Johnston, L.; Farokhzad, O. C.; Langer, R.; Scott, D. W.; von Andrian, U. H.; Kishimoto, T. K. Polymeric Synthetic Nanoparticles for the Induction of Antigen Specific Immunological Tolerance. *Proc. Natl. Acad. Sci. U. S. A.* **2015**, *112*, 156−165.
(40) Coffinier, Y.; Olivier, C.; Perzyna, A.; Grandidier, B.; Wallart, X.; Durand, J. O.; Melnyk, O.; Stievenard, D. Semicarbazide Functionalized Si(111) Surfaces for the Site Specific Immobilization of Peptides. *Langmuir* **2005**, *21*, 1489−1496.

DOI: 10.1021/acsnano.8b01625
ACS Nano 2018, 12, 6637−6647

CONCLUSION

In conclusion, we have demonstrated the ability of DC-SIGN pSiNP to track to DC populations *in vitro*. We then explored the effect rapamycin loaded pSiNP would have on DC phenotype by identify the maturation resistance characteristic of DC preconditioned with rapamycin. Next, we demonstrated the poor allogeneic stimulatory capacity of these DC *in vitro*, utilising mixed lymphocyte reactions. *In vivo*, we concluded that CD11c functionalised pSiNP had significantly enhanced tracking ability to splenic DC population. Within the non-human primates, age related illnesses possibly skewed the full tracking potential of these DC targeting pSiNP, showing high levels of accumulation within the lungs of the animals. This was one of the major limitation within this research. With a pre-existing lung condition, it is difficult to identify the metabolism of DC-SIGN coated pSiNP accurately within the non-human promote model. A benefit of exploring the pSiNP tracking in animals with a lung pathology is that it did highlight the enhanced pulmonary targeting of the nanoparticles within this setting. This offers an alternative use of these nanoparticle in the treatment of chronic obstructive pulmonary disease (COPD). Due to the variation of tracking within the DC-SIGN pSiNP marmosets, it definitely warrants repetition in younger, healthier animals to truly highly their benefit. *In vivo* functional tests of rapamycin loaded pSiNP successfully promoted regulatory T-cell generation when specifically targeting DC. However, histological sections also identified large aggregates of nanoparticles deposited within some of the tissues, including the kidney and liver. Translating this into a human therapy could poses a potential problem with the chance of the particles aggregating, leading to the development of an emboli and potentially death. *In vitro* studies with these pSiNP should be carried out to identify potential factors that can inhibit the internal aggregation seen *in vivo*. This may be as simple as resuspending the pSiNP in a heparinised saline before i.v. injection or a physical coating of aspirin over the pSiNP to prevent platelet activation and inevitably the coagulation cascade. The studies performed here, highlight the importance of nanoparticles functionalisation for specific *in vivo* cell targeting. Future experiments should explore the functionalisation of pSiNP with alternative targeting antigens, exploring the full ability of these nanoparticles to deliver drugs, peptide or genomic fragments to multiple cell types within the body.

REFERENCES

1. Misra R, Sahoo SK. Intracellular Trafficking of Nuclear Localization Signal Conjugated Nanoparticles for Cancer Therapy. European journal of pharmaceutical sciences : official journal of the European Federation for Pharmaceutical Sciences. **2010**;39:152-63.

2. Choi HS, Liu W, Liu F, Nasr K, Misra P, Bawendi MG, et al. Design Considerations for Tumour-Targeted Nanoparticles. Nature nanotechnology. **2010**;5:42-7.

3. Vannucci L, Fiserova A, Sadalapure K, Lindhorst TK, Kuldova M, Rossmann P, et al. Effects of N-Acetyl-Glucosamine-Coated Glycodendrimers as Biological Modulators in the B16f10 Melanoma Model in Vivo. International journal of oncology. **2003**;23:285-96.

4. Shaunak S, Thomas S, Gianasi E, Godwin A, Jones E, Teo I, et al. Polyvalent Dendrimer Glucosamine Conjugates Prevent Scar Tissue Formation. Nat Biotechnol. **2004**;22:977-84.

5. Okamoto S, Yoshii H, Matsuura M, Kojima A, Ishikawa T, Akagi T, et al. Poly-Gamma-Glutamic Acid Nanoparticles and Aluminum Adjuvant Used as an Adjuvant with a Single Dose of Japanese Encephalitis Virus-Like Particles Provide Effective Protection from Japanese Encephalitis Virus. Clinical and vaccine immunology : CVI. **2012**;19:17-22.

6. Uto T, Akagi T, Toyama M, Nishi Y, Shima F, Akashi M, et al. Comparative Activity of Biodegradable Nanoparticles with Aluminum Adjuvants: Antigen Uptake by Dendritic Cells and Induction of Immune Response in Mice. Immunology letters. **2011**;140:36-43.

7. Uto T, Akagi T, Yoshinaga K, Toyama M, Akashi M, Baba M. The Induction of Innate and Adaptive Immunity by Biodegradable Poly(Gamma-Glutamic Acid) Nanoparticles Via a Tlr4 and Myd88 Signaling Pathway. Biomaterials. **2011**;32:5206-12.

8. Jose M, Caring for Australians with Renal I. The Cari Guidelines. Calcineurin Inhibitors in Renal Transplantation: Adverse Effects. Nephrology. **2007**;12 Suppl 1:S66-74.

9. Riminton DS, Hartung HP, Reddel SW. Managing the Risks of Immunosuppression. Current opinion in neurology. **2011**;24:217-23.

10. Carbone J, del Pozo N, Gallego A, Sarmiento E. Immunological Risk Factors for Infection after Immunosuppressive and Biologic Therapies. Expert review of anti-infective therapy. **2011**;9:405-13.

11. Bangham A. Liposomes: The Babraham Connection. Chemistry and physics of lipids. **1993**;64:275-85.

12. Torchilin VP. Recent Advances with Liposomes as Pharmaceutical Carriers. Nature reviews Drug discovery. **2005**;4:145.

13. Felgner PL, Gadek TR, Holm M, Roman R, Chan HW, Wenz M, et al. Lipofection: A Highly Efficient, Lipid-Mediated DNA-Transfection Procedure. Proceedings of the National Academy of Sciences. **1987**;84:7413-7.

14. Bulbake U, Doppalapudi S, Kommineni N, Khan W. Liposomal Formulations in Clinical Use: An Updated Review. Pharmaceutics. **2017**;9:12.

15. Gref R, Minamitake Y, Peracchia MT, Trubetskoy V, Torchilin V, Langer R. Biodegradable Long-Circulating Polymeric Nanospheres. Science. **1994**;263:1600-3.

16. Torchilin VP. Micellar Nanocarriers: Pharmaceutical Perspectives. Pharmaceutical research. **2007**;24:1.

17. Pillai C, Paul W, Sharma CP. Chitin and Chitosan Polymers: Chemistry, Solubility and Fiber Formation. Progress in polymer science. **2009**;34:641-78.

18. Lee E, Khan S, Lim K-H. Gelatin Nanoparticle Preparation by Nanoprecipitation. Journal of Biomaterials Science, Polymer Edition. **2011**;22:753-71.

19. Sarei F, Dounighi NM, Zolfagharian H, Khaki P, Bidhendi SM. Alginate Nanoparticles as a Promising Adjuvant and Vaccine Delivery System. Indian journal of pharmaceutical sciences. **2013**;75:442.

20. Filippov SK, Starovoytova L, Koňák Cer, Hrubý M, Macková H, Karlsson Gr, et al. Ph Sensitive Polymer Nanoparticles: Effect of Hydrophobicity on Self-Assembly. Langmuir. **2010**;26:14450-7.

21. Wang AZ, Gu F, Zhang L, Chan JM, Radovic-Moreno A, Shaikh MR, et al. Biofunctionalized Targeted Nanoparticles for Therapeutic Applications. Expert opinion on biological therapy. **2008**;8:1063-70.

22. Medina SH, El-Sayed ME. Dendrimers as Carriers for Delivery of Chemotherapeutic Agents. Chemical reviews. **2009**;109:3141-57.

23. Fréchet JM. Dendrimers and Supramolecular Chemistry. Proceedings of the National Academy of Sciences. **2002**;99:4782-7.

24. Svenson S, Tomalia DA. Dendrimers in Biomedical Applications—Reflections on the Field. Advanced drug delivery reviews. **2012**;64:102-15.

25. Mintzer MA, Grinstaff MW. Biomedical Applications of Dendrimers: A Tutorial. Chemical Society Reviews. **2011**;40:173-90.

26. Harries M, Ellis P, Harper P. Nanoparticle Albumin–Bound Paclitaxel for Metastatic Breast Cancer. American Society of Clinical Oncology; 2005.

27. Gradishar WJ, Tjulandin S, Davidson N, Shaw H, Desai N, Bhar P, et al. Phase Iii Trial of Nanoparticle Alubmin-Bound Paclitaxel Compared with Polyethylated Castor Oil-Based Paclitaxel in Women with Breast Cancer. J clin Oncol. **2005**;23:7794-803.

28. Gradishar WJ. Albumin-Bound Paclitaxel: A Next-Generation Taxane. Expert opinion on pharmacotherapy. **2006**;7:1041-53.

29. Jovin TM. Quantum Dots Finally Come of Age. Nature Publishing Group; 2003.

30. Chang YP, Pinaud F, Antelman J, Weiss S. Tracking Bio-Molecules in Live Cells Using Quantum Dots. Journal of biophotonics. **2008**;1:287-98.

31. Chan WC, Maxwell DJ, Gao X, Bailey RE, Han M, Nie S. Luminescent Quantum Dots for Multiplexed Biological Detection and Imaging. Current opinion in biotechnology. **2002**;13:40-6.

32. Weissleder R. Molecular Imaging in Cancer. Science. **2006**;312:1168-71.

33. Daniel M-C, Astruc D. Gold Nanoparticles: Assembly, Supramolecular Chemistry, Quantum-Size-Related Properties, and Applications toward Biology, Catalysis, and Nanotechnology. Chemical reviews. **2004**;104:293-346.

34. Castelló J, Gallardo M, Busquets MA, Estelrich J. Chitosan (or Alginate)-Coated Iron Oxide Nanoparticles: A Comparative Study. Colloids and Surfaces A: Physicochemical and Engineering Aspects. **2015**;468:151-8.

35. Millon A, Dickson S, Klink A, Izquierdo-Garcia D, Bini J, Lancelot E, et al. Monitoring Plaque Inflammation in Atherosclerotic Rabbits with an Iron Oxide (P904) and 18f-Fdg Using a Combined Pet/Mr Scanner. Atherosclerosis. **2013**;228:339-45.

36. Sigovan M, Boussel L, Sulaiman A, Sappey-Marinier D, Alsaid H, Desbleds-Mansard C, et al. Rapid-Clearance Iron Nanoparticles for Inflammation Imaging of Atherosclerotic Plaque: Initial Experience in Animal Model. Radiology. **2009**;252:401-9.

37. Li L, Jiang W, Luo K, Song H, Lan F, Wu Y, et al. Superparamagnetic Iron Oxide Nanoparticles as Mri Contrast Agents for Non-Invasive Stem Cell Labeling and Tracking. Theranostics. **2013**;3:595.

38. Wang Y-XJ, Hussain SM, Krestin GP. Superparamagnetic Iron Oxide Contrast Agents: Physicochemical Characteristics and Applications in Mr Imaging. European radiology. **2001**;11:2319-31.

39. Mahmoudi M, Sant S, Wang B, Laurent S, Sen T. Superparamagnetic Iron Oxide Nanoparticles (Spions): Development, Surface Modification and Applications in Chemotherapy. Advanced drug delivery reviews. **2011**;63:24-46.

40. Huang X, Jain PK, El-Sayed IH, El-Sayed MA. Gold Nanoparticles: Interesting Optical Properties and Recent Applications in Cancer Diagnostics and Therapy. **2007**.

41. Nie S, Emory SR. Probing Single Molecules and Single Nanoparticles by Surface-Enhanced Raman Scattering. science. **1997**;275:1102-6.

42. Wagner V, Dullaart A, Bock A-K, Zweck A. The Emerging Nanomedicine Landscape. Nature biotechnology. **2006**;24:1211.

43. Petros RA, DeSimone JM. Strategies in the Design of Nanoparticles for Therapeutic Applications. Nature reviews Drug discovery. **2010**;9:615.

44. Cai W, Chen X. Nanoplatforms for Targeted Molecular Imaging in Living Subjects. Small. **2007**;3:1840-54.

45. Huang S, Song L, Xiao Z, Hu Y, Peng M, Li J, et al. Graphene Quantum Dot-Decorated Mesoporous Silica Nanoparticles for High Aspirin Loading Capacity and Its Ph-Triggered Release. Analytical Methods. **2016**;8:2561-7.

46. Tu J, Boyle AL, Friedrich H, Bomans PH, Bussmann J, Sommerdijk NA, et al. Mesoporous Silica Nanoparticles with Large Pores for the Encapsulation and Release of Proteins. ACS applied materials & interfaces. **2016**;8:32211-9.

47. Singh K, Sun S, Vezina C. Rapamycin (Ay-22,989), a New Antifungal Antibiotic. Iv. Mechanism of Action. The Journal of antibiotics. **1979**;32:630-45.

48. Reffitt DM, Jugdaohsingh R, Thompson RP, Powell JJ. Silicic Acid: Its Gastrointestinal Uptake and Urinary Excretion in Man and Effects on Aluminium Excretion. Journal of Inorganic Biochemistry. **1999**;76:141-7.

49. Chougule MB, Padhi BK, Misra A. Nano-Liposomal Dry Powder Inhaler of Amiloride Hydrochloride. Journal of nanoscience and nanotechnology. **2006**;6:3001-9.

50. Konduri KS, Nandedkar S, Düzgünes N, Suzara V, Artwohl J, Bunte R, et al. Efficacy of Liposomal Budesonide in Experimental Asthma. Journal of allergy and clinical immunology. **2003**;111:321-7.

51. Wu J, Lu Y, Lee A, Pan X, Yang X, Zhao X, et al. Reversal of Multidrug Resistance by Transferrin-Conjugated Liposomes Co-Encapsulating Doxorubicin and Verapamil. J Pharm Pharm Sci. **2007**;10:350-7.

52. Spangler RS. Insulin Administration Via Liposomes. Diabetes care. **1990**;13:911-22.

53. Khanna C, Anderson PM, Hasz DE, Katsanis E, Neville M, Klausner JS. Interleukin-2 Liposome Inhalation Therapy Is Safe and Effective for Dogs with Spontaneous Pulmonary Metastases. Cancer. **1997**;79:1409-21.

54. Leonard SC, Lee H, Gaddy DF, Klinz SG, Paz N, Kalra AV, et al. Extended Topoisomerase 1 Inhibition through Liposomal Irinotecan Results in Improved Efficacy over Topotecan and Irinotecan in Models of Small-Cell Lung Cancer. Anti-cancer drugs. **2017**;28:1086-96.

55. Joshi M, Misra A. Dry Powder Inhalation of Liposomal Ketotifen Fumarate: Formulation and Characterization. International journal of pharmaceutics. **2001**;223:15-27.

56. Jones S, Merkel O. Tackling Breast Cancer Chemoresistance with Nano-Formulated Sirna. Gene therapy. **2016**;23:821.

57. Marier J, Brazier J, Lavigne J, Ducharme M. Liposomal Tobramycin against Pulmonary Infections of Pseudomonas Aeruginosa: A Pharmacokinetic and Efficacy Study Following Single and Multiple Intratracheal Administrations in Rats. Journal of antimicrobial chemotherapy. **2003**;52:247-52.

58. De Witt M, Gamble A, Hanson D, Markowitz D, Powell C, Al Dimassi S, et al. Repurposing Mebendazole as a Replacement for Vincristine for the Treatment of Brain Tumors. Molecular Medicine. **2017**;23:50.

59. Gong F, Tang H, Lin Y, Gu W, Wang W, Kang M. Gene Transfer of Vascular Endothelial Growth Factor Reduces Bleomycin-Induced Pulmonary Hypertension in Immature Rabbits. Pediatrics international. **2005**;47:242-7.

60. Yao Y-C, Zhan X-Y, Zhang J, Zou X-H, Wang Z-H, Xiong Y-C, et al. A Specific Drug Targeting System Based on Polyhydroxyalkanoate Granule Binding Protein Phap Fused with Targeted Cell Ligands. Biomaterials. **2008**;29:4823-30.

61. Chittasupho C, Xie S-X, Baoum A, Yakovleva T, Siahaan TJ, Berkland CJ. Icam-1 Targeting of Doxorubicin-Loaded Plga Nanoparticles to Lung Epithelial Cells. European journal of pharmaceutical sciences. **2009**;37:141-50.

62. Liang C, Yang Y, Ling Y, Huang Y, Li T, Li X. Improved Therapeutic Effect of Folate-Decorated Plga–Peg Nanoparticles for Endometrial Carcinoma. Bioorganic & medicinal chemistry. **2011**;19:4057-66.

63. Kocbek P, Obermajer N, Cegnar M, Kos J, Kristl J. Targeting Cancer Cells Using Plga Nanoparticles Surface Modified with Monoclonal Antibody. Journal of controlled release. **2007**;120:18-26.

64. Villaverde A. Nanoparticles in Translational Science and Medicine: Academic Press; **2011**.

65. Lee CC, Gillies ER, Fox ME, Guillaudeu SJ, Fréchet JM, Dy EE, et al. A Single Dose of Doxorubicin-Functionalized Bow-Tie Dendrimer Cures Mice Bearing C-26 Colon Carcinomas. Proceedings of the National Academy of Sciences. **2006**;103:16649-54.

66. Pyreddy S, Kumar PD, Kumar PV. Polyethylene Glycolated Pamam Dendrimers-Efavirenz Conjugates. International journal of pharmaceutical investigation. **2014**;4:15.

67. Blanzat M, Turrin CO, Aubertin AM, Couturier-Vidal C, Caminade AM, Majoral JP, et al. Dendritic Catanionic Assemblies: In Vitro Anti-Hiv Activity of Phosphorus-Containing Dendrimers Bearing Galβ1cer Analogues. ChemBioChem. **2005**;6:2207-13.

68. Dutta T, Jain NK. Targeting Potential and Anti-Hiv Activity of Lamivudine Loaded Mannosylated Poly (Propyleneimine) Dendrimer. Biochimica et Biophysica Acta (BBA)-General Subjects. **2007**;1770:681-6.

69. Weber N, Ortega P, Clemente MI, Shcharbin D, Bryszewska M, de la Mata FJ, et al. Characterization of Carbosilane Dendrimers as Effective Carriers of Sirna to Hiv-Infected Lymphocytes. Journal of Controlled Release. **2008**;132:55-64.

70. Goldberg DS, Vijayalakshmi N, Swaan PW, Ghandehari H. G3. 5 Pamam Dendrimers Enhance Transepithelial Transport of Sn38 While Minimizing Gastrointestinal Toxicity. Journal of controlled release. **2011**;150:318-25.

71. Kensinger RD, Catalone BJ, Krebs FC, Wigdahl B, Schengrund C-L. Novel Polysulfated Galactose-Derivatized Dendrimers as Binding Antagonists of Human Immunodeficiency Virus Type 1 Infection. Antimicrobial agents and chemotherapy. **2004**;48:1614-23.

72. Poller JM, Zaloga J, Schreiber E, Unterweger H, Janko C, Radon P, et al. Selection of Potential Iron Oxide Nanoparticles for Breast Cancer Treatment Based on in Vitro Cytotoxicity and Cellular Uptake. International journal of nanomedicine. **2017**;12:3207.

73. Yen SK, Padmanabhan P, Selvan ST. Multifunctional Iron Oxide Nanoparticles for Diagnostics, Therapy and Macromolecule Delivery. Theranostics. **2013**;3:986.

74. Ma X, Gong A, Chen B, Zheng J, Chen T, Shen Z, et al. Exploring a New Spion-Based Mri Contrast Agent with Excellent Water-Dispersibility, High Specificity to Cancer Cells and Strong Mr Imaging Efficacy. Colloids and Surfaces B: Biointerfaces. **2015**;126:44-9.

75. Shevtsov MA, Nikolaev BP, Yakovleva LY, Marchenko YY, Dobrodumov AV, Mikhrina AL, et al. Superparamagnetic Iron Oxide Nanoparticles Conjugated with Epidermal Growth Factor (Spion–Egf) for Targeting Brain Tumors. International journal of nanomedicine. **2014**;9:273.

76. Liao N, Wu M, Pan F, Lin J, Li Z, Zhang D, et al. Poly (Dopamine) Coated Superparamagnetic Iron Oxide Nanocluster for Noninvasive Labeling, Tracking, and Targeted Delivery of Adipose Tissue-Derived Stem Cells. Scientific Reports. **2016**;6:18746.

77. Kalangi SK, Sathyavathi R, Rao DN, Pallu R. Bioimaging of 5 Fluorouracil Conjugated to Cdte Quantum Dots in Mcf-7 Breast Cancer Cells. Journal of Bionanoscience. **2012**;6:17-22.

78. Savla R, Taratula O, Garbuzenko O, Minko T. Tumor Targeted Quantum Dot-Mucin 1 Aptamer-Doxorubicin Conjugate for Imaging and Treatment of Cancer. Journal of controlled release. **2011**;153:16-22.

79. D Mahajan S, Roy I, Xu G, Yong K-T, Ding H, Aalinkeel R, et al. Enhancing the Delivery of Anti Retroviral Drug "Saquinavir" across the Blood Brain Barrier Using Nanoparticles. Current HIV research. **2010**;8:396-404.

80. Chen Y-H, Tsai C-Y, Huang P-Y, Chang M-Y, Cheng P-C, Chou C-H, et al. Methotrexate Conjugated to Gold Nanoparticles Inhibits Tumor Growth in a Syngeneic Lung Tumor Model. Molecular pharmaceutics. **2007**;4:713-22.

81. Podsiadlo P, Sinani VA, Bahng JH, Kam NWS, Lee J, Kotov NA. Gold Nanoparticles Enhance the Anti-Leukemia Action of a 6-Mercaptopurine Chemotherapeutic Agent. Langmuir. **2008**;24:568-74.

82. Dreaden EC, Mwakwari SC, Sodji QH, Oyelere AK, El-Sayed MA. Tamoxifen− Poly (Ethylene Glycol)− Thiol Gold Nanoparticle Conjugates: Enhanced Potency and Selective Delivery for Breast Cancer Treatment. Bioconjugate chemistry. **2009**;20:2247-53.

83. Liong M, Lu J, Kovochich M, Xia T, Ruehm SG, Nel AE, et al. Multifunctional Inorganic Nanoparticles for Imaging, Targeting, and Drug Delivery. ACS nano. **2008**;2:889-96.

84. Ma X, Zhao Y, Ng KW, Zhao Y. Integrated Hollow Mesoporous Silica Nanoparticles for Target Drug/Sirna Co-Delivery. Chemistry-A European Journal. **2013**;19:15593-603.

85. Gary-Bobo M, Hocine O, Brevet D, Maynadier M, Raehm L, Richeter S, et al. Cancer Therapy Improvement with Mesoporous Silica Nanoparticles Combining Targeting, Drug Delivery and Pdt. International journal of pharmaceutics. **2012**;423:509-15.

86. Mamaeva V, Rosenholm JM, Bate-Eya LT, Bergman L, Peuhu E, Duchanoy A, et al. Mesoporous Silica Nanoparticles as Drug Delivery Systems for Targeted Inhibition of Notch Signaling in Cancer. Molecular Therapy. **2011**;19:1538-46.

87. Zhang L, Wang T, Yang L, Liu C, Wang C, Liu H, et al. General Route to Multifunctional Uniform Yolk/Mesoporous Silica Shell Nanocapsules: A Platform for Simultaneous Cancer-Targeted Imaging and Magnetically Guided Drug Delivery. Chemistry-A European Journal. **2012**;18:12512-21.

88. Sanchez–Fueyo A, Strom TB. Immunologic Basis of Graft Rejection and Tolerance Following Transplantation of Liver or Other Solid Organs. Gastroenterology. **2011**;140.

89. Comber JD, Philip R. Mhc Class I Antigen Presentation and Implications for Developing a New Generation of Therapeutic Vaccines. Therapeutic advances in vaccines. **2014**;2:77-89.

90. Janeway Jr CA, Travers P, Walport M, Shlomchik MJ. The Major Histocompatibility Complex and Its Functions. **2001**.

91. van de Weijer ML, Luteijn RD, Wiertz EJ. Viral Immune Evasion: Lessons in Mhc Class I Antigen Presentation. Seminars in immunology. **2015**.

92. Dauer M, Obermaier B, Herten J, Haerle C, Pohl K, Rothenfusser S, et al. Mature Dendritic Cells Derived from Human Monocytes within 48 Hours: A Novel Strategy for Dendritic Cell Differentiation from Blood Precursors. Journal of immunology (Baltimore, Md : 1950). **2003**;170:4069-76.

93. Castiello L, Sabatino M, Jin P, Clayberger C, Marincola FM, Krensky AM, et al. Monocyte-Derived Dc Maturation Strategies and Related Pathways: A Transcriptional View. Cancer immunology, immunotherapy : CII. **2011**;60:457-66.

94. Sato M, Takayama T, Tanaka H, Konishi J, Suzuki T, Kaiga T, et al. Generation of Mature Dendritic Cells Fully Capable of T Helper Type 1 Polarization Using Ok-432 Combined with Prostaglandin E(2). Cancer science. **2003**;94:1091-8.

95. Verneris MR, Lee SJ, Ahn KW, Wang H-L, Battiwalla M, Inamoto Y, et al. Hla Mismatch Is Associated with Worse Outcomes after Unrelated Donor Reduced-Intensity Conditioning Hematopoietic Cell Transplantation: An Analysis from the Center for International Blood and Marrow Transplant Research. Biology of Blood and Marrow Transplantation. **2015**;21:1783-9.

96. Gilks WR, Bradley BA, Gore SM, Klouda PT. Substantial Benefits of Tissue Matching in Renal Transplantation. Transplantation. **1987**;43:669-74.

97. Doxiadis II, de Fijter JW, Mallat MJ, Haasnoot GW, Ringers J, Persijn GG, et al. Simpler and Equitable Allocation of Kidneys from Postmortem Donors Primarily Based on Full Hla-Dr Compatibility. Transplantation. **2007**;83:1207-13.

98. Coupel S, Giral-Classe M, Karam G, Morcet J-F, Dantal J, Cantarovich D, et al. Ten-Year Survival of Second Kidney Transplants: Impact of Immunologic Factors and Renal Function at 12 Months. Kidney international. **2003**;64:674-80.

99. Thaiss CA, Semmling V, Franken L, Wagner H, Kurts C. Chemokines: A New Dendritic Cell Signal for T Cell Activation. Frontiers in immunology. **2011**;2:31.

100. Lafferty KJ, Woolnough J. The Origin and Mechanism of the Allograft Reaction. Immunological reviews. **1977**;35:231-62.

101. Fracchia KM, Pai C, Walsh CM. Modulation of T Cell Metabolism and Function through Calcium Signaling. Frontiers in immunology. **2013**;4:324.

102. Foulds CE, Nelson ML, Blaszczak AG, Graves BJ. Ras/Mitogen-Activated Protein Kinase Signaling Activates Ets-1 and Ets-2 by Cbp/P300 Recruitment. Molecular and cellular biology. **2004**;24:10954-64.

103. Liu X, Berry CT, Ruthel G, Madara JJ, MacGillivray K, Gray CM, et al. T Cell Receptor-Induced Nuclear Factor Kb (Nf-Kb) Signaling and Transcriptional Activation Are Regulated by Stim1- and Orai1-Mediated Calcium Entry. Journal of Biological Chemistry. **2016**;291:8440-52.

104. Brincks EL, Woodland DL. Novel Roles for Il-15 in T Cell Survival. F1000 biology reports. **2010**;2.

105. Obar JJ, Molloy MJ, Jellison ER, Stoklasek TA, Zhang W, Usherwood EJ, et al. Cd4+ T Cell Regulation of Cd25 Expression Controls Development of Short-Lived Effector Cd8+ T Cells in Primary and Secondary Responses. Proceedings of the National Academy of Sciences. **2010**;107:193-8.

106. Grewal IS, Flavell RA. The Role of Cd40 Ligand in Costimulation and T-Cell Activation. Immunological reviews. **1996**;153:85-106.

107. Trinchieri G. Interleukin-12 and the Regulation of Innate Resistance and Adaptive Immunity. Nature reviews Immunology. **2003**;3:133-46.

108. Filatenkov AA, Jacovetty EL, Fischer UB, Curtsinger JM, Mescher MF, Ingulli E. Cd4 T Cell-Dependent Conditioning of Dendritic Cells to Produce Il-12 Results in Cd8-Mediated Graft Rejection and Avoidance of Tolerance. Journal of immunology (Baltimore, Md : 1950). **2005**;174:6909-17.

109. Ray JP, Staron MM, Shyer JA, Ho P-C, Marshall HD, Gray SM, et al. The Interleukin-2-Mtorc1 Kinase Axis Defines the Signaling, Differentiation, and Metabolism of T Helper 1 and Follicular B Helper T Cells. Immunity. **2015**;43:690-702.

110. Mao Y, van Hoef V, Zhang X, Wennerberg E, Lorent J, Witt K, et al. Il-15 Activates Mtor and Primes Stress-Activated Gene Expression Leading to Prolonged Antitumor Capacity of Nk Cells. Blood. **2016**;128:1475-89.

111. Rojas-Canales D. Studies of Clinically Applicable Human Tolerogenic Dendritic Cells and Pd-L2 Genetic Modification of Human Islet Allograft to Promote Graft Tolerance: The University of Adelaide; 2011.

112. Sheppard KA, Fitz LJ, Lee JM, Benander C, George JA, Wooters J, et al. Pd-1 Inhibits T-Cell Receptor Induced Phosphorylation of the Zap70/Cd3zeta Signalosome and Downstream Signaling to Pkctheta. FEBS letters. **2004**;574:37-41.

113. Okazaki T, Chikuma S, Iwai Y, Fagarasan S, Honjo T. A Rheostat for Immune Responses: The Unique Properties of Pd-1 and Their Advantages for Clinical Application. Nature immunology. **2013**;14:1212.

114. Zhu J, Yamane H, Paul WE. Differentiation of Effector Cd4 T Cell Populations. Annual review of immunology. **2010**;28:445-89.

115. MacLeod MKL, Kappler JW, Marrack P. Memory Cd4 T Cells: Generation, Reactivation and Re-Assignment. Immunology. **2010**;130:10-5.

116. Sallusto F, Geginat J, Lanzavecchia A. Central Memory and Effector Memory T Cell Subsets: Function, Generation, and Maintenance. Annu Rev Immunol. **2004**;22:745-63.

117. Romagnani S. T-Cell Subsets (Th1 Versus Th2). Annals of Allergy, Asthma & Immunology.85:21.

118. Romagnani S. T-Cell Subsets (Th1 Versus Th2). Annals of allergy, asthma & immunology : official publication of the American College of Allergy, Asthma, & Immunology. **2000**;85:9-18; quiz , 21.

119. Akyol S, Hanci M. Th1 and Th2 Cytokines Production and Nk Cell Level Assessment in Peripheral Blood of Patients with Ddh. The Indian journal of surgery. **2013**;75:294-7.

120. Fairfax KC, Everts B, Amiel E, Smith AM, Schramm G, Haas H, et al. Il-4-Secreting Secondary T Follicular Helper (Tfh) Cells Arise from Memory T Cells, Not Persisting Tfh Cells, through a B Cell-Dependent Mechanism. Journal of immunology (Baltimore, Md : 1950). **2015**;194:2999-3010.

121. Murphy K, Weaver C. Janeway's Immunobiology: Garland Science; **2016**.

122. Stone KD, Prussin C, Metcalfe DD. Ige, Mast Cells, Basophils, and Eosinophils. The Journal of allergy and clinical immunology. **2010**;125:S73-80.

123. Fiorentino DF, Zlotnik A, Vieira P, Mosmann TR, Howard M, Moore KW, et al. Il-10 Acts on the Antigen-Presenting Cell to Inhibit Cytokine Production by Th1 Cells. Journal of immunology (Baltimore, Md : 1950). **1991**;146:3444-51.

124. Yao Z, Fanslow WC, Seldin MF, Rousseau AM, Painter SL, Comeau MR, et al. Herpesvirus Saimiri Encodes a New Cytokine, Il-17, Which Binds to a Novel Cytokine Receptor. Journal of immunology (Baltimore, Md : 1950). **2011**;187:4392-402.

125. Shalom-Barak T, Quach J, Lotz M. Interleukin-17-Induced Gene Expression in Articular Chondrocytes Is Associated with Activation of Mitogen-Activated Protein Kinases and Nf-Kappab. The Journal of biological chemistry. **1998**;273:27467-73.

126. Schwandner R, Yamaguchi K, Cao Z. Requirement of Tumor Necrosis Factor Receptor-Associated Factor (Traf)6 in Interleukin 17 Signal Transduction. The Journal of experimental medicine. **2000**;191:1233-40.

127. Dong C. Diversification of T-Helper-Cell Lineages: Finding the Family Root of Il-17-Producing Cells. Nature Reviews Immunology. **2006**;6:329.

128. Collin M, McGovern N, Haniffa M. Human Dendritic Cell Subsets. Immunology. **2013**;140:22-30.

129. Zhou LJ, Tedder TF. Cd14+ Blood Monocytes Can Differentiate into Functionally Mature Cd83+ Dendritic Cells. Proceedings of the National Academy of Sciences of the United States of America. **1996**;93:2588-92.

130. Ito T, Inaba M, Inaba K, Toki J, Sogo S, Iguchi T, et al. A Cd1a+/Cd11c+ Subset of Human Blood Dendritic Cells Is a Direct Precursor of Langerhans Cells. Journal of immunology (Baltimore, Md : 1950). **1999**;163:1409-19.

131. Banchereau J, Briere F, Caux C, Davoust J, Lebecque S, Liu YJ, et al. Immunobiology of Dendritic Cells. Annual review of immunology. **2000**;18:767-811.

132. Haller Hasskamp J, Zapas JL, Elias EG. Dendritic Cell Counts in the Peripheral Blood of Healthy Adults. American journal of hematology. **2005**;78:314-5.

133. Lozach P-Y, Amara A, Bartosch B, Virelizier J-L, Arenzana-Seisdedos F, Cosset F-L, et al. C-Type Lectins L-Sign and Dc-Sign Capture and Transmit Infectious Hepatitis C Virus Pseudotype Particles. Journal of Biological Chemistry. **2004**;279:32035-45.

134. Geijtenbeek TB, Kwon DS, Torensma R, van Vliet SJ, van Duijnhoven GC, Middel J, et al. Dc-Sign, a Dendritic Cell–Specific Hiv-1-Binding Protein That Enhances Trans-Infection of T Cells. Cell. **2000**;100:587-97.

135. Wu L, Martin TD, Vazeux R, Unutmaz D, KewalRamani VN. Functional Evaluation of Dc-Sign Monoclonal Antibodies Reveals Dc-Sign Interactions with Icam-3 Do Not Promote Human Immunodeficiency Virus Type 1 Transmission. Journal of virology. **2002**;76:5905-14.

136. Edwards AD, Chaussabel D, Tomlinson S, Schulz O, Sher A, e Sousa CR. Relationships among Murine Cd11chigh Dendritic Cell Subsets as Revealed by Baseline Gene Expression Patterns. The Journal of Immunology. **2003**;171:47-60.

137. Caminschi I, Corbett AJ, Zahra C, Lahoud M, Lucas KM, Sofi M, et al. Functional Comparison of Mouse Cire/Mouse Dc-Sign and Human Dc-Sign. International immunology. **2006**;18:741-53.

138. Wierecky J, Müller MR, Wirths S, Halder-Oehler E, Dörfel D, Schmidt SM, et al. Immunologic and Clinical Responses after Vaccinations with Peptide-Pulsed Dendritic Cells in Metastatic Renal Cancer Patients. Cancer Research. **2006**;66:5910-8.

139. Van Tendeloo VF, Van de Velde A, Van Driessche A, Cools N, Anguille S, Ladell K, et al. Induction of Complete and Molecular Remissions in Acute Myeloid Leukemia by Wilms' Tumor 1 Antigen-Targeted Dendritic Cell Vaccination. Proceedings of the National Academy of Sciences. **2010**;107:13824-9.

140. Rosenblatt J, Avivi I, Vasir B, Uhl L, Munshi NC, Katz T, et al. Vaccination with Dendritic Cell/Tumor Fusions Following Autologous Stem Cell Transplant Induces Immunologic and Clinical Responses in Multiple Myeloma Patients. Clinical Cancer Research. **2013**;19:3640-8.

141. Himmel ME, MacDonald KG, Garcia RV, Steiner TS, Levings MK. Helios+ and Helios- Cells Coexist within the Natural Foxp3+ T Regulatory Cell Subset in Humans. Journal of immunology (Baltimore, Md : 1950). **2013**;190:2001-8.

142. Rutella S, Danese S, Leone G. Tolerogenic Dendritic Cells: Cytokine Modulation Comes of Age. Blood. **2006**;108:1435-40.

143. Steinman RM, Hawiger D, Liu K, Bonifaz L, Bonnyay D, Mahnke K, et al. Dendritic Cell Function in Vivo During the Steady State: A Role in Peripheral Tolerance. Annals of the New York Academy of Sciences. **2003**;987:15-25.

144. Kalinski P. Dendritic Cells in Immunotherapy of Established Cancer: Roles of Signals 1, 2, 3 and 4. Current opinion in investigational drugs (London, England : 2000). **2009**;10:526-35.

145. Morelli AE. The Immune Regulatory Effect of Apoptotic Cells and Exosomes on Dendritic Cells: Its Impact on Transplantation. American journal of transplantation : official journal of the American Society of Transplantation and the American Society of Transplant Surgeons. **2006**;6:254-61.

146. Wang Z, Larregina AT, Shufesky WJ, Perone MJ, Montecalvo A, Zahorchak AF, et al. Use of the Inhibitory Effect of Apoptotic Cells on Dendritic Cells for Graft Survival Via T-Cell Deletion and Regulatory T Cells. American journal of transplantation : official journal of the American Society of Transplantation and the American Society of Transplant Surgeons. **2006**;6:1297-311.

147. Wu J, Li S, Zheng Y, Zhang M, Zhang H, Sun Y, et al. Silencing of Lncrna Neat1 Induces Tolerogenic Dendritic Cells and Immune Tolerance in Heart Transplantation. Am Assoc Immnol; 2017.

148. Ezzelarab M, Zahorchak A, Lu L, Morelli A, Chalasani G, Demetris A, et al. Regulatory Dendritic Cell Infusion Prolongs Kidney Allograft Survival in Nonhuman Primates. American Journal of Transplantation. **2013**;13:1989-2005.

149. Geissler EK. The One Study Compares Cell Therapy Products in Organ Transplantation: Introduction to a Review Series on Suppressive Monocyte-Derived Cells. Transplantation research. **2012**;1:11.

150. Thomson AW, Zahorchak AF, Ezzelarab MB, Butterfield LH, Lakkis FG, Metes DM. Prospective Clinical Testing of Regulatory Dendritic Cells in Organ Transplantation. Frontiers in immunology. **2016**;7.

151. Vezina C, Kudelski A, Sehgal SN. Rapamycin (Ay-22,989), a New Antifungal Antibiotic. I. Taxonomy of the Producing Streptomycete and Isolation of the Active Principle. The Journal of antibiotics. **1975**;28:721-6.

152. Sehgal SN, Baker H, Vezina C. Rapamycin (Ay-22,989), a New Antifungal Antibiotic. Ii. Fermentation, Isolation and Characterization. The Journal of antibiotics. **1975**;28:727-32.

153. Baker H, Sidorowicz A, Sehgal SN, Vezina C. Rapamycin (Ay-22,989), a New Antifungal Antibiotic. Iii. In Vitro and in Vivo Evaluation. The Journal of antibiotics. **1978**;31:539-45.

154. Wicker LS, Boltz RC, Jr., Matt V, Nichols EA, Peterson LB, Sigal NH. Suppression of B Cell Activation by Cyclosporin a, Fk506 and Rapamycin. European journal of immunology. **1990**;20:2277-83.

155. Yoshimura S, Bondeson J, Foxwell BM, Brennan FM, Feldmann M. Effective Antigen Presentation by Dendritic Cells Is Nf-Kappab Dependent: Coordinate Regulation of Mhc, Co-Stimulatory Molecules and Cytokines. International immunology. **2001**;13:675-83.

156. Powell JD, Lerner CG, Schwartz RH. Inhibition of Cell Cycle Progression by Rapamycin Induces T Cell Clonal Anergy Even in the Presence of Costimulation. Journal of immunology (Baltimore, Md : 1950). **1999**;162:2775-84.

157. Fischer R, Turnquist HR, Taner T, Thomson AW. Use of Rapamycin in the Induction of Tolerogenic Dendritic Cells. Dendritic Cells: Springer; 2009. p. 215-32.

158. Hackstein H, Taner T, Zahorchak AF, Morelli AE, Logar AJ, Gessner A, et al. Rapamycin Inhibits Il-4—Induced Dendritic Cell Maturation in Vitro and Dendritic Cell Mobilization and Function in Vivo. Blood. **2003**;101:4457-63.

159. Adorini L, Penna G. Induction of Tolerogenic Dendritic Cells by Vitamin D Receptor Agonists. Dendritic Cells: Springer; 2009. p. 251-73.

160. Buckland M, Lombardi G. Aspirin and the Induction of Tolerance by Dendritic Cells. Dendritic Cells: Springer; 2009. p. 197-213.

161. Lenicov FR, Rodrigues CR, Sabatté J, Cabrini M, Jancic C, Ostrowski M, et al. Semen Promotes the Differentiation of Tolerogenic Dendritic Cells. The Journal of Immunology. **2012**;189:4777-86.

162. Zoncu R, Efeyan A, Sabatini DM. Mtor: From Growth Signal Integration to Cancer, Diabetes and Ageing. Nature reviews Molecular cell biology. **2011**;12:21.

163. Augustine JJ, Bodziak KA, Hricik DE. Use of Sirolimus in Solid Organ Transplantation. Drugs. **2007**;67:369-91.

164. Choo AY, Yoon S-O, Kim SG, Roux PP, Blenis J. Rapamycin Differentially Inhibits S6ks and 4e-Bp1 to Mediate Cell-Type-Specific Repression of Mrna Translation. Proceedings of the National Academy of Sciences. **2008**;105:17414-9.

165. Garcia JA, Danielpour D. Mammalian Target of Rapamycin Inhibition as a Therapeutic Strategy in the Management of Urologic Malignancies. Molecular Cancer Therapeutics. **2008**;7:1347-54.

166. Molano RD, Pileggi A, Berney T, Poggioli R, Zahr E, Oliver R, et al. Long-Term Islet Allograft Survival in Nonobese Diabetic Mice Treated with Tacrolimus, Rapamycin, and Anti-Interleukin-2 Antibody. Transplantation. **2003**;75:1812-9.

167. Toso C, Morel P, Bucher P, Mathe Z, Demuylder-Mischler S, Bosco D, et al. Insulin Independence after Conversion to Tacrolimus and Sirolimus-Based Immunosuppression in Islet-Kidney Recipients. Transplantation. **2003**;76:1133-4.

168. Berney T, Secchi A. Rapamycin in Islet Transplantation: Friend or Foe? Transplant International. **2009**;22:153-61.

169. Laugharne M, Cross S, Richards S, Dawson C, Ilchyshyn L, Saleem M, et al. Sirolimus Toxicity and Vascular Endothelial Growth Factor Release from Islet and Renal Cell Lines. Transplantation. **2007**;83:1635-8.

170. Zhang N, Su D, Qu S, Tse T, Bottino R, Balamurugan A, et al. Sirolimus Is Associated with Reduced Islet Engraftment and Impaired B-Cell Function. Diabetes. **2006**;55:2429-36.

171. Bussiere CT, Lakey JR, Shapiro AM, Korbutt GS. The Impact of the Mtor Inhibitor Sirolimus on the Proliferation and Function of Pancreatic Islets and Ductal Cells. Diabetologia. **2006**;49:2341-9.

172. Larsen JL, Bennett RG, Burkman T, Ramirez AL, Yamamoto S, Gulizia J, et al. Tacrolimus and Sirolimus Cause Insulin Resistance in Normal Sprague Dawley Rats. Transplantation. **2006**;82:466-70.

173. Lopez-Talavera JC, Garcia-Ocana A, Sipula I, Takane KK, Cozar-Castellano I, Stewart AF. Hepatocyte Growth Factor Gene Therapy for Pancreatic Islets in Diabetes: Reducing the Minimal Islet Transplant Mass Required in a Glucocorticoid-Free Rat Model of Allogeneic Portal Vein Islet Transplantation. Endocrinology. **2004**;145:467-74.

174. Hyder A, Laue C, Schrezenmeir J. Effect of the Immunosuppressive Regime of Edmonton Protocol on the Long-Term in Vitro Insulin Secretion from Islets of Two Different Species and Age Categories. Toxicology in vitro : an international journal published in association with BIBRA. **2005**;19:541-6.

175. Kneteman NM, Lakey JR, Wagner T, Finegood D. The Metabolic Impact of Rapamycin (Sirolimus) in Chronic Canine Islet Graft Recipients. Transplantation. **1996**;61:1206-10.

176. Kidszun A, Schneider D, Erb D, Hertl G, Schmidt V, Eckhard M, et al. Isolated Pancreatic Islets in Three-Dimensional Matrices Are Responsive to Stimulators and Inhibitors of Angiogenesis. Cell transplantation. **2006**;15:489-97.

177. Fabian MC, Lakey JR, Rajotte RV, Kneteman NM. The Efficacy and Toxicity of Rapamycin in Murine Islet Transplantation. In Vitro and in Vivo Studies. Transplantation. **1993**;56:1137-42.

178. Paty BW, Harmon JS, Marsh CL, Robertson RP. Inhibitory Effects of Immunosuppressive Drugs on Insulin Secretion from Hit-T15 Cells and Wistar Rat Islets. Transplantation. **2002**;73:353-7.

179. Bell E, Cao X, Moibi JA, Greene SR, Young R, Trucco M, et al. Rapamycin Has a Deleterious Effect on Min-6 Cells and Rat and Human Islets. Diabetes. **2003**;52:2731-9.

180. Taner T, Hackstein H, Wang Z, Morelli AE, Thomson AW. Rapamycin-Treated, Alloantigen-Pulsed Host Dendritic Cells Induce Ag-Specific T Cell Regulation and Prolong Graft Survival. American journal of transplantation : official journal of the American Society of Transplantation and the American Society of Transplant Surgeons. **2005**;5:228-36.

181. Yin C, Hong B, Gong Z, Zhao H, Hu W, Lu X, et al. Fluorescent Oligo(P-Phenyleneethynylene) Contained Amphiphiles-Encapsulated Magnetic Nanoparticles for Targeted Magnetic Resonance and Two-Photon Optical Imaging in Vitro and in Vivo. Nanoscale. **2015**.

182. Horcajada P, Chalati T, Serre C, Gillet B, Sebrie C, Baati T, et al. Porous Metal-Organic-Framework Nanoscale Carriers as a Potential Platform for Drug Delivery and Imaging. Nature materials. **2010**;9:172-8.

183. Koppolu B, Zaharoff DA. The Effect of Antigen Encapsulation in Chitosan Particles on Uptake, Activation and Presentation by Antigen Presenting Cells. Biomaterials. **2013**;34:2359-69.

184. Vallhov H, Gabrielsson S, Stromme M, Scheynius A, Garcia-Bennett AE. Mesoporous Silica Particles Induce Size Dependent Effects on Human Dendritic Cells. Nano letters. **2007**;7:3576-82.

185. Dasary SS, Rai US, Yu H, Anjaneyulu Y, Dubey M, Ray PC. Gold Nanoparticle Based Surface Enhanced Fluorescence for Detection of Organophosphorus Agents. Chemical physics letters. **2008**;460:187-90.

186. Baier G, Baumann D, Siebert JM, Musyanovych A, Mailander V, Landfester K. Suppressing Unspecific Cell Uptake for Targeted Delivery Using Hydroxyethyl Starch Nanocapsules. Biomacromolecules. **2012**;13:2704-15.

187. Maldonado RA, LaMothe RA, Ferrari JD, Zhang AH, Rossi RJ, Kolte PN, et al. Polymeric Synthetic Nanoparticles for the Induction of Antigen-Specific Immunological Tolerance. Proc Natl Acad Sci U S A. **2015**;112:E156-65.

188. Sarparanta M, Bimbo LM, Rytkonen J, Makila E, Laaksonen TJ, Laaksonen P, et al. Intravenous Delivery of Hydrophobin-Functionalized Porous Silicon Nanoparticles: Stability, Plasma Protein Adsorption and Biodistribution. Molecular pharmaceutics. **2012**;9:654-63.

189. Gu L, Ruff LE, Qin Z, Corr M, Hedrick SM, Sailor MJ. Multivalent Porous Silicon Nanoparticles Enhance the Immune Activation Potency of Agonistic Cd40 Antibody. Advanced materials. **2012**;24:3981-7.

190. Secret E, Smith K, Dubljevic V, Moore E, Macardle P, Delalat B, et al. Antibody-Functionalized Porous Silicon Nanoparticles for Vectorization of Hydrophobic Drugs. Advanced healthcare materials. **2013**;2:718-27.

SUPPLEMENTARY INFORMATION 1

MANIPULATING HUMAN DENDRITIC CELL PHENOTYPE AND FUNCTION WITH TARGETED POROUS SILICON NANOPARTICLES

Table S1. Antibodies used for *in vitro* pSiNP targeting.

Antigen	Fluorophore	Clone	Ig Class	Manufacturer
Lineage				
CD2	e450	RPA-2.10	m IgG1	eBioscience
CD3		OKT3	m IgG2a	
CD14		61D3	m IgG1	
CD16		CB16	m IgG1	
CD19		HIB19	m IgG1	
CD56		CB56	m IgG1	
CD235a		HIR2	m IgG2b	
HLA-DR	Pe-Cy7	G46-6	m IgG2a	BD Biosciences
CD11c	APC	S-HCL-3	m IgG2b	eBioscience
BDCA-2 (CD303)	PE	AC144	m IgG1	Miltenyi Biotec

Table S2. Antibodies used for phenotyping of monocyte-derived DC.

Antigen	Fluorophore	Clone	Ig Class	Manufacturer
HLA-ABC	APC	W6/32	m IgG2a	eBioscience
HLA-DR	APC	L243	m IgG2a	Biolegend
CD11c	APC	3.9	m IgG1	eBioscience
	PE	S-HCL-3	m IgG2b	
CD14	PE	61D3	m IgG1	BD Biosciences
CD40	APC e450	5C3	m IgG1	eBioscience
CD80	FITC	MAB104	m IgG1	Beckman Coulter
CD83	FITC	HB15e	m IgG1	eBioscience
CD86	Alexa Fluor® 488	IT2.2	m IgG2b	Biolegend
CD209	PE	DCN46	m IgG2b	BD Biosciences

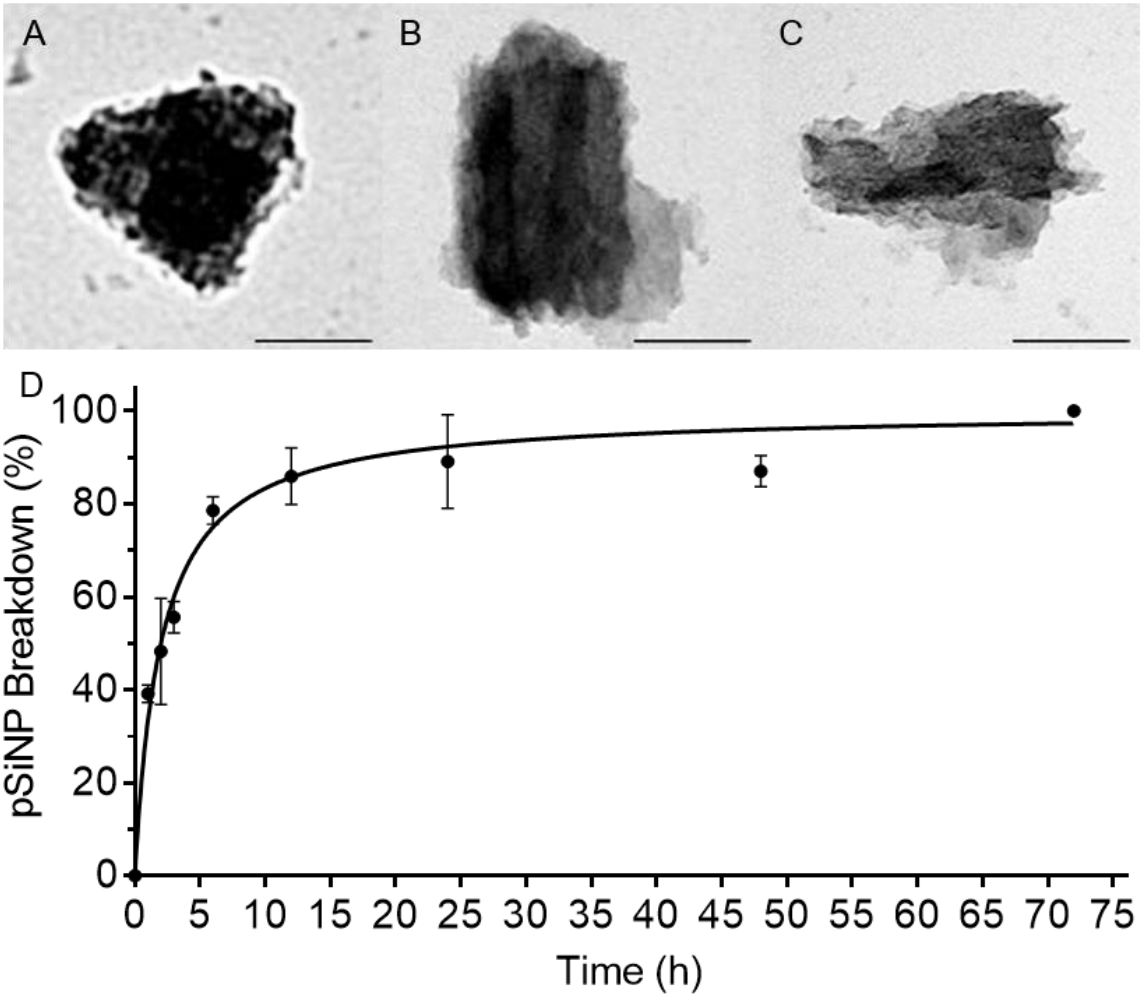

Figure S1 (A-C). Top view, front view and side view transmission electron micrographs of individual pSiNP. Intermittent light and dark regions indicate nanoparticle pores, scale bar represents 100 nm. DLS calculated particle mean size was 160 ± 4 nm. (D). Nanoparticle breakdown kinetics obtained by ICP-MS analysis of elemental silicon. Ninety percent of the pSiNP were broken down within the first 24 h; n = 3.

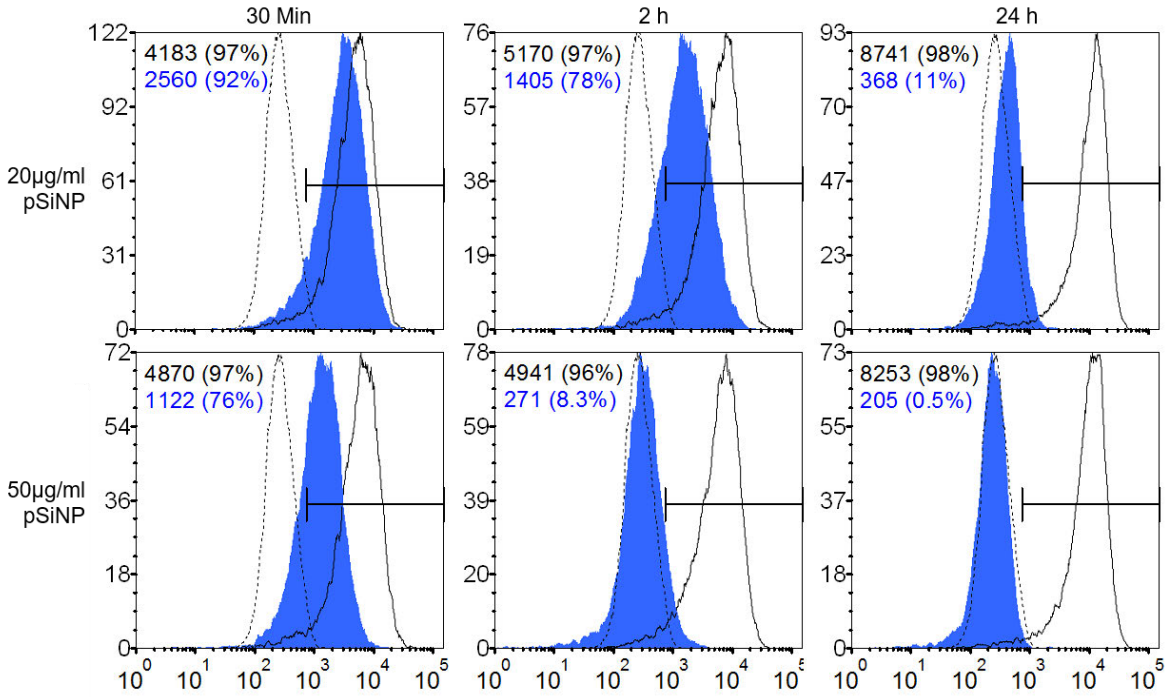

Figure S2. DC-SIGN expression of monocyte-derived DC treated with functionalised pSiNP. DC cultured with DC-SIGN pSiNP (Blue shaded) showed decreased DC-SIGN surface expression in a time and dose dependant manner due to the competitive binding of the pSiNP for the same receptor epitope, preventing DC-SIGN-PE from binding. DC cultured with Isotype pSiNP (Black line) continued to have DC-SIGN receptor expression > 96% indicating that pSiNP functionalisation with DC-SIGN allowed for specific receptor mediated binding. Dashed line represents unstained control. Histograms show MFI with % positivity in parentheses, n = 9.

SUPPLEMENTARY INFORMATION 2

MURINE AND NON-HUMAN PRIMATE DENDRITIC CELL TARGETING NANOPARTICLES FOR *IN VIVO* GENERATION OF REGULATORY T-CELLS

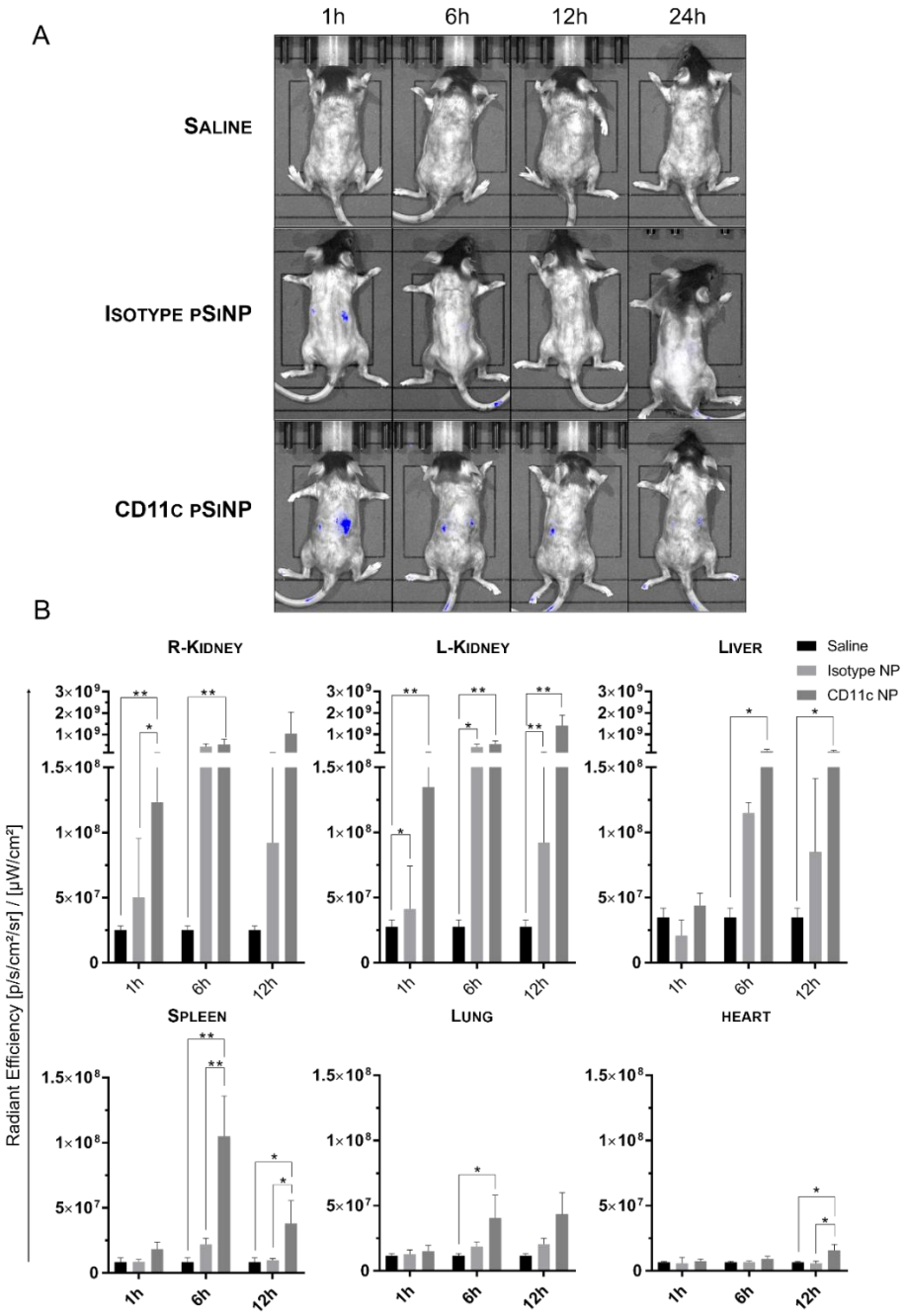

Figure S1. Kidneys accumulate the higher proportion of fluorescent pSiNP in mice. (A) Topographical distribution of fluorescent pSiNP over 1, 6, 12 and 24 h indicated by blue colour. High level of accumulation was seen in the kidneys at 1 h which dissipated at 24 h. (B) Time course tracking experiments indicated that CD11c pSiNP tracked to the kidneys, liver, spleen and lungs with minimal detection in the heart. Isotype pSiNP tracked predominantly to the kidneys and liver with low level detection within the spleen, lungs and heart of mice. (Data are represented as mean ± SD, n = 3 per group, significance determined by one-way ANOVA, * $p < 0.05$, ** $p < 0.01$).

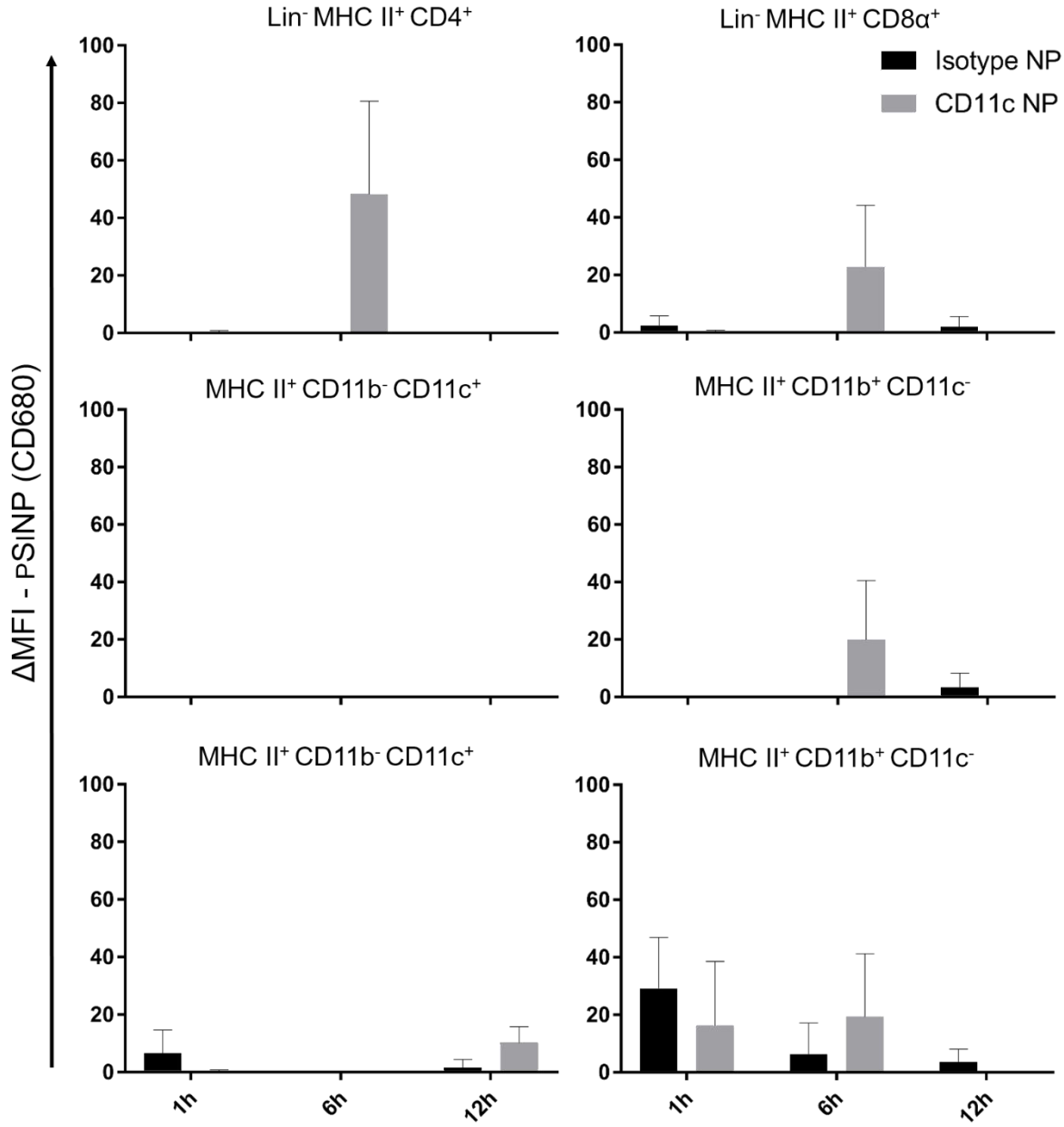

Figure S2. Murine splenic DC preferentially uptake CD11c pSiNP *in vivo*. Time course uptake of pSiNP by mice shows that CD11c pSiNP are taken up more readily over isotype pSiNP by $CD4^+$ and $CD8\alpha^+$ splenic DC at 6 h. Data are presented as delta (Δ) MFI ± SD, normalised to the baseline fluorescence in saline injected control animals. (n = 3 per group, statistical significance determined by two-tailed T-test).

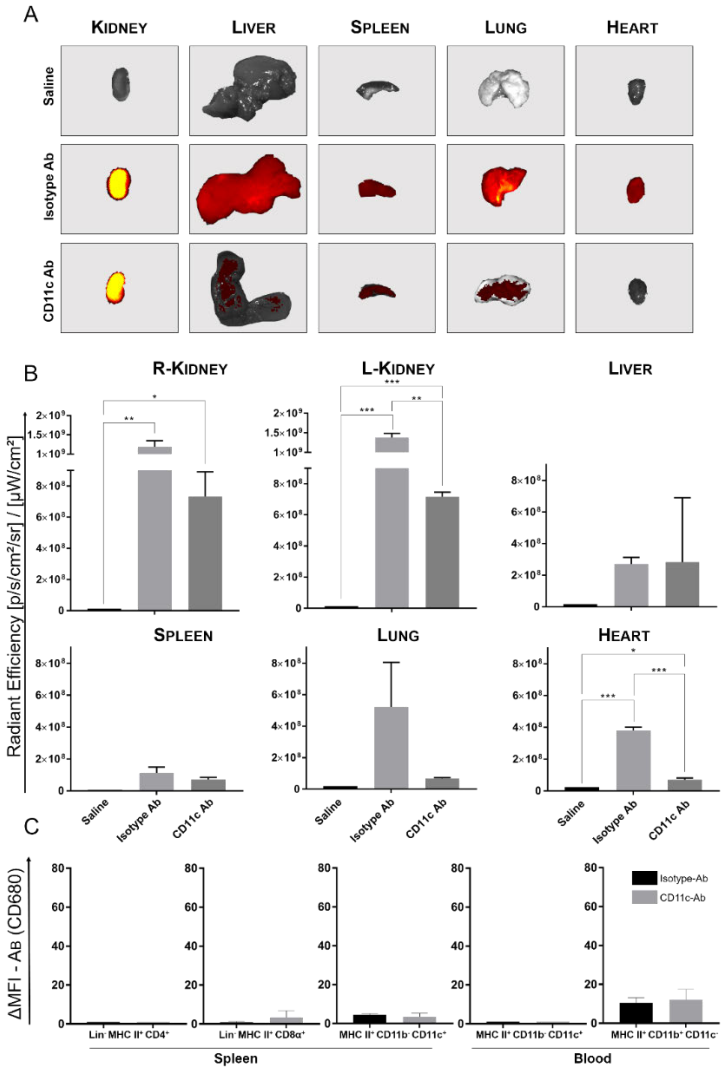

Figure S3. Fluorescently labelled antibodies (Ab) showed markedly different biodistribution in the absence of pSiNP. (A) Individual organs taken from the mice at 24 h post injection (i.v.) with fluorescent Ab. Heat map (red to yellow) indicates presence of antibody. Non-targeting isotype-Ab shows systemic distribution to all major organs. (B) Quantification of total fluorescence as radiant efficiencies (RE) of each of the organs at 24 h. Kidneys expressed the highest accumulation of antibodies with the spleen showing no significant uptake of CD11c-Ab, contrary to CD11c-pSiNP. (C) Quantification of the mean fluorescence intensity (MFI), representative of Ab accumulation, within splenic and blood DC and macrophage populations. No significantly increased detectable levels of antibody fluorophore was seen in any of the conventional DC populations in mice injected with either isotype or CD11c-Ab. (Data is represented as mean RE or ΔMFI ± SD, n = 3 per group, significance determined by one-way ANOVA, * $p < 0.05$, ** $p < 0.01$, *** $p < 0.001$).

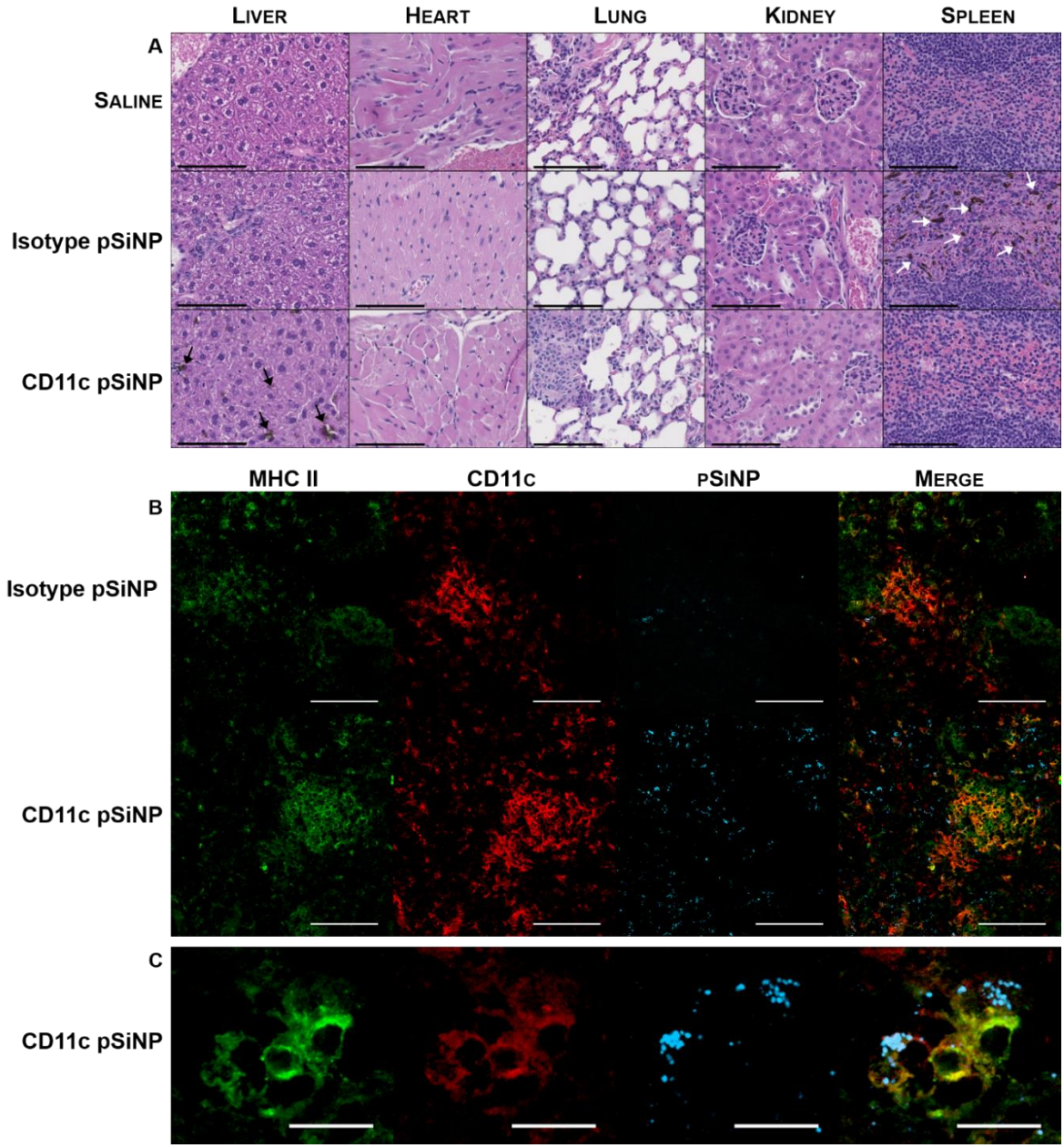

Figure S4. CD11c pSiNP track to splenic DC in mice. (A) General histology of mouse organs, haematoxylin and eosin (H&E). Arrows in CD11c pSiNP liver and isotype pSiNP spleen indicate large brown pSiNP aggregates ranging up to 8 μm in diameter (24 h post injection, scale bar = 100 μm). (B) Immunofluorescent staining of spleens from mice injected with isotype or CD11c pSiNP (blue) co-stained with MHC II (green) and CD11c (red). The spleen displayed a higher level of CD11c pSiNP distribution compared to isotype pSiNP control mice (scale bar = 100 μm). (C) Magnified section of spleen from a CD11c pSiNP mouse showing co-localised staining of CD11c, MHC II and pSiNP (scale bar = 25 μm).

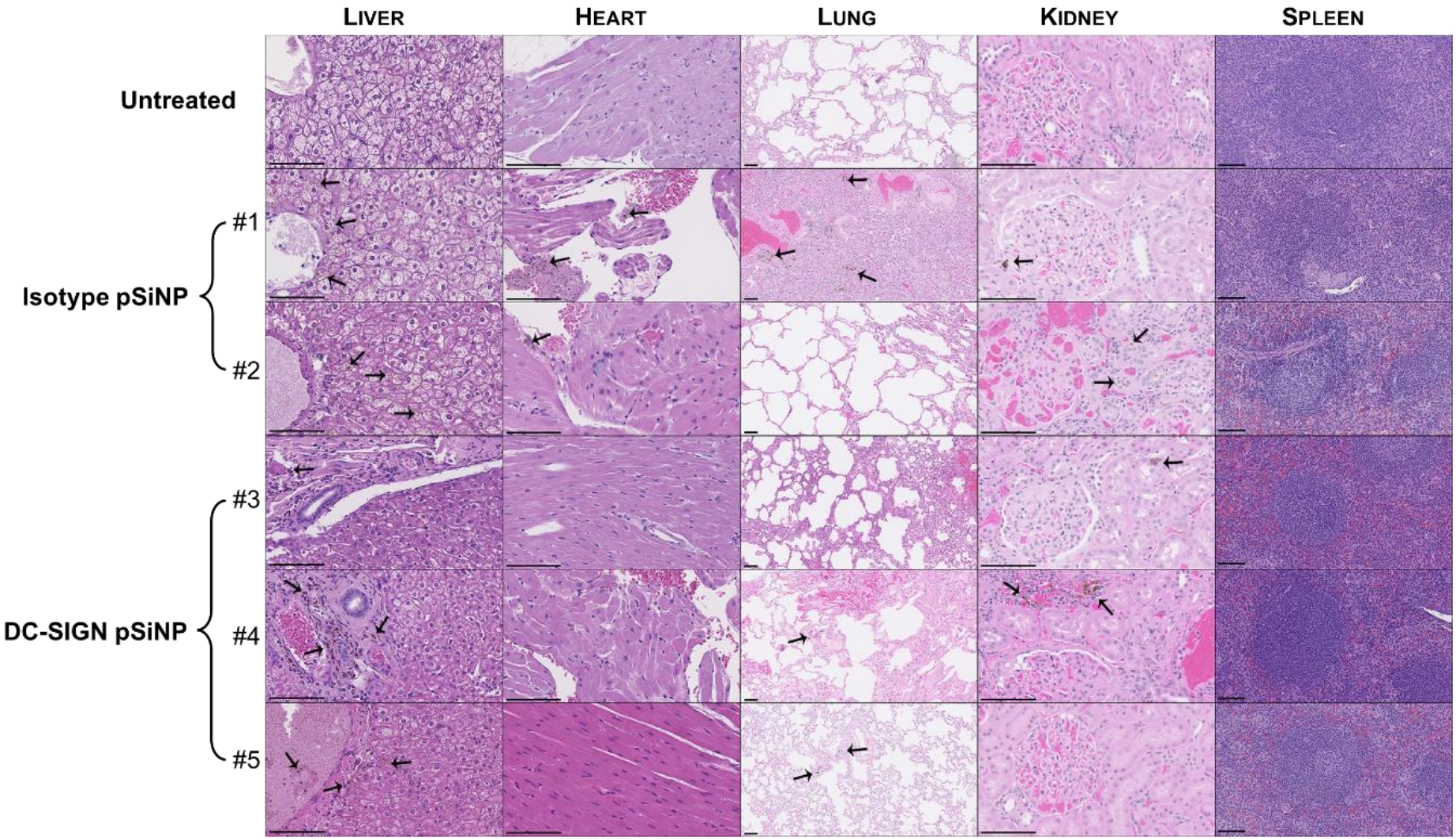
LIVER
HEART
LUNG
KIDNEY
SPLEEN
Untreated
Isotype pSiNP
#1
#2
DC-SIGN pSiNP
#3
#4
#5

Figure S5. Histology shows aggregates of pSiNP within tissue. H&E histological staining showed that a majority of the marmosets had lung tissue with increased compliance and destruction of the alveolar walls, consistent with chronic lung damage. Marmoset organ histology, arrows indicating aggregates of pSiNP within the liver, heart lungs and kidneys (scale bar = 100 μm). CD11c pSiNP aggregated in the lungs ranged from 1 - 10 μm and highly dispersed throughout the tissue compared to isotype pSiNP. Within the liver, isotype pSiNP were smaller (≤ 4.5 μm) compared to CD11c pSiNP.

Table S1. **Murine antibodies used in this study.**

Antigen	Fluorophore	Clone	Ig Class	Manufacturer
Lineage				
CD3ε	FITC	145-2C11	IgG1	BioLegend
CD45R/B220		RA3-6B2	IgG2a	
Ly-6G/Ly-6C		RB6-8C5	IgG2b	
TER-119		TER-119		
MHC Class II (I-A/I-E)	PE-Cy7	M5/114.15.2	IgG2b	BioLegend
	FITC	NIMR-4		eBioscience
CD4	PE	RM4-5	IgG2a	BioLegend
	APC-eFluor 780	GK1.5	IgG2b	eBioscience
CD8α	Pacific Blue	53-6.7	IgG2a	BioLegend
CD11b	eFluor 450	M1/70	IgG2b	eBioscience
CD11c	Purified	HL3	IgG1	BD Bioscience
	PerCP-Cy5.5	N418		eBioscience
CD25	PE	7D4	IgM	Miltenyi Biotec
FoxP3	APC	3G3	IgG1	Miltenyi Biotec

Table S2. **Marmoset antibodies used in this study.**

Antigen	Fluorophore	Clone	Ig Class	Manufacturer
Lineage				
CD3	FITC	SP34	IgG3	BD Biosciences
CD14		M5E2	IgG2a	
CD20		2H7	IgG2b	
CD56		NCAM16.2		
MHC Class II (HLA-DR)	PE-Cy7	L243	IgG2a	BD Biosciences
CD11c	PE	S-HCL-3	IgG2b	BD Biosciences
DC-SIGN (CD209)	Purified	DCN46	IgG2b	BD Biosciences